ISSN 2409-9074

Міністерство освіти і науки України
Національний університет
«Полтавська політехніка імені Юрія Кондратюка»

Ministry of Education and Science of Ukraine
National University
«Yuri Kondratyuk Poltava Polytechnic»

ЗБІРНИК НАУКОВИХ ПРАЦЬ

ГАЛУЗЕВЕ МАШИНОБУДУВАННЯ, БУДІВНИЦТВО

Випуск 2 (63)′ 2024

ACADEMIC JOURNAL

INDUSTRIAL MACHINE BUILDING, CIVIL ENGINEERING

Issue 2 (63)′ 2024

Міністерство освіти і науки України

Національний університет
«Полтавська політехніка імені Юрія Кондратюка»

Ministry of Education and Science of Ukraine

National University «Yuri Kondratyuk Poltava Polytechnic»

ЗБІРНИК НАУКОВИХ ПРАЦЬ

ГАЛУЗЕВЕ МАШИНОБУДУВАННЯ,
БУДІВНИЦТВО

Випуск 2 (63)′ 2024

ACADEMIC JOURNAL

INDUSTRIAL MACHINE BUILDING,
CIVIL ENGINEERING

Issue 2 (63)′ 2024

Полтава – 2024

Poltava – 2024











www.znp.nupp.edu.ua
http://journals.nupp.edu.ua/znp

**Збірник наукових праць. Галузеве машинобудування, будівництво /
Національний університет «Полтавська політехніка імені Юрія Кондратюка»**

Збірник наукових праць видається з 1999 р., періодичність – двічі на рік.

Засновник і видавець – Національний університет «Полтавська політехніка імені Юрія Кондратюка».

Ідентифікатор медіа R30-04133 згідно з рішенням Національної ради України з питань телебачення і радіомовлення від 25.04.2024 No 1416.

Збірник наукових праць уключений до переліку наукових фахових видань (категорія Б), у яких можуть публікуватися результати дисертаційних робіт (Наказ МОН України №1218 від 07.11.2018 року).

Збірник наукових праць рекомендовано до опублікування вченою радою Національного університету «Полтавська політехніка імені Юрія Кондратюка» протокол №20 від 20.12.2024 р.

У збірнику представлені результати наукових і науково-технічних розробок у галузі машинобудування, автомобільного транспорту та механізації будівельних робіт; із проектування, зведення, експлуатації та реконструкції будівельних конструкцій, будівель і споруд; їх основ та фундаментів; будівельної фізики та енергоефективності будівель і споруд; а також у галузях гірництва, нафтогазової інженерії та технологій, екології.

Призначений для наукових й інженерно-технічних працівників, аспірантів і магістрів.

Адреса видавця та редакції – Національний університет «Полтавська політехніка імені Юрія Кондратюка»
Науково-дослідницька частина, к. 320Ф, Першотравневий проспект, 24, м. Полтава, 36011.
Тел.: (05322) 29875; e-mail: v171@pntu.edu.ua; www.pntu.edu.ua
Макет та тиражування виконано у поліграфічному центрі Національного університету «Полтавська політехніка імені Юрія Кондратюка», Першотравневий проспект, 24, м. Полтава, 36011.
Свідоцтво про внесення суб'єкта видавничої справи до державного реєстру видавців, виготівників і розповсюджувачів видавничої продукції (ДК № 3130 від 06.03.2008 р.).
Комп'ютерна верстка – Д.М.Овсій.
Підписано до друку 25.12.2024 р.
Папір ксерокс. Друк різограф. Формат 60x80 1/8. Ум. Друк. Арк. – 10,73.
Тираж 300 прим.

Academic journal. Industrial Machine Building, Civil Engineering / National University «Yuri Kondratyuk Poltava Polytechnic»

Academic journal was founded in 1999, the publication frequency of the journal is twice a year.

Founder and Publisher is National University «Yuri Kondratyuk Poltava Polytechnic».

Media ID R30-04133 according to the decision of the National Council of Ukraine on Television and Radio Broadcasting dated 04/25/2024 No. 1416.

Academic journal is included into the list of specialized academic publications where graduated thesis results could be presented (Order of Department of Education and Science of Ukraine № 1218 dated 07.11.2018).

Academic journal was recommended for publication by the Academic Board of National University «Yuri Kondratyuk Poltava Polytechnic», transactions №20 of 20.12.2024.

The results of scientific and scientific-technical developments in the sphere of mechanical engineering, automobile transport and mechanization of construction works; designing, erection, operation and reconstruction of structural steels, buildings and structures; its bases and foundations; building physics and energy efficiency of buildings and structures are presented in the collection; as well as in the fields of mining, oil and gas engineering and technology; ecology.

Academic journal is designed for researchers and technologists, postgraduates and senior students.

Address of Publisher and Editorial Board − National University «Yuri Kondratyuk Poltava Polytechnic», Research Centre, room 320-F, Pershotravnevyi Avenue, 24, Poltava, 36011, Ukraine.
tel.: (05322) 29875; e-mail: v171@pntu.edu.ua; www.pntu.edu.ua
Layout and printing made in the printing center of National University «Yuri Kondratyuk Poltava Polytechnic», Pershotravnevyi Avenue, 24, Poltava, 36011, Ukraine.
Registration certificate of publishing subject in the State Register of Publishers Manufacturers and Distributors of publishing products (DK № 3130 from 06.03.2008).
Desktop Publishing – D. Ovsii.
Authorize for printing 25.12.2024.
Paper copier. Print rizograf. Format 60x80 1/8. Conventionally printed sheets – 13,25.
Circulation 300 copies.

Збірник наукових праць. Галузеве машинобудування, будівництво
Збірник наукових праць. Галузеве машинобудування, будівництво
Academic journal. Industrial Machine Building, Civil Engineering
http://journals.nupp.edu.ua/znp
https://doi.org/10.26906/znp.2024.63.3550

UDC 699.85:721.012.1-047.44

Olena Filonenko
National University «Yuri Kondratyuk Poltava Polytechnic»
https://orcid.org/0000-0001-8571-9089

Ihor Yurchenko *
National University «Yuri Kondratyuk Poltava Polytechnic»
https://orcid.org/0009-0001-7314-8933

Tetiana Lvovska
Geotechnical laboratory "ISOTOP", Haifa, Israel
https://orcid.org/0000-0002-4747-3353

Nataliia Mahas
Slovak University of Technology in Bratislava, Bratislava, Slovakia
https://orcid.org/0000-0002-4459-3704

Analysis of spatial planning solutions for civil protection structures according to regulatory requirements

The article presents an analysis of the normative-legal documentation regulating the construction and reconstruction of civil protection shelters in countries such as Israel and Ukraine. A comparative analysis method was employed to identify the differences in shelter requirements between the two countries. Specific technical requirements that significantly impact the design and construction process were highlighted. The study compared the approach to determining the required area of shelters in both countries for various facilities. An overview and description of the requirements for ventilation systems, water supply, drainage, and electrical connections were provided. Additionally, the general approach to selecting finishing materials and types of coverings for internal and external structural elements was described. Significant discrepancies in the requirements and approaches to the construction or reconstruction of shelters in these countries were identified. The findings can be used to enhance the efficiency of shelter design and construction in Ukraine, which is particularly relevant in the current context of increased risks to the civilian population.
Keywords: DBN of Ukraine, shelters, dual-purpose structures, Israel's standards

*Corresponding author E-mail: i.a.yurchenko@ukr.net

Introduction

The modern challenges faced by Ukraine constantly introduce new demands for protecting the population from military threats. The issues of construction, reconstruction, and modernization of civil defense shelters are highly relevant and urgent. State regulatory documents governing these processes must be continuously improved, drawing on both contemporary Ukrainian experience and the practices of other countries.

Review of the research sources and publications

State requirements for civil defense shelters are outlined in [1], while Israel's regulatory documents are presented in [2-3]. The study [4] examines the improvement of national legislation in the field of civil defense under martial law. Several scientific studies address the legislative regulation of civil defense issues during the pre-war period, including amendments to Ukraine's Civil Defense Code. The authors of [5] highlighted shortcomings in the approach to forming the protective properties of civil defense structures and the criteria defining them. They analyzed statistical data on the functioning of such structures in Ukraine and the level of protection provided per one thousand people.

Definition of unsolved aspects of the problem.

Although the requirements for civil defense shelters in Ukraine were updated in 2023, numerous unresolved issues remain. These issues lead to increased time and resource expenditures for design and construction. In some cases, they also impose additional financial and economic burdens on the state budget.

Problem statement

The aim of this study is to analyze the spatial and planning solutions for civil defense structures based on the regulatory requirements of Ukraine and Israel. The review of Israel's requirements is conducted with the goal of potentially adopting certain technical aspects that could significantly improve and accelerate the design and construction processes, as well as enhance cost-efficiency in the implementation of such projects.

Analyzing spatial and planning solutions in both countries allows for the identification of key differences and similarities that can be valuable when adapting modern design methods for various conditions, particularly in situations with limited resources and the need for rapid execution of work.

Basic material and results

Let us consider the regulation of certain technical issues based on Israeli legislation.

In Israel, protective structures are divided into several types based on volume and area, such as A-1, A-2, B-1, B-2, C-1, and C-2, as well as into groups by purpose. These include shelters like K1, K2, K3, "forward shelters" or "frontline shelters," "bomb shelters" or "rear shelters," "protected space," "residential safe space," "protected premises in healthcare institutions," "public protected space," and "floor-protected premises." In Fig. 1, a safe space on the premises of a private house is presented. The type and area of a shelter are determined according to the building's purpose and the settlement classification, which is explicitly stated in regulatory documents.

Each type of shelter has both general and specific requirements, ensuring the appropriate use of certain materials or technologies for each type. It is specified that the design of a shelter, its contents, and the characteristics of floor-level and apartment-level protected spaces, including ventilation and filtration systems, sanitary facilities, electrical and communication equipment, must strictly adhere to the examples outlined in state regulations.

Figure 1 - A safe space on the premises of a private house.

Clear minimum and maximum area limits are defined. If a shelter is used as a multipurpose space, the primary area may be increased to accommodate equipment or furniture, provided that this additional space does not exceed 20% of the shelter's main area and does not require significant deviations from standard solutions, except for increasing the number of ventilation and lighting systems, markings, and signage.Table 1 provides an example of how area standards are organized for different building types. Shelters are typically constructed using B-30 concrete, with B15 concrete used for flooring. Walls are 20-40 cm thick, and all interior walls are also made of reinforced concrete. During the casting process, samples are collected for testing in a licensed laboratory to ensure the concrete's strength. In Fig. 2, the method for testing the compressive strength of concrete is illustrated.

Figure 2 - The method for testing the compressive strength of concrete.

After casting an underground shelter, a water-tightness test is conducted by flooding all underground components of the structure with water up to the ceiling. The water remains in the structure for 48 hours, and any detected leaks must be repaired before further work proceeds.

Special attention is paid to ventilation systems. During threats, filtered air is supplied, while natural ventilation is used in peacetime. One supply and one exhaust air duct are designed for every 25 m² of space. The equipment is calculated based on a density of 0.4 m² per person and at least 16 air exchanges per hour.

In Fig. 3, the elements of a ventilation system are depicted.

In A-1 type shelters, there is no obligation to install sinks and faucets. In other shelters, one sink and faucet with running water are installed for every 50 square meters of the main area or any part thereof. Wastewater disposal is generally done by gravity, except in cases where this is not possible. For buildings equipped with a generator, and where the competent authority confirms that gravity drainage is not feasible, wastewater may be removed using pumping systems. Appropriate measures are taken to prevent backflow, including mechanical devices.

A drinking water storage tank is installed in each shelter, calculated at 5 liters per square meter of the shelter's main area. The capacity of a single drinking water storage tank must not exceed 500 liters.

A clear categorization of shelter types in Israel allows implementation of a protected window opening, Fig. 5

Table 1. Shelter Area Standards for Different Building Types in Israel

Building Type	Required Protected Space Area	Minimum Protected Space Area, m²
Office Building	3% of the main area	10
Laboratories	3% of the main area	10
Banks	2% of the main area	10
Post Offices	4% of the main area	10
- Courtrooms	5 m² per courtroom	10
- Offices	3% of the main area	10
Religious Buildings:		
- Synagogues	1% of the main area	10
- Ritual Buildings	1% of the main area	10
- Mosques, Churches	1% of the main area	10
- Prayer Halls	1% of the main area	10
Protected Housing and Nursing Homes	2.5 m² for residential units with up to 2 rooms	10
Hotels, Sanatoriums, Guesthouses	1 m² per residential unit	10
Dormitories, Boarding Schools	20% of the main area	-
Clinics, Mother and Child Rooms, etc.	3% of the main area	10
Community Centers, Youth Clubs	2% of the main area	10
Industrial Buildings:		
- Offices and High-Tech Industry	3% of the main area	10
- Production Workshops	2% of the main area	10
- Warehouses	0.8% of the warehouse area	10

for the standardization of required electrical connections.

For instance, it is explicitly stated that A- 2 and B-1 type shelters must be connected to a single- phase power supply with a capacity of 40 amps. B-2 type shelters must be connected to either a single-phase supply of 40 amps or a three-phase supply of 25 amps. C-1 type shelters without central ventilation and filtration rooms are connected to a three-phase power supply of 25 amps. For C-1 shelters with ventilation rooms and C-2 shelters, the power requirements are determined by the designer. In shelters equipped with power generators, switching between power sources is done manually. To monitor the generator's load, ammeters are installed in the premises, marked with a red line indicating the maximum allowable current.

Regarding finishing works, the regulations specify that the concrete surface must be smooth after casting. Plastering, stone cladding, or the use of tiles of any kind is prohibited. Only painting or the application of decorative coatings with a layer no thicker than 2 mm is allowed. PVC panels are permitted on slopes.

Exterior wall surfaces above ground level can either remain as painted concrete or be plastered. Stairs, emergency exits, and access routes, excluding floors, are whitewashed with lime or synthetic lime or painted in white or other light shades at the designer's discretion.

The use of materials other than those specified in the standard is allowed only with the approval of the relevant defense ministry authorities. Elements such as entrance doors, airtight doors, soundproof doors, windows, steel pipes with a diameter of 4" or more, and all connecting elements, as well as floor hatch covers, must be certified and bear approval marks from the Standards Institute. Fig. 4 presents an example of the shows the results of testing doors that do not meet the requirements.

The concept of "Owner" in Israeli legislation is defined as the recipient or the person entitled to receive income from a property, or who would receive income if the property generated it, as well as those with ownership rights or acting as trustees. This applies regardless of whether the owner is registered. In the case of leased properties with a fixed lease term of 25 years or more, the lessee is considered the "Owner."

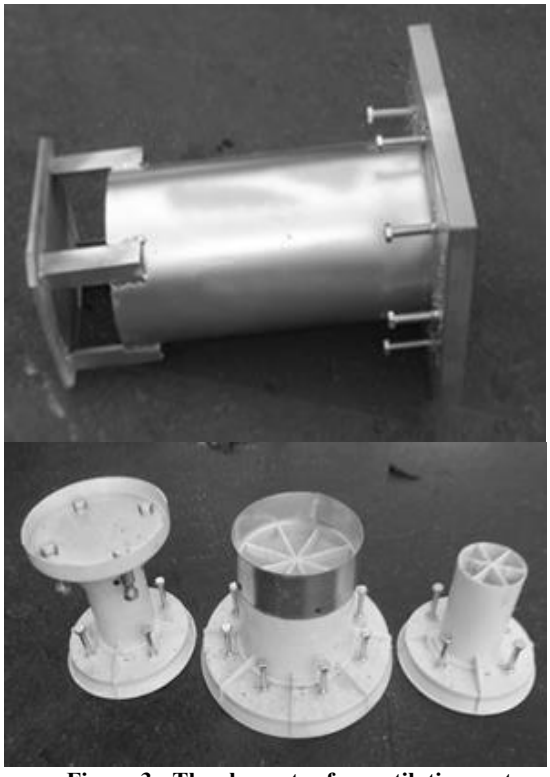

Figure 3 - The elements of a ventilation system.

Thus, the responsibility for maintaining shelters falls not only on property owners but also on those using the building or deriving income from it. Additionally, if a building lacks a shelter, the owner is obligated to arrange one within or near the building at a time and location specified by the local authority through written instructions.

Figure 4 – Example of the implementation of a protected window opening.

Exemptions from the obligation to build or expand a shelter may be granted if it is proven that construction or expansion is impossible at the site. In such cases, the applicant must contribute to a fund dedicated to creating, improving, or expanding public shelters. The contribution should not exceed the costs of constructing or expanding the shelter on-site. Exemptions may also depend on the presence of an existing shelter accessible to users of the building or factory.

Expenses incurred by the owner for equipping, repairing, or reconstructing a shelter can be partially recouped from building occupants, ranging from 25% to 50% depending on specific conditions.

Let’s return to the regulatory documentation of Ukraine.

In 2023, Ukraine approved DBN V.2.2-5:2023 "Protective Structures of Civil Defense," which replaced DBN V.2.2.5-97 "Protective Structures of Civil Defense," which, in turn, was based on construction norms from the USSR in the 1950s and 1970s, with certain changes and revisions over time. During this period, some provisions were canceled, while others were modified or supplemented.

In Ukraine, the following types of civil defense structures are distinguished: shelters, radiation protection shelters, dual-use structures with shelter properties, dual-use structures with radiation protection shelter properties, primary (mobile) shelters, and the simplest shelters. Each of these types has general requirements according to state norms. Each shelter is designed considering its purpose, location, structural, and other technical issues, which are individually resolved by the designer for each project.

Civil defense structures and dual-use structures are designed and constructed in such a way as to create appropriate conditions for the accommodation of people requiring shelter and to provide the necessary level of protection from the anticipated impacts of hazardous factors that may arise as part of dangerous events during emergencies, military (combat) operations, and terrorist acts. These structures are designed to support the presence of people for up to 48 hours.

The required number and capacity of each protective structure and dual-purpose structure are determined during the design phase, based on the estimated number of people needing shelter. For educational institutions, shelters must accommodate 100% of the participants in the educational process and other staff members. However, during the reconstruction or new construction of separate or attached protective structures or dual-purpose structures within the grounds of existing educational institutions, the capacity of the protective structures may be reduced to 50% of the total capacity of the institution, provided that sheltering is available for all individuals who may be in the building at the same time, according to the institution's operational schedule during the most populated shift. The total capacity of protective structures and dual-purpose structures in public buildings is determined by the possibility of sheltering 100% of the estimated number of people who periodically stay on the premises (calculated according to DSTU 8855), residential buildings – 100% of the estimated number of people who permanently stay on the premises, and buildings intended for production, storage, and administrative and household purposes – 100% of the estimated number of people who periodically stay on the premises.

The minimum area of the main and auxiliary rooms of shelters and dual-purpose structures with shelter properties is specified in the current DBN, while the upper limit is not restricted.

For the construction of concrete, reinforced concrete, and steel-reinforced concrete structures for protective structures and dual-purpose structures, heavy concrete with a density of at least 2000 kg/m³ and a class not

Figure 5 – Results of testing doors that do not comply with the requirements.

lower than C12/15 should be used. For columns and beams, the class should not be lower than C20/25. Concrete blocks for walls should be designed from concrete with a class not lower than C8/10. The mortar for sealing the walls of prefabricated reinforced concrete structures must not be lower than C8/10.

There is a provision concerning the airtightness of shelters, which states: "External enclosing structures (foundations, floors, walls, ceilings, and roofs), along with their waterproofing, must protect the shelter from the negative impact of groundwater, flooding, and ensure the airtightness of the shelter." However, no detailed testing requirements are provided.

Ventilation systems must meet the needs of people for clean air for 6-48 hours, depending on the ventilation mode (I, II, or III). Air intake must be cleaned of solid particles and dust by installing coarse air filters. The minimum air exchange rate in the rooms where individuals will be sheltered should be 6-10 air exchanges per hour, depending on the functional features of the room.

There is a requirement to install at least one washbasin for every 200 people, but no fewer than one per sanitary unit. Wastewater discharge can be handled either by gravity or by using a pumping station for pumping (if gravity discharge is not possible) with the installation of a valve inside the structure.

The reserve of drinking water in containers is calculated at 3 liters per day per person who is to be sheltered.

Regarding electrical connections, it is recommended that the power supply for electrical receivers be provided from a network with a nominal voltage of 230/400 V. The reliability of the power supply for electrical receivers used in peacetime is determined according to the relevant norms for such a type of structure. The power capacity for connection is not standardized and not limited.

There are general requirements for finishing works; the use of suspended ceilings, false floors, glass cladding, ceramic tiles, or other materials that could create sharp fragments when broken is prohibited.

Conclusions

Modern realities impose continuous adjustments that are far from final. Therefore, existing regulatory documents must evolve, be supplemented, and optimized further. The integration of advanced technologies, the experience of other countries, and contemporary requirements for civil defense will contribute to improving the efficiency and timeliness of constructing protective structures.

The ongoing process of improving the regulatory framework is essential to ensure an adequate level of protection for the population and infrastructure in the face of modern threats. This will help reduce resource costs, enhance design quality, and accelerate the adoption of innovations in the field of civil defense.

References

1. Мінрегіон України. (2023). *ДБН В.2.2.5-2023. Захисні споруди цивільного захисту* (120 с.). Київ: Мінрегіон України.
2. Israel Defense Regulations. (2024*). Official text as of 2024*. Retrieved from https://www.nevo.co.il/law_html/law01/125_020.htm#Seif274
3. Israel Civil Defense Regulations. (2024). *Official text as of 2024.* Retrieved from

1. Ministry for Communities and Territories Development of Ukraine. (2023). *DBN B.2.2.5-2023. Civil protection shelters* (120 p.). Kyiv.
2. Israel Defense Regulations. (2024). *Official text as of 2024*. Retrieved from https://www.nevo.co.il/law_html/law01/125_020.htm#Seif274
3. Israel Civil Defense Regulations. (2024). *Official text as of 2024*. Retrieved from

https://www.nevo.co.il/law_html/law01/125_020.htm#med0
4. Бойко, О. (2022). Державне управління у сфері цивільного захисту: подальше вдосконалення законодавства в умовах дії воєнного стану. *Науковий вісник: Державне управління*, (2)12, 195–217. https://doi.org/10.33269/2618-0065-2022-2(12)-195-217
5. Некора, В., Ніжник, В., Поздєєв, С., Луценко, Ю., & Михайлов, В. (2023). Особливості та перспективи ефективного функціонування захисних споруд цивільного захисту в умовах бойових дій. *Науковий вісник: Цивільний захист та пожежна безпека,* (1)15, 149–157. https://doi.org/10.33269/nvcz.2023.1(15).149-157
6. Джеджула, В. В. (2023). Особливості влаштування вентиляції в захисних спорудах цивільного захисту. *Сучасні технології в будівництві*, 35(2), 185–189.
7. Sobchenko, T., Kin, O., & Vorozhbit-Gorbatyuk, V. (2023). Creation of a safe educational space in educational institutions under the conditions of martial state. *New Collegium*, 3(111), 39–42. https://doi.org/10.30837/nc.2023.3.39
8. Sehida, K., & Chekhov, S. (2023). Spatial analysis of provision the population of Kharkiv with civil defense facilities. *Human Geography Journal*, 34, 14–26. https://doi.org/10.26565/2076-1333-2023-34-02
9. ASME. (2023). Features in civil defense facilities. *ASME Journal of Nuclear Radiation Science*, *10*(4). https://doi.org/10.1115/1.4065463
10. Glasstone, S., & Dolan, P. J. (1977). *The effects of nuclear weapons* (3rd ed.). United States Department of Defense and United States Department of Energy.
11. Al-Maliky, S. J. (2008). Basic concepts for the design of nuclear shelters and the calculation of wall thickness against a nuclear explosion of 20 kT. *Journal of Engineering and Development*, 12(2), 17. https://jeasd.uomustansiriyah.edu.iq/index.php/jeasd/article/view/1659/1319

https://www.nevo.co.il/law_html/law01/125_020.htm#med0
4. Boiko, O. (2022). State management in the field of civil protection: Further improvement of legislation under martial law. *Scientific Bulletin: Public Administration*, (2)12, 195–217. https://doi.org/10.33269/2618-0065-2022-2(12)-195-217
5. Nekora, V., Nizhnyk, V., Pozdeyev, S., Lutsenko, Yu., & Mykhailov, V. (2023). Features and prospects for the efficient functioning of civil protection shelters under combat conditions. *Scientific Bulletin: Civil Protection and Fire Safety*, (1)15, 149–157. https://doi.org/10.33269/nvcz.2023.1(15).149-157
6. Djedzhula, V. V. (2023). Features of ventilation arrangement in civil protection shelters. *Modern Technologies in Construction*, 35(2), 185–189.
7. Sobchenko, T., Kin, O., & Vorozhbit-Gorbatyuk, V. (2023). Creation of a safe educational space in educational institutions under the conditions of martial state. *New Collegium*, 3(111), 39–42. https://doi.org/10.30837/nc.2023.3.39
8. Sehida, K., & Chekhov, S. (2023). Spatial analysis of provision the population of Kharkiv with civil defense facilities. *Human Geography Journal*, 34, 14–26. https://doi.org/10.26565/2076-1333-2023-34-02
9. ASME. (2023). Features in civil defense facilities. *ASME Journal of Nuclear Radiation Science*, *10*(4). https://doi.org/10.1115/1.4065463
10. Glasstone, S., & Dolan, P. J. (1977). *The effects of nuclear weapons* (3rd ed.). United States Department of Defense and United States Department of Energy.
11. Al-Maliky, S. J. (2008). Basic concepts for the design of nuclear shelters and the calculation of wall thickness against a nuclear explosion of 20 kT. *Journal of Engineering and Development*, 12(2), 17. https://jeasd.uomustansiriyah.edu.iq/index.php/jeasd/article/view/1659/1319

Філоненко О.І.
Національний університет «Полтавська політехніка імені Юрія Кондратюка»
https://orcid.org/0000-0001-8571-9089

Юрченко І.О. *
Національний університет «Полтавська політехніка імені Юрія Кондратюка»
https://orcid.org/0009-0001-7314-8933

Львовська Т.В.
Геотехнічна лабораторія «ISOTOP», Хайфа, Ізраїль
https://orcid.org/0000-0002-4747-3353

Магас Н.М.
Словацький технічний університет у Братиславі, Братислава, Словаччина
https://orcid.org/0000-0002-4459-3704

Аналіз об’ємно-планувальних рішень споруд цивільного захисту за нормативними вимогами

В статті представлено аналіз нормативно-правової документації, яка регулює будівництво та реконструкцію укриттів цивільного захисту таких країн як Ізраїль та Україна. У дослідженні використано метод порівняльного аналізу для ідентифікації розбіжностей у вимогах до укриттів між країнами. Було виділено конкретні технічні вимоги, які мають вагомий вплив на процес проєктування та будівництва. Проведене порівняння підходу до визначення необхідної площі укриттів в обох країнах для різних об’єктів. Зроблено огляд і опис вимог до систем вентиляції, водопостачання та водовідведення, електричних підключень. Описано загальний підхід до вибору оздоблювальних матеріалів та типів покриттів внутрішніх та зовнішніх конструктивних елементів. Виявлено значні розбіжності в вимогах та підходах до будівництва чи реконструкції укриттів в цих країнах. Результати можуть бути використані для підвищення ефективності проєктування та будівництва укриттів в Україні, що є особливо актуальним у сучасних умовах підвищеного ризику для цивільного населення.
Ключові слова: ДБН України, укриття, споруди подвійного призначення, норми Ізраїля
*Адреса для листування E-mail: i.a.yurchenko@ukr.net

Збірник наукових праць. Галузеве машинобудування, будівництво
Academic journal. Industrial Machine Building, Civil Engineering
http://journals.nupp.edu.ua/znp
https://doi.org/10.26906/znp.2024.63.3865

UDC 624.046.5

Sergii Pichugin
National University «Yuri Kondratyuk Poltava Polytechnic»
https://orcid.org/0000-0001-8505-2130

Analysis of trends in the development of load codes for building structures

The content of the article is a consistent review of approaches to considering loads on building structures and their reflection in regulatory documents of different years. Attention is focused on the continuity of the method of limit states and the method of permissible stresses in the part of the description of loads. With regard to climatic loads (snow, wind), attention is paid to changes in territorial zoning and calculation coefficients, the assignment of normative and calculation values and the involvement of experimental statistical data. Attention is also paid to the connection between the development of codes of crane loads and the results of experimental studies of these loads.

Keywords: reliability, design codes, limit states, snow loads, wind loads, crane loads

*Corresponding author E-mail: pichugin.sf@gmail.com

Introduction

Engineers always face the question of how the builders of the past ensured the reliability of buildings and structures that have been safely preserved to this day. At the same time, issues of substantiation of some calculated parameters and coefficients of the allowable stress method, which later became part of the codes of the limit states method, remain unclear. These and other questions are answered by the study of the development of domestic and foreign design codes, the relevance of which is connected not only with the fact that history provides factual knowledge about past construction experience, but allows predicting trends in the development of building codes.

Review of the latest sources and publications

Separate stages of the development of building mechanics, building structures and building design codes are covered in domestic articles and monographs of different years [1,2]. From foreign publications dedicated to this topic, major reviews stand out [3,4]. The analysis of the evolution of building design codes should begin with the capital Urgent position, which regulated construction activities on the territory of Ukraine from the middle of the 19th century to the beginning of the 20th century [5]. Foreign construction regulation, in particular in Germany, in the same period is represented by the multi-volume HŰTTE handbook, which was quite popular until the 1930s [6]. The period 1930-1955 is characterized by constant development and revision of domestic design codes based on the allowable stress method, which was later replaced by the limit state method, the features of which are analyzed in monographs [7,8]. An important direction in the development t of design codes is the clarification of the calculated values of loads acting on the building and having a complex probabilistic nature [9]. Domestic studies of loads have intensified in recent decades in connection with the implementation of the State Building Codes of Ukraine [10-12].

Definition of unsolved aspects of the problem.

It should be noted that currently there are not enough scientific publications in which the chronological development of the method of allowable stresses, which was the basis of the design of building structures for more than 100 years, until the middle of the 20th century, was analyzed in detail. Therefore, it can be assumed that the long-term positive potential of the allowable stress method, on the basis of which the transition to the modern calculation of building structures according to limit states was made in the 1950s, was generally ignored.

Problem statement

The aim and objectives of the study are a consistent review of approaches to the consideration of loads on building structures and their reflection in regulatory documents of different years. Attention is focused on the continuity of the method of limit states and the method of allowable stresses in the part of the load description. With regard to climatic loads (snow, wind), attention is paid to changes in territorial zoning and calculation coefficients, the assignment of normative and calculation values, and the involvement of experimental statistical data. Attention is also paid to

the connection between the development of codes of crane loads and the results of experimental studies of these loads.

Basic material and results

As indicated above, the first normative document that was effective in the territory of Ukraine was "Urgent position: a guide for drawing up and checking estimates, designing and performing works" [5]. This document contained some provisions of the structure calculation methodology. It is interesting to note that its author was Count De Rochefort N.I. (1846 – 1903), civil engineer and architect, builder of railways, highways and palaces. The Urgent position is a unique manual that served as a reference for builders and architects, a textbook for teachers, and a guide for construction contractors. For the first time, it explained the building regulations and rules and contained the necessary reference material related to construction. The Urgent position came into effect for the first time in 1869, it was republished with changes 13 times, the last edition was printed in 1930. The Urgent position had an important state status and was mandatory for use throughout the country.

In the second half of the 19th century and at the beginning of the 20th century, domestic technical literature was practically absent. Therefore, translated technical publications, mainly German, were popular. Such a publication was the Hütte handbook - a multi-volume "Handbook for engineers, technicians and students" [6]. The first German edition of the Handbook was published in Germany in 1857, it included sections: mathematics and mechanics, mechanical engineering and construction. Soon, in 1863, the first Russian translation of the Handbook was published. Before World War II, Hütte was one of the most common technical reference books in our country. The Handbook continued to be published in the post-war years, the last 34th edition was printed in 2012.

Changes in snow load rationing. Based on these and other sources, let's first consider how the regulation of such an important and dangerous force on buildings as snow load changed over time. The Urgent provision contained some instructions regarding loads on structures, in particular, on rafter trusses. The load from own weight was regulated in the range of 20 – 70 kgf/m^2, variable loads – at 160 kgf/m^2. It can be assumed that this variable load with a margin took into account the snow load in the main territory of the country, and the total calculated load of 180 – 230 kgf/m^2, together with a margin for strength, ensured a certain level of safety of structures made according to competent calculations. It should be noted that the specified recommendations regarding the total loads on the roof corresponded to the German codes of that time for pitched roofs in Germany [6].

In the first post-revolutionary Unified Rules for Building Design (1931), the snow load P_c (kgf/m^2) was determined by a formula that is quite unusual from a modern point of view:

$$P_c = P_c^0\left(1+0.002h\right)\left(45^\circ-\alpha\right), \qquad (1)$$

where P_c^0 – an empirical value that depended on the geographical location of the area (latitude and longitude), and was found in the corresponding table with latitude values in the range of 40 – 70^o and longitude 20 – 190^o; h – height of the area above sea level (in meters); α is the angle of inclination to the horizon (in degrees) of the surface that received the snow load.

To specify the recommendations of the Uniform Rules regarding snow load, we will perform calculations for three geographical points:

• Poltava: latitude 44°35′, longitude 34°34′, h = 146 m, P_c^0 = 1.33, according to formula (1) the estimated snow load on the horizontal surface (α = 0°) was

$$P_c = 1,33\left(1+0,002\cdot 146\right)45^\circ = 77,5 \text{ kgf/m}^2;$$

• Kyiv: latitude 50°27′, longitude 30°30′, h = 183 m, P_c^0 = 0.94

$$P_c = 0,94\left(1+0,002\cdot 183\right)45^\circ = 57,8 \text{ kgf/m}^2.$$

• Kropyvnytskyi: latitude 48°31′, longitude 32°17′, h = 127 m, P_c^0 =1.10

$$P_c = 1,10\left(1+0,002\cdot 127\right)45^\circ = 62,0 \text{ kgf/m}^2.$$

As can be seen, the values of snow load regulated by the Uniform Rules were significantly lower than those previously contained in the Urgent provision.

In the next normative on the height of the snow cover h, and the average document of 1933, the snow load was standardized differently, depending maximum height for the last ten years was taken into account. So, the calculated height of the snow cover had some statistical justification. At the same time, the density of snow was assumed to be ρ = 100 kg/m^3 without sufficient explanation. The calculated value of the snow load was determined as $p = 1,6\rho h$. 4 regions were determined with heights of snow cover in the range of 30 sm>h>80 sm and corresponding snow load p = 25 – 120 kgf/m^2 [2].

It is interesting to note that the codes of 1933 (that is, 90 years ago) contained detailed recommendations regarding the possible reduction of snow loads due to melting:

a) for moderately insulated roofs (with a thermal resistance of 0.75...1.10 (m^2·°C)/W) at an internal temperature of 15˚C, 2/3 of which are located above the heated rooms, the snow load was reduced by 50%;

b) for roofs of buildings with large heat emissions (heat flow over 800 cal/h/m^2) with thermal resistance less than 0.75 (m^2·°C)/W – the snow load was reduced by 75%.

In the future, these valid recommendations were omitted, and they are missing from domestic snow codes to this day, although their relevance is obvious, which is confirmed by the presence of similar recommendations in the Eurocode.

In the following codes (1940), when justifying the snow load standard, the snow density was increased with a differentiation of ρ = 200 – 250 kg/m^3 depending

on the height of the snow cover. The territory of the country was divided into 5 snow regions with the values of the snow cover height h and the calculated snow weight p on the ground surface of a slightly higher level compared to the previous codes. At the same time, the territory of Ukraine was attributed to the I region (h up to 20 cm, weight p = 50 kgf/m^2) and II region (h from 20 to 40 cm, p = 70 kgf/m^2). These unjustified standards ignored the climatic features of Ukraine and were significantly lower than the actual snow loads on its territory. Nevertheless, these standards were left in subsequent editions of the load codes and transferred as normative values to the SNiP, which regulated the calculations of structures for limit states.

A number of researchers have identified significant shortcomings of SNiP regarding the standardization of snow loads [2].

1. Underestimation of the calculated values of snow load, which is the result of the imperfection of the methodology for their justification, as a result of which they are exceeded quite often, in some areas every 5...10 years. This is largely due to the fact that methodological approaches to the standardization of snow loads, appropriate for areas with heavy snow winters, have not been sufficiently justified in areas with unstable snow cover (which includes, for example, most of Ukraine). Here, the snow load has significant specifics, in particular, it cannot be described by the normal distribution law, which satisfactorily assesses the snow load in continental areas. As a result, on average across Ukraine, the calculated values of snow load were underestimated by 50...60% compared to the values necessary to ensure a minimum sufficient level of reliability of load-bearing structures. Such a serious discrepancy between snow standards and reality was the cause of a large number of accidents in building structures.

2. Overly generalized zoning of the territory of the former USSR (6 snow regions), which ignored the specifics of individual regions of the country. To a large extent, this situation is attributed to the territory of Ukraine with various physical and geographical features and climatic regions, such as coastal, mountainous, steppe, forest and other areas. As a result, the changeable Ukrainian winters form a territorial distribution of snow cover, which is significantly different from the zoning map of snow load according to SNiP. Here we give the remarks of R.I. Kinash [2], who, as a curiosity, noted that in terms of snow load, Lviv (in which in 1995/96 and 1996/97 the snow lay for almost 6 months) was attributed to the same region as Tashkent and Ashgabat, and Vinnytsia, close to Lviv, to a remote continental high-snowfall region of inland Asia with markedly different climatic characteristics. Obviously, for a vast territory that constituted one sixth of the Earth's landmass, such a generalized zoning with a limited number of snowy areas can be considered forcibly justified, but insufficiently differentiated.

3. The lack of a clear connection between the snow load standard and its recurrence period, which makes it impossible to take into account the service life of buildings, as a result of which they are designed for an indefinite service life, which supports the misconception: "Buildings should stand forever!".

4. Disadvantages in the standardization of the long-term component of the snow load, which is not regulated at all for I and II snow regions. Such an approach is illogical, since whatever the nature of the change in the snow load in low-snow regions (to which I and II regions belong), it will still create rheological phenomena in structures (even if insignificant and have little effect on the operation of the structure). Therefore, long-term components should also be established for I and II regions, at least from a methodological point of view.

5. The fundamental incorrectness of taking into account the differentiated reliability coefficient γ_f = 1.4...1.6 depending on the weight of the roof. Taking into account the necessity of such an approach, it should be emphasized that this coefficient depends only on the probabilistic properties of the snow load and is not related to the design and weight of the roof.

With the collapse of the USSR, the new independent states had the opportunity to move away from the crude Soviet snow standardization and develop their own, more differentiated snow zoning. Further development of snow standards in the CIS was implemented in the form of national standards of individual states. The codes of Ukraine DBN V.1.2-2:2006 “Loads and loadings” finally (after 70 years!) introduced statistically justified increased values of snow load. Compiled on the basis of research by domestic scientists [9], these codes regulate the characteristic values of snow load, in particular, for Poltava and Kyiv 1600 Pa (160 kgf/m^2 – 5th region), for Kropyvnytskyi 1400 Pa (140 kgf/m^2 – 4 region). A more detailed description of the evolution of snow load standardization is given in the publication [10].

Evolution of normalization of wind loads. The beginning of this was laid in 1931 with the publication of "Uniform codes of construction design". There was already a certain scientific basis for substantiating the codes in that period: long-term meteorological wind observations (3 times a day) with the measurement of wind speed by a Wild weathervane with two-minute averaging; aerodynamic studies that have been carried out since pre-revolutionary times in laboratories and institutes. In the Uniform codes, the wind load was determined by the formula, which also had a rather unusual appearance from a modern point of view:

$$p_в = k\left(p_в^0 + k_1 h\right) \qquad (2)$$

where $p_в$ – the wind pressure in kgf/m^2; k – coefficient of flow, which depended on the shape and position of the object exposed to the wind; $p_в^0$ – the highest pressure in kgf/m^2 when the air flow is directed normally to the surface; h is the total height of the building (m) above the edge of the foundation; k_1 – calculation coefficient, which was taken

depending on the nature of the wind flow around the buildings.

Territorial zoning in the first wind codes was practically absent, since the same maximum wind pressure $p_в^0$ = 50 kgf/m^2 was assumed for the entire country, except for the coasts of seas and the mouths of large rivers 75 – 100 kgf/m^2.

Standardization of wind load was developed in the codes introduced in 1933 [2]. In them, the wind load was determined by a different formula:

$$P_a = k \cdot q \quad (3)$$

where k is the flow coefficient; q – wind pressure, similar to $p_в^0$ in the formula (2).

The wind division was maintained for the above-mentioned three geographical areas, and for the entire territory the pressure was reduced to 45 kgf/m^2.

Evaluating the described wind codes, it should be noted that the first wind zoning was not differentiated enough and regulated only one basic value of wind pressure of $q = 45$ kgf/m^2 for the entire territory of the country (with few exceptions). It was not sufficiently statistically substantiated. As subsequent studies have shown, this value turned out to be underestimated and was subsequently increased. Perhaps the authors of the codes took this into account, so they recommended the designers to use the additionally known Beaufort wind force scale, supplemented with wind pressure values [11]. According to this scale, the normalized value of 45 kgf/m^2 corresponds to 8 points and "very strong wind" with a speed of 18 – 20 m/s. At the same time, judging by the Beaufort scale, during storms and hurricanes (9 – 12 points), the wind speed and the corresponding wind pressure can be much higher. It should be noted that the first codes already took into account the increase in wind load with height, the impact of the protection of buildings and the nature of the flow around buildings of different configurations.

Over the next ninety years, the design codes of building structures regarding the standardization of wind loads have undergone significant changes and expanded their statistical bases. Territorial wind zoning has been developed, the number of wind regions has increased. In particular, according to the current DBN V.1.2-2:2006 "Loads and loadings", the characteristic value of wind pressure W_0 is equal to the average (static) component of wind pressure at a height of 10 m above the ground surface, which can be exceeded, unlike SNiP, on average once in 50 years (similar to Eurocode standards). The characteristic value of wind pressure W_0 is determined depending on the wind region according to a map or tabular appendix. It should be noted that the wind zoning of the territory of Ukraine according to the DBN takes into account significant territorial variability of wind load, which is noticeably different from its overly generalized standardization of SNiP, according to which almost the entire territory of Ukraine was classified as II (normative load W_0 = 0.3 kPa, design load 0.42 kPa) and III (W_0 = 0.38 kPa, design load 0.53 kPa) wind regions. A more detailed territorial zoning of Ukraine by characteristic values of wind load includes five territorial regions with characteristic values from 0.4 to 0.6 kPa. The lowest values of wind load are observed in the central and northwestern regions of Ukraine, as well as in Transcarpathia. Large wind loads are realized in the Carpathians, Precarpathian and coastal regions. Territorial zoning of Ukraine by characteristic values of wind pressure was performed according to the method developed by V.A. Pashinsky [9]. A probabilistic model of a non-stationary normal random field was used, the ordinates of which were the values of the loads of individual weather stations located at distances of 30…60 km. The smoothing procedure made it possible to obtain a smooth surface of the mathematical expectation of the wind load, free from random fluctuations of the data of individual weather stations. Region values of the design wind load were set so that the excess reserves of the territorial zoning were minimal.

Comparison of wind zoning according to DBN with SNiP reveals a relatively small difference in the calculated velocity pressures. In the central regions, Crimea, Lviv, Odessa, Kherson and Luhansk, the wind load is lower than in the SNiP. In the Azov region, on the contrary, the wind load is much higher. On average in Ukraine, zoning according to the DBN underestimates the wind load by 4%. At the same time, for 34% of observation points, wind load is underestimated by 15…25%, and for 12% of points, it is increased by 25…65%.

Stages of crane loads normalization. The beginning of domestic standardization of crane loads was laid in 1931 with the introduction of the "Uniform codes of construction design" [2]. Due to the fact that at that time the relevant experimental works were not carried out, the basis of the adopted standards were foreign codes, works of crane operators and reference publications, for example [6].

The horizontal loads transmitted from the cranes to the crane tracks and directed along the building were determined as

$$H = 0{,}1Pn \quad (4)$$

where P is the calculated vertical pressure on the crane wheel; n is the number of brake crane wheels located on the crane beam.

At the same time, the values of forces of normal intensity were taken to be equal to 0.5 of the values obtained by formula (4) (obviously, this was the first attempt to take into account the mode of operation of bridge cranes).

The transverse crane load was taken as that created by braking of cart with a cargo, and was determined by the formula

$$T = \frac{0{,}1(Q+q)n}{n_0} \quad (5)$$

where Q is the weight of the cargo; q – cart weight; n_0 – the number of all wheels of the crane; n is the number of brake wheels of the crane.

This effort was distributed between the crane beams in proportion to their lateral stiffnesses.

Formulas (4) and (5) take into account that the friction force F is equal to the normal pressure N multiplied by the coefficient of friction between the rails and the wheels of the crane or cart f , which is equal to 0.1.

For especially fast or slow working cranes, it was allowed to determine horizontal forces using the formula:

$$H = \frac{\sum Q}{10} \cdot \frac{v}{t} \qquad (6)$$

where $\sum Q/10$ is the mass of moving goods (the number 10 in the denominator approximately takes into account $g = 9{,}8\ \text{m/s}^2$); v – the maximum speed of the crane (cart); t – braking time.

Formula (6) was obtained from the condition of equality of the kinetic energy of motion and the work of the force H. For increasing speed according to the law of the triangle, this formula determines the average value of the force, which is equal to half of the maximum instantaneous force H_{max}, which is detected during braking. In subsequent editions of the codes, formula (6) was deleted.

In subsequent years, the crane load codes were gradually changed [12], but only in 2006, in the national standards DBN V.1.2-2:2006 “Loads and loadings”, the erroneous braking force formula (5) was replaced by the formulas for lateral forces caused by skewing of bridge cranes and non-parallelism of crane tracks. Lateral forces are regulated separately for four-wheeled cranes of small lifting capacity, prone to skewing during movement. For these bridge cranes, the lateral force formula has the following form:

$$H_{\kappa} = 0{,}1F_{\max} + \alpha(F_{\max} - F_{\min})\frac{L_{cr}}{B} \qquad (7)$$

where $F_{\max}$ and $F_{\min}$ are the wheel pressures of greater and less loaded side of the crane; L_{cr}, B are the span and base of the crane; α is a coefficient equal to 0.01 for cranes with a separate drive of the movement mechanism and 0.03 for cranes with a central drive.

In the above formula, the first term gives the transverse force from the wheel skew, the second term gives the horizontal component on the wheel flange, which limits the skew of the bridge. This formula provides a fairly close match with the experimental values [12].

The lateral forces H_k, calculated by formula (7), can be applied:

• to the wheels of one side of the crane and directed in different directions (inside or outside the span of the building under consideration), which corresponds to the limitation of the crane skew by the wheels of one side;

• to the wheels along the diagonal of the crane and also directed in different directions (inside or outside the span of the building under consideration), which corresponds to the case of limiting the crane skew by the wheels located along the diagonal of the crane.

In this case, forces equal to $0{,}1F^n_{\max}$ ($0{,}1F^n_{\min}$) , directed in the most unfavorable direction (inside or outside the span under consideration), are applied to the other wheels.

For multi-wheel cranes with a large load capacity, not prone to skewing during movement, a new lateral force standard has been introduced based on the results of many years of testing of such cranes. The characteristic value of the lateral force on the wheel of multi-wheel cranes with flexible load suspension is taken as 0.1 of the vertical load on the wheel, calculated under the condition that the trolley with a load equal to the crane's rated load capacity is located in the middle of the bridge. The following formula can be used in this case:

$$H^n_k = 0{,}1\left(G_M + G_B + Q\right)/2n_0 \qquad (8)$$

where G_M is the weight of the crane bridge; G_B is the weight of the trolley; Q is the lifting capacity of the bridge crane; n_0 is the number of wheels on one side of the crane.

For multi-wheel cranes with rigid suspension of the load, a characteristic lateral force H^n_k is taken equal to 0.1 of the maximum vertical load on the wheel. When determining the characteristic values H^n_k, it is taken into account that the lateral forces from two multi-wheel cranes are transmitted to both sides of the crane track. On each side of the crane, the lateral forces have one direction – outward or inward, on different tracks they are directed in opposite directions (both inward or both outward). On one of the tracks, the full lateral force is taken, on the other track, half of the lateral force is applied.

The consequences of implementing the recommendations of DBN V.1.2-2:2006 “Loads and loadings” in terms of bridge crane loads [2] were analysed. It was found that the horizontal loads on the wheel of four-wheel bridge cranes determined according to DBN were 1.3…9.6 times higher than the loads calculated according to SNiP. When determining the force effects of four-wheel bridge cranes according to DBN, the bending moments in the columns of the transverse frames of one-story industrial buildings (OIB) from lateral forces increase by 1.9…6.9 times, compared with the efforts from braking forces according to SNiP, and the bending moments in the structures of crane beams increase by 1.2…7.8 times. As a result, there is a slight increase in the material consumption of crane beams, which is on average 1.1%, as well as a detected increase of up to 24% in the material consumption of crane parts of columns of buildings equipped with four-wheel cranes.

Under the conditions of action on the structures of multi-wheel overhead cranes, the loads on the wheel of multi-wheel cranes according to DBN exceed the loads according to SNiP by 1.3…1.7 times. It was found that

the bending moments in the transverse frames increase by 1.1…1.2 times and up to 1.6 times in the crane beams. Based on the tests of the bearing capacity of the structures of the OIB, it was established that in the case of equipping buildings with multi-wheel overhead cranes, the transition to determining the loads according to DBN does not lead to an increase in the material consumption of the structures of the crane beams and columns.

To neutralize the consequences of the introduction of load standards into the practice of design, it is recommended to use such a reserve of steel frames of the OIB as the spatial work of the frames. It has been established that taking into account the effect of spatial work of frames in the calculation of transverse frames of the OIB for combinations of loads allows to approximate the results of calculations of frames for loads according to SNiP 2.01.07-85 and avoid additional material consumption.

Conclusions.

It is shown how, during the last ninety years, the design codes of building structures regarding the normalization of loads have significant changes and expanded their statistical bases. Territorial snow and wind zoning has been developed, the number of regions on the territory of Ukraine has increased. The normalization of crane loads has been significantly changed, especially in the part of lateral forces of bridge cranes. The substantiation of normative (characteristic) and calculated values of climatic and crane loads based on an increased recurrence period has been modified. The high scientific level of codes DBN B.1.2-2006 "Loads and loadings" was noted, which have a modern statistical basis, are associated with Eurocode codes and ensure the required level of reliability of building structures

References

1. Баженов В.А., Ворона Ю.В., Перельмутер А.В. (2016). Будівельна механіка і теорія споруд. Нариси з історії. К.: Каравела. ISBN 978-966-222-968-8/

2. Пічугін С.Ф. (2024). Етапи розвитку загальної методики розрахунку будівельних конструкцій. Полтава: ТОВ «АСМІ». ISBN 978-966-182-699-0

3. Elishakoff I. (1999). Probabilistic Theory of Structures. New York: Dover Publications

4.Truesdell C.A. (1968). Essays in the History of Mechanics. Berlin: Springer Verlag

5. Де-Рошефор Н.І. (1916). Урочне положення. Шосте виправлене видання. Петроград: Видання К.Л. Раккера.

6. HŰTTE. (1935). Довідник для інженерів, техніків і студентів. Том другий. П'ятнадцяте видання (переклад з 26-го німецького видання). М.: Держмашметвидав.

7. Перельмутер А.В., Пічугін С.Ф. (2024). Метод граничних станів. Загальні положення та застосування в нормах проєктування. К.: «Софія-А». ISBN 978-617-8382-12-4

8. Пічугін СФ. (2016). Розрахунок надійності будівельних конструкцій. Полтава: ТОВ «АСМІ», ISBN 978-966-182-418-8

9. Пашинський В.А. (1999). Атмосферні навантаження на будівельні конструкції для території України. К.: УкрНДІПСК,

10. Pichugin Sergii. (2020). Probabilistic basis development of standartization of snow loads on building structures. Industrial Machine Building, Civil Engineering, 2(55). 5-14.
https://doi.org/10.26906/znp.2020.55.2335

11. Pichugin Sergii. (2021). Many years of experience of standarding the medium component of wind load on building structures. Industrial Machine Building, Civil Engineering. 2 (57). 5-13.
https://doi.org/10.26906/znp.2021.57.2579

12. Pichugin Sergii. (2021). Development of crane load codes on the basis of experimental research. Industrial Machine Building, Civil Engineering. 1 (56). 18-29.
https://doi.org/10.26906/znp.2021.56.2493

1. Bazhenov V.A. Vorona Y.V., Perelmuter A.V. (2016). *Construction mechanics and theory of buildings*. *Essays on history*. K.:Caravela. ISBN 978-966-222-968-8

2. Pichugin S.F. (2024). *Development stages of general methodology for building structure calculation.* Poltava: TOV "ASMI". ISBN 978-966-182-699-0

3. Elishakoff I. (1999). *Probabilistic Theory of Structures*. New York: Dover Publications

4.Truesdell C.A. (1968). *Essays in the History of Mechanics*. Berlin: Springer Verlag

5. De Rochefort N.I. (1916). *Urgent position*. Sixth revised edition. Petrograd: K. L. Rakker Edition.

6. HŰTTE. (1935). *Handbook for engineers, technicians and students*. Volume 2. Fifteenth edition (translated from the 26th German edition). M.: Gosmashmetizdat

7. Perelmuter A.V., Pichugin S.F. (2024). *Method of limit states. General provisions and application in design codes*. K.: "Sofia-A" ISBN 978-617-8382-12-4

8. Pichugin S.F. (2016). *Reliability calculation of building structures*. Poltava: TOV "ASMI" ISBN 978-966-182-418-8

9. Pashynskyi V.A. (1999). *Atmospheric loads on building structures for the territory of Ukraine*. K.: UkrNDIPSK

10. Pichugin Sergii. (2020). Probabilistic basis development of standartization of snow loads on building structures. *Industrial Machine Building, Civil Engineering,* 2(55). 5-14.
https://doi.org/10.26906/znp.2020.55.2335

11. Pichugin Sergii. (2021). Many years of experience of standarding the medium component of wind load on building structures. *Industrial Machine Building, Civil Engineering.* 2 (57). 5-13.
https://doi.org/10.26906/znp.2021.57.2579

12. Pichugin Sergii. (2021). Development of crane load codes on the basis of experimental research. *Industrial Machine Building, Civil Engineering.* 1 (56). 18-29.
https://doi.org/10.26906/znp.2021.56.2493

Sergii Pichugin
Національний університет «Полтавська політехніка імені Юрія Кондратюка»
https://orcid.org/0000-0001-8505-2130

Аналіз тенденцій розвитку норм навантажень на будівельні конструкції

У статті послідовно розглянуті підходи до врахування навантажень на будівельні конструкцій та їхнє відображення у нормативних документах різних років. Зосереджено увагу на спадкоємність методу граничних станів і методу допустимих напружень у частині опису навантажень. Показано, як протягом останніх дев'яноста років норми проектування будівельних конструкцій щодо нормування навантажень зазнали значних змін і розширили свої статистичні основи. Перші рекомендації, що містилися в Урочному положенні, із запасом враховували снігове навантаження на основній території країни. Початкове нормування вітрового навантаження регламентувало однаковий вітровий тиск для всіх місцевостей. З роками стосовно кліматичних навантажень (снігових, вітрових) приділялась увага змінам територіального районування (кількість районів на території України було збільшено) та розрахункових коефіцієнтів, призначенню нормативних і розрахункових значень та залученню до цього дослідних статистичних даних. Приділено також увагу зв’язку розвитку норм кранових навантажень з результатами експериментальних досліджень цих навантажень. Норми кранових навантажень поступово змінювали, але тільки у 2006 р в національних нормах ДБН В.1.2-2:2006 «Навантаження і впливи» помилкову формулу гальмівних сил було замінено на формулу бічних сил, що спричиняються перекосами мостових кранів і непаралельністю кранових колій. Модифіковано обґрунтування нормативних (характеристичних) та розрахункових значень кліматичних і кранових навантажень на основі збільшеного періоду повторюваності. Вітчизняні дослідження навантажень активізувалися останні десятиліття у зв’язку із впровадженням Державних будівельних норм України. Відзначено високий науковий рівень вітчизняних норм ДБН В.1.2-2006 «Навантаження та впливи», які мають сучасний статистичний базис, асоціюються з нормами Єврокод та забезпечують необхідний рівень надійності будівельних конструкцій.

Ключові слова: надійність, норми проєктування, граничні стани, снігове навантаження, вітрове навантаження, кранове навантаження

*Адреса для листування E-mail: pichugin.sf@gmail.com

Збірник наукових праць. Галузеве машинобудування, будівництво
Academic journal. Industrial Machine Building, Civil Engineering
http://journals.nupp.edu.ua/znp
https://doi.org/10.26906/znp.2024.63.3881

UDC 627.824.2/3

Volodymyr Shapoval *
Dnipro University of Technology
https://orcid.org/0000-0003-2993-1311

Valerii Shuminskyi
SE "State Research Institute Of Building Constructions"
https://orcid.org/0000-0002-8751-1983

Oleksandr Skobenko
Dnipro University of Technology
https://orcid.org/0000-0002-8122-6583

Volodymyr Konoval
Cherkasy National Technological University
https://orcid.org/0000-0002-6740-6617

Determination of settlement profiles of foundations composed of weak soils for railway and road embankments, dams, and levees made of earth materials

The article is dedicated to the issue of foundation settlements in railway, road, and other embankments, as well as earth dams and dikes, especially when constructed on weak soils with low deformation modulus. It emphasizes that in such cases, settlements can be comparable to the height of the embankment, requiring settlement profiles to be considered during design. A simple iterative algorithm developed by the authors is proposed for calculating settlement profiles and is recommended for inclusion in the draft Ukrainian State Building Code "Earth Dams. General Requirements." An example of the algorithm's application is provided, demonstrating its advantages over conventional graphical and tabular methods. The algorithm ensures simplicity, fast convergence, and results consistent with those obtained using the finite element method. Additionally, the study highlights the limitations of FEM when regulatory guidance on key parameters such as boundary conditions and mesh configuration is lacking. The authors conclude that their proposed algorithm can be effectively implemented in engineering practice for the design of embankments and dams on weak soils with a trapezoidal cross-section.

Keywords: earth dams, embankments, foundation settlement, long embankment, trapezoidal embankment, weak foundation soils, plane strain condition, compressed soil depth, settlement profile, material volume for embankment on weak soils

*Corresponding author E-mail: shapvv27@gmail.com

Introduction

The determination of settlements of foundations for railway, highway, and other embankments, as well as for earth dams and levees during their design, construction, and operation is a mandatory procedure [1, 2].

If the foundation consists of soils with a low modulus of overall deformation (such as silts, peats, peaty soils, and similar types), it is necessary not only to determine the average settlement and differential settlement (as is typically done for conventional foundations), but also to determine the settlement profiles. This requirement arises because, in such cases, the settlement values can be of the same order of magnitude as the height of the embankment, dam, or levee. Therefore, when calculating the volume of earth material required for constructing such structures, these settlements must be taken into account. Accordingly, it becomes necessary to construct settlement profiles both within the embankment body and beyond its boundaries [1, 2, 3, 4, 5].

This article presents an example of the application of an algorithm we developed for the Ukrainian State Building Code (DSTU XXXX:202X "Earth Dams. General Requirements") to calculate settlement profiles of railway, highway, and other embankments, as well as earth dams and levees [6]. The theoretical background of the settlement calculation algorithm presented in [6] is described in detail in works [7] and [8].

Methods.

Theoretical investigation of geomechanical processes using analytical and numerical mathematical methods. Analysis and generalization of the results of theoretical studies.

Results.

A simple algorithm has been developed to determine the required volume of material for the construction of embankments (dams and levees) made of earth materials when founded on weak soils. The algorithm is based on a simple iterative process.

Scientific novelty.

It has been shown that a simple iterative process can be applied to determine the theoretical volume of material required for the construction of embankments (dams and levees) made of earth materials.

Practical significance.

The main practical outcome of this study is the development of a method for calculating the volume of material required to achieve the design profile of an embankment (dam or levee) built on weak soils.

Review of achievements in this field.

To determine the settlements of dams (including those constructed from earth materials), the current building codes in force in Ukraine use either the graphical-analytical method (which provides only approximate results), or a tabular method (in which settlements can be calculated only along a vertical line passing either through the center or the corner of a rectangular area loaded with uniformly distributed pressure) [1, 2, 3, 4, 5]. These data are clearly insufficient for constructing the settlement profile of the base of an embankment (dam or levee). Therefore, the algorithm proposed in [6] for calculating the settlements of embankments and earth dams or levees is considered in more detail.

The settlement of the foundation of an earth embankment (dam or levee) along a computational vertical line S_j, which passes through a point x_j (see Fig. 1), should be calculated using the formulas proposed in [6]:

$$\left.\begin{aligned} S_j &= 0,8 \cdot \sum\nolimits_{(i=1)}^{n} S_i(x_j); \\ S_i(x_j) &= \frac{W(x_j, z_{i+1}) - W(x_j, z_i)}{E_i} \end{aligned}\right\}, \qquad (1)$$

where: S_j – is the settlement of the embankment (dam or levee) base along the computational vertical located at a horizontal distance x_j from the left edge of the structure (i.e., the origin of coordinates; see Fig. 1); $\beta = 0,8$; $S_i(x_j)$ – is the settlement of the i-th layer of the foundation with thickness $h_i = z_{i+1} - z_i$, whose top is at depth z_i and bottom at depth z_{i+1}; $W(x,z)$ – is the vertical displacement of the foundation at point with coordinates *x* (horizontal) and z (vertical); $W(x_j, z_i)$ *ma* $W(x_j, z_{i+1})$ – are, respectively, the displacements at the top and bottom of the i-th soil layer in the foundation with deformation modulus E_i.

The displacement of the foundation $W(x,z)$ at the calculation depth z should be determined using formulas specified in Eq. 1.

$$\left.\begin{aligned} &W(x,z) = k_1 \cdot (\xi_1 + \xi_2 + \xi_3 + \xi_4 + \xi_5 + \xi_6 + \xi_7 + \xi_8 + \xi_9 + \xi_{10} + \xi_{11} + \xi_{12}) \\ &k_1 = \frac{\gamma_c \cdot h}{2\pi \cdot L_1 \cdot y_4};\ y_1 = -L_1 - b_1 + x_j;\ y_2 = -L_1 + x_j;\ y_3 = b + x_j;\ y_4 = b - L_1 - b_1; \\ &\xi_1 = -L_1 \cdot y_1^2 \cdot \ln(y_1^2 + z^2);\quad \xi_2 = -y_2^2 \cdot y_4 \cdot \ln(y_2^2 + z^2);\quad \xi_3 = L_1 \cdot y_3^2 \cdot \ln(y_3^2 + z^2); \\ &\xi_4 = -2 \cdot z \cdot L_1 \cdot y_1 \cdot arctg\left(\frac{y_1}{z}\right);\quad \xi_5 = -2 \cdot z \cdot y_2 \cdot y_4 \cdot arctg\left(\frac{y_4}{z}\right);\quad \xi_6 = 2 \cdot z \cdot L_1 \cdot y_3 \cdot arctg\left(\frac{y_3}{z}\right); \\ &\xi_7 = x_j^2 \cdot y_4 \cdot \ln(x_j^2 + z^2);\quad \xi_8 = 2 \cdot x_j \cdot z \cdot y_4 \cdot arctg\left(\frac{x_j}{z}\right);\quad \xi_9 = 2 \cdot L_1 \cdot y_1^2 \cdot \ln(-y_1); \\ &\xi_{10} = 2 \cdot y_2^2 \cdot y_4 \cdot \ln(-y_2);\qquad \xi_{11} = 2 \cdot L_1 \cdot y_3^2 \cdot \ln(y_3);\qquad \xi_{12} = 2 \cdot x_j^2 \cdot y_4 \cdot \ln(x_j). \end{aligned}\right\} \qquad (2)$$

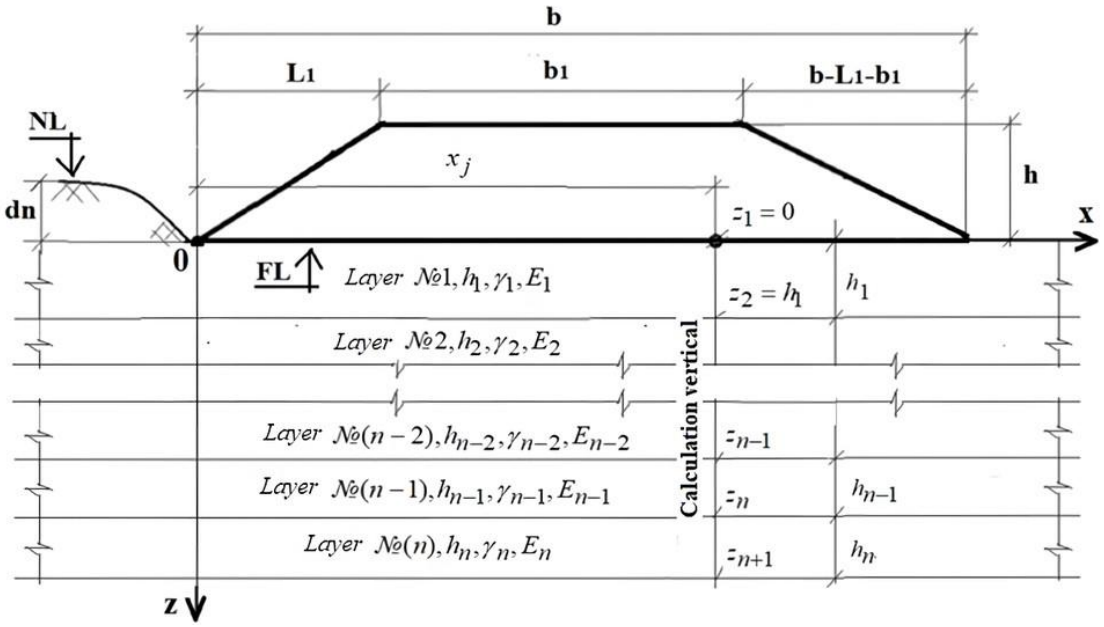

Figure 1 – Scheme for Determining the Settlements of the Foundation of an Earth Dam (Embankment or Dike): if the distance $x_j < 0$ or $x_j > b$, then the calculated vertical lies outside the base of the dam (embankment or dike); $E_{1...n}$; $\gamma_{1...n}$ – deformation moduli and densities of the 1 to n soil layers, respectively.

The additional vertical stresses at the foundation from the dam (embankment or dike) weight $\sigma_{zp}(z)$, required to determine the lower boundary of the compressible stratum along the calculated vertical at position x_j , should be determined using the following expression:

$$\sigma_{zr}(z) = \frac{2 \cdot \gamma_c \cdot h}{\pi(b - b_1)} \times \times \left[b \cdot arctan\left(\frac{b}{2z}\right) - b_1 \cdot arctan\left(\frac{b_1}{2z}\right) \right], \quad (3)$$

where: d_n, h, b, b_1 and L_1 are the geometric parameters of the dam (embankment or dike) as shown in Figure 1; γ_c is the unit weight of the dam (embankment or dike) material; if the calculated depth z=0, then in formulas (2) and (3), use z=0.0001 m.

Eqs. (1), (2) and (3) allow determining settlements of the foundation both within and beyond the base of a homogeneous dam (embankment or dike, see Figure 1).

Settlement Calculation Procedure

1. Determine the Design Location of the Calculation Vertical Line – usually specified in the design brief. The calculation vertical can be located either within or beyond the dam base.

2. Calculate the Foundation Settlement S_j at the vertical position x_j using Eqs. (1) and (2).

3. Determine the Depth of the Compressible Layer H_{st}, which satisfies the condition:

$$\sigma_{zr}(0, H_{st}) = k \cdot \sigma_{zq}(x_j, H_{st}), \quad (4)$$

where: k=0.2 for $b \leq 5$ m; k=0.5 for $b > 20$ m; for $5 < b \leq 20$ m, use linear interpolation. $\sigma_{zp}(0, H_{st})$ – the additional vertical stress from the dam weight (use Eq. 3); $\sigma_{zq}(0, H_{st})$ – the vertical stress from soil weight, calculated as:

$$\left.\begin{aligned} \sigma_{zq}(0, H_{st}) &= \gamma' \cdot d_n + \sum_{i=1}^{n} \gamma_i \cdot h_i; \\ H_{st} &= d_n + \sum_{i=1}^{n} h_i \end{aligned}\right\} \quad (5)$$

where: γ' denotes the density of the soil located above the base of the dam (embankment or levee); γ_i and h_i represent, respectively, the density and thickness of the i-th soil layer; d_n – see explanation in Figure 1.

4. If the point at which the stresses from the self-weight of the soil are calculated is located below the groundwater level, then instead of γ_i, the density of the soil in a submerged state should be adopted. This density is determined according to the expression:

$$\gamma_{sb,i} = \frac{\gamma_{s,i} - \gamma_w}{1 + e_i} \quad (6)$$

where: $\gamma_{s,i}$ is the density of soil particles; γ_w is the density of water; e_i is the soil porosity ratio; i – denotes the number of the elementary soil layer.

Features of Settlement Calculation for Dike Foundations Composed of Weak Soils

1. When calculating settlements of foundations composed of weak soils, it is recommended to take into account the fact that the settlements may be of the same order of magnitude as the dimensions of the dike. In addition, it is necessary to consider the significant nonlinearity of the deformation and strength properties of the foundation under external loading.

2. The task of the calculation is to determine such a filling contour that, when settlements of the foundation are considered, the dike contour coincides with the design one.

3. For calculation purposes, it is recommended to adopt the standard values of the deformation properties of the foundation soil.

4. The computational domain should be defined as follows: vertically, down to the lower boundary of the compressed stratum, which should be determined either according to the requirements of the recommended Annex D of DBN V.2.1-10, or to the upper boundary of the rigid underlying soil (e.g., rock or coarse-grained deposits); horizontally −5-b, where b is the dike width.

The calculation is recommended to be performed using the method of successive approximations (iterations) in the following sequence:

5.1. First, the load on the foundation from the dike with design dimensions is determined.

5.2. Then, using formulas (1)…(5), the settlements of the foundation are calculated.

5.3. If the settlements exceed the design value, the calculated settlement values are added to the coordinates of the design contour.

5.4. The load on the foundation from the dike with the contour established according to Step 3 is determined, and settlements are recalculated in the second approximation.

5.5. The process is repeated until the filling contour, adjusted for foundation settlements, does not differ from the design contour by more than a predetermined value (this parameter should be specified in the project technical assignment).

To illustrate the application of the proposed settlement calculation algorithm, the filling contour for the dike shown in Fig. 2 was determined with consideration of soil foundation settlements. The properties of the soil layers underlying the dam are presented in Table 1. The groundwater level is located at a depth of 2 m. The unit weight of the dam body is $\gamma = 18$ kN/m³. The soil foundation consists of weak soil underlain by bedrock. All further calculations were performed using the "MAPLE-2021" software package, which is freely available.

An identical example was also considered by the authors of study [9].

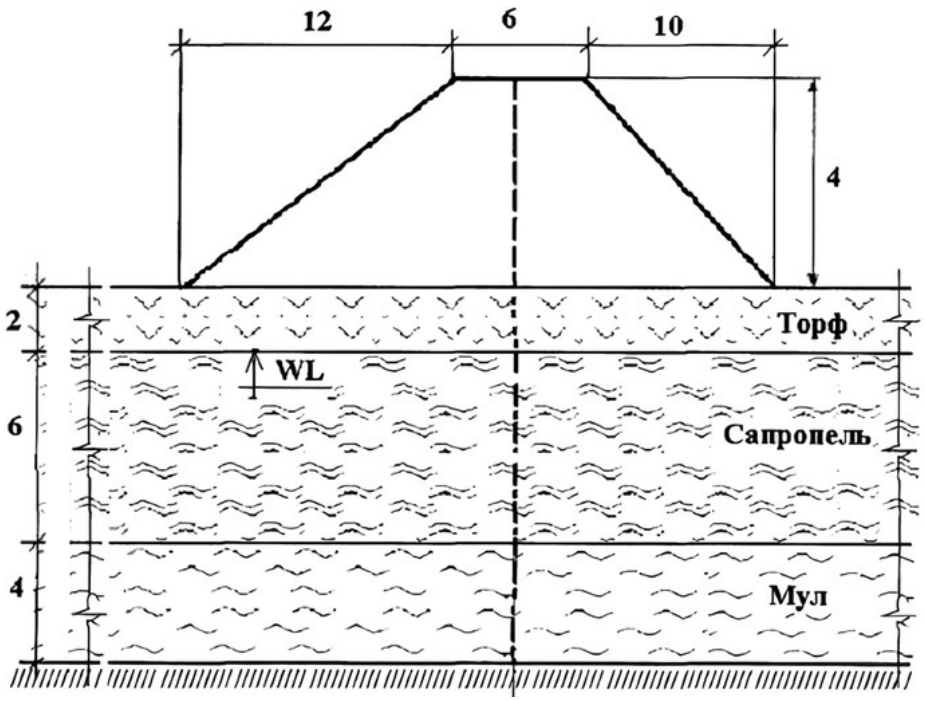

Figure 2 – Computational scheme of the dam

In the first approximation, the load on the foundation was assumed to correspond to row 1 in Fig. 3. This load results in settlements (Fig. 4, row 1) and the dam profile shown in Fig. 5 (row 1). The volume of material required for the construction of 1 linear meter of the embankment amounts: $\frac{6+28}{2} \cdot 4 \cdot 1 = 60 м^3$..

In the second approximation, the load on the foundation was assumed to correspond to row 2 in Figure 3. This load results in settlements (Fig. 4, row 2) and the dam profile shown in Figure 5 (row 2). The volume of material required for the construction of 1 linear meter of the embankment amounts: $\frac{6+28}{2} \cdot 4,85 \cdot 1 = 72,75 м^3$.

Table 1 – Properties of soil layers of the dam base

№	Soil name	Distance from the surface, m	Soil moisture, %	Density of soil particles, kN/m^3	Soil density, kN/m^3	Density of dry soil, kN/m^3	Porosity coefficient, p.u.	Modulus of total deformation, kPa
1	Low-moisture peat	0-2	55	16,30	8,57	13,29	0,901	330
2	Organomineral sapropel	2-6	62	15,5	7,95	12,87	0,951	500
3	Clay silt	6-10	57	2,55	16,01	25,13	0,593	3600
4	Rock	Unlimited	0-2	-	27,2	-	-	$78 \cdot 10^6$

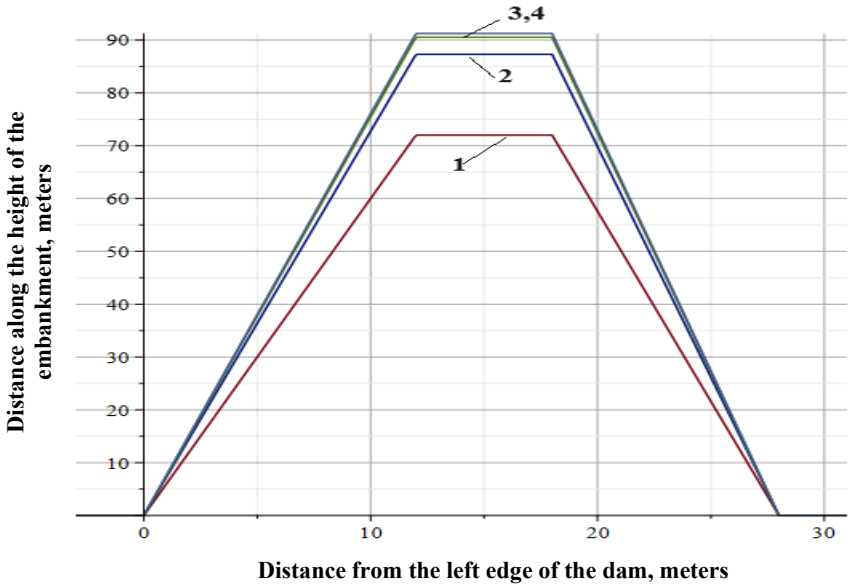

Figure 3 – Loading on the dam foundation.
Row 1 – load assumed in the first approximation; Row 2 – the same, in the second approximation;
Row 3 – the same, in the third approximation; Row 4 – the same, in the fourth approximation.
Note: rows 3 and 4 coincide.

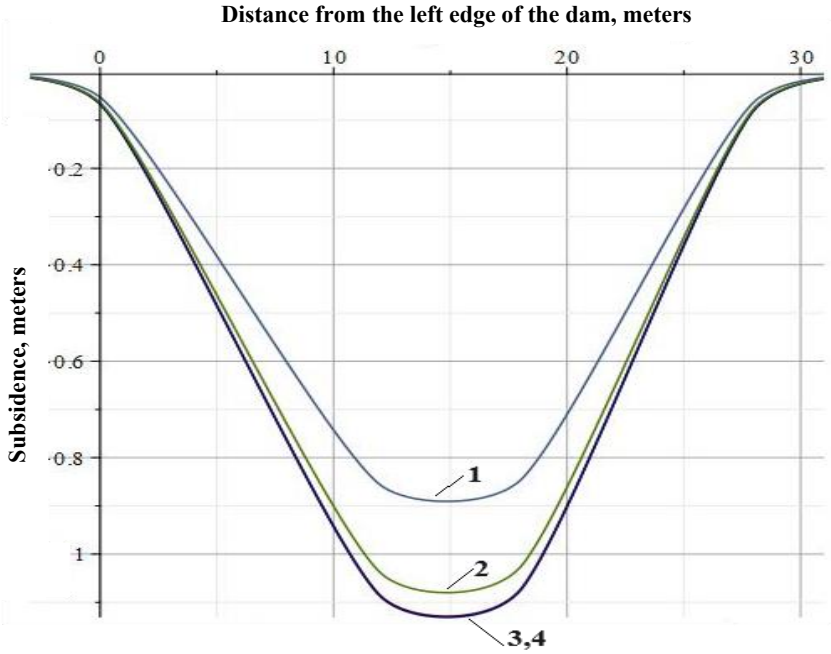

Figure 4 – Settlements of the dam foundation:
Row 1 – settlement calculated in the first approximation; Row 2 – the same, in the second approximation;
Row 3 – the same, in the third approximation; Row 4 – the same, in the fourth approximation.
Note: rows 3 and 4 coincide.

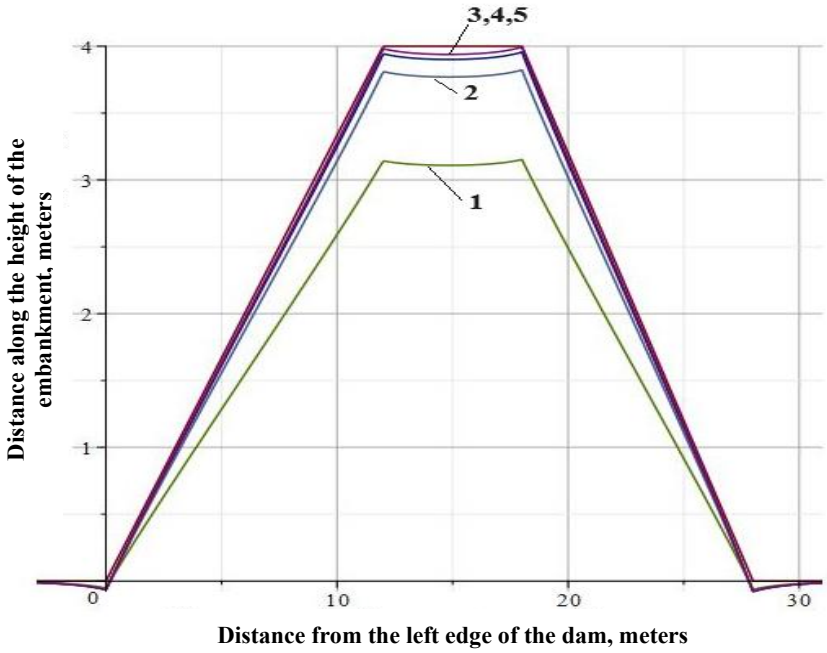

Figure 5 – Settlements of the dam foundation:
Row 1 – settlement calculated in the first approximation; Row 2 – the same, in the second approximation;
Row 3 – the same, in the third approximation; Row 4 – the same, in the fourth approximation.
Note: rows 3 and 4 coincide.

In the third approximation, the foundation loading corresponding to row 3 in Figure 3 was adopted. This loading corresponds to the settlements (Fig. 4, row 3) and the dam contour shown in Fig. 5 (row 3). The volume of material required for the construction of 1 linear meter of the dam is equal to 76.05 m³.

In the fourth approximation, the foundation loading corresponding to row 4 in Figure 3 was adopted. This loading corresponds to the settlements (Fig. 4, row 4) and the dam contour presented in Fig. 5 (row 4). The volume of material required for the construction of 1 linear meter of the dam is equal to 76.20 m³.

Thus, the volumes of material required for the construction of one linear meter of the dam, calculated in the third and fourth approximations, differ by only 0.2%. This result should be considered satisfactory and entirely acceptable for further development of the technical part of the dam construction project.

Moreover, according to the obtained calculation results, in order to ensure the design profile of the dam, it is necessary to use 76.20 m³ of soil instead of 60 m³ (the latter figure was obtained without accounting for foundation settlements). The difference between these values is 27%. This result is fully suitable for further development of the organizational-technological, economic, and cost-estimation parts of the dam construction project.

Conclusions

The research results presented in this paper allow us to draw the following conclusions:

1. Using a specific example, it has been demonstrated that the proposed algorithm for calculating the settlement profiles of railway, highway, and other embankments, as well as earth dams with a trapezoidal cross-section, is sufficiently simple and convenient to apply. Therefore, it can undoubtedly be incorporated into the Ukrainian State Standards (DSTU XXXX:202X “Earth Dams. General Requirements”).

2. It has been shown that the proposed algorithm for calculating dam and embankment settlements on weak soil foundations, which is based on an iterative process, is both straightforward to use and exhibits rapid convergence.

3. The obtained results show good agreement with the data presented in [9], which were derived when solving an identical problem using the finite element method [10]. However, the data obtained by the authors of [9] compared to those in the present study have the following drawbacks:

3.1. The calculated settlement profiles, load distributions, and dam profiles appear not as continuous but as broken lines (a drawback inherently associated with the finite element method).

3.2. The current regulatory documents in force in Ukraine provide no answers to several critical questions arising when applying the finite element method to the calculation of settlements of earth dams and embankments [10]:

3.2.1. What should be the dimensions of the computational foundation domain?

3.2.2. What should be the boundary conditions for the computational foundation domain?

3.2.3. What should be the dimensions and configuration of the finite elements?

All of the above allows us to conclude that the algorithms for determining settlements of embankments and dams made of soil materials

proposed in this study can be widely applied in the design of embankments and dams with trapezoidal cross-sections.

References

1.ДБН В.2.4-20:2014. (2014). *Греблі з ґрунтових матеріалів. Основні положення*.

2.Кирієнко, І. І., & Хімерік, Ю. А. (1987). *Гідротехнічні споруди. Проектування та розрахунок: навчальний посібник.* Київ: Вища школа.

3.ДБН В.2.1-10:2009. (2009). *Основи та фундаменти споруд. Основні положення проектування*.

*4.*ДБН В.2.1-10:2019. (2019). *Основи та фундаменти споруд. Основні положення проектування.*

5.ДСТУ-Н Б В.1.1-38:2016. (2016). *Настанова щодо інженерного захисту територій, будівель і споруд від підтоплення та затоплення.*

6.Шаповал, В. Г., Шумінський, В. Д., Скобенко, О. В., & Кулівар, В. В. (2024). *Розрахунок осідань основ гребель із ґрунтових матеріалів.* У *Матеріали регіональної науково-практичної конференції до Всесвітнього дня води* (с. 101–103). Дніпро: ДДАЕУ.

7.Шаповал, В., Шашенко, О., Скобенко, О., Гапєєв, С., & Коновал, В. (2022). *Напружено-деформований стан основ гребель із ґрунтового матеріалу з трапецеїдальним поперечним профілем.* У *Scientific foundations for research in engineering: collective monograph* (с. 646–660). Boston: Primedia eLaunch.

8.Shapoval, V. H., Pavluchenko, A. V., Shuminskys, V. D., Skobenko, O. V., & Barsukova, S. O. (2023*). Stressed-deformed state of dam foundation made of soil material with a trapezoidal transverse profile*. In *Scientific research in engineering: collective monograph* (pp. 212–227). Petrosani, Romania: UNIVERSITAS Publishing.

9.ДСТУ-Н Б В.1.1-38:2016. (2016). *Настанова щодо інженерного захисту територій, будівель і споруд від підтоплення та затоплення*

10. Shapoval, V., Shashenko, O., Skobenko, O., Konoval, V., & Shuminskyi, V. (2024). *Technical, agricultural and physical sciences as the main human sciences*. In *Collective monograph.* Boston: Primedia eLaunch, International Science Group (pp. 91–107)

1. DBN V.2.4-20:2014. (2014). *Earth dams. Main provisions*

2. Kirienko, I. I., & Khimerik, Yu. A. (1987). *Hydraulic structures: Design and calculation: Textbook*. Kyiv: Vyscha Shkola.

3. DBN V.2.1-10:2009. (2009). *Bases and foundations of structures. Design provisions.*

4. DBN V.2.1-10:2019. (2019). *Bases and foundations of structures. Design provisions.*

5. DSTU-N B V.1.1-38:2016. (2016). *Guideline for engineering protection of territories, buildings, and structures against flooding.*

6. Shapoval, V. H., Shuminskyi, V. D., Skobenko, O. V., & Kulivar, V. V. (2024). *Settlement calculation of earth dam foundations.* In *Materials of regional scientific-practical conference dedicated to World Water Day* (pp. 101–103). Dnipro: DDAEU.

7. Shapoval, V., Shashenko, O., Skobenko, O., Gapeev, S., & Konoval, V. (2022*). Stressed-deformed state of dam foundations made of soil material with trapezoidal transverse profile*. In *Scientific foundations for research in engineering: Collective monograph* (pp. 646–660). Boston: Primedia eLaunch.

8. Shapoval, V. H., Pavluchenko, A. V., Shuminskys, V. D., Skobenko, O. V., & Barsukova, S. O. (2023). *Stressed-deformed state of dam foundation made of soil material with a trapezoidal transverse profile*. In *Scientific research in engineering: Collective monograph* (pp. 212–227). Petrosani, Romania: UNIVERSITAS Publishing.

9. DSTU-N B V.1.1-38:2016. (2016). *Guideline for engineering protection of territories, buildings, and structures against flooding*.

10. Shapoval, V., Shashenko, O., Skobenko, O., Konoval, V., & Shuminskyi, V. (2024). *Technical, agricultural and physical sciences as the main human sciences.* In *Collective monograph* (pp. 91–107). Boston: Primedia eLaunch, International Science Group.

Шаповал В.Г *
Національний технічний університет "Дніпровська політехніка"
https://orcid.org/0000-0003-2993-1311

Шумінський В.Д
ДП «Державний науково-дослідницький інститут будівельних конструкцій»
https://orcid.org/0000-0002-8751-1983

Скобенко О.В.
Національний технічний університет "Дніпровська політехніка"
https://orcid.org/0000-0002-8122-6583

Коновал В.М.
Черкаський державний технологічний університет
https://orcid.org/0000-0002-6740-6617

Визначення профілів осідань складених слабкими ґрунтами основ залізничних та автодорожніх насипів, гребель і дамб із ґрунтових матеріалів

Стаття присвячена проблемі визначення осідань основи залізничних, автодорожніх та інших насипів, а також гребель і дамб із ґрунтових матеріалів, особливо при будівництві на слабких ґрунтах. У таких випадках осідання можуть бути співмірними з висотою насипу, що потребує не лише оцінки середнього осідання, а й побудови повного профілю

осідання у межах споруди та за її межами. У роботі проаналізовано обмеження традиційних методів, передбачених чинними будівельними нормами, зокрема графоаналітичного й табличного, які не забезпечують достатньої точності. Для усунення цих недоліків запропоновано простий ітераційний алгоритм розрахунку профілів осідань. Алгоритм базується на поетапному наближенні та дає змогу розраховувати осідання основ під насипами з трапецеїдальним перерізом. Запропонований підхід демонструє добру збіжність результатів з розрахунками, виконаними методом скінченних елементів, але при цьому не має його недоліків — таких як ламаність профілю та потреба в деталізованих граничних умовах. У статті також обґрунтовано доцільність включення цього алгоритму до проєкту нових ДСТУ щодо проектування гребель з ґрунтових матеріалів. Отримані результати можуть бути використані в інженерній практиці для підвищення точності розрахунків об’ємів матеріалу та формування проектного профілю насипів і гребель на слабких ґрунтах.

Ключові слова: ґрунтові греблі, дамби, осідання основи, довгий насип, трапецієподібна форма насипу, слабкі ґрунти, плоска деформація, глибина стиснення ґрунту, профіль осідання, обсяг матеріалу для насипу на слабких ґрунтах.

*Адреса для листування E-mail: shapvv27@gmail.com

Збірник наукових праць. Галузеве машинобудування, будівництво
Academic journal. Industrial Machine Building, Civil Engineering
http://journals.nupp.edu.ua/znp
https://doi.org/10.26906/znp.2024.63.3880

UDC 556.3

Dmitro Dmitirev *
SE "State Research Institute Of Building Constructions"
https://orcid.org/0000-0003-2993-1311

Olena Perlova
SE "State Research Institute Of Building Constructions"
https://orcid.org/0000-0002-8751-1983

Building drainage in dense urban areas

This article analyzes the specific challenges of constructing underground structures under complex hydrogeological conditions in densely built-up urban environments. The construction of pile foundations, tunnels, utility networks, and underground parking areas often obstructs natural groundwater flow, leading to localized flooding. The underground space of a modern city is saturated with water-bearing utility lines prone to unpredictable leaks. In such cases, it is essential to preserve the existing hydrogeological regime and prevent additional structural deformations of adjacent buildings. Therefore, the regulatory framework for the protection of underground structures must be improved in accordance with contemporary engineering standards.

Keywords: hydrogeological conditions, groundwater level, construction dewatering, filtration coefficient, needle filters.

*Corresponding author E-mail: dmitrievgts71@gmail.com

Introduction

The construction of underground structures (parking lots, bomb shelters, foundations, retaining structures) and utility networks (water, storm water, sewerage, power supply networks, etc.) requires additional measures to protect them from groundwater impact during their construction and operation.

In such cases, hydrogeological conditions and soil filtration properties play a significant role (often a decisive one). New construction sites are often located in dense urban areas. All these factors should be taken into account when designing and performing construction work, as well as during operation.

Review of the latest research sources and publications

Numerous regulatory documents and scientific studies [1÷6] address the issue of groundwater impact on underground structures. It is usually emphasized that during the construction period, various construction dewatering techniques must be applied, and during the operation period, drainage and waterproofing should be installed.

Definition of unsolved aspects of the problem

A wide range of factors and initial data should be taken into account for the qualitative selection of a dewatering method for the construction period. First and foremost, these are the engineering, geological and hydrogeological conditions of the site, the design of underground structures, the possibility of discharging water pumped out during dewatering beyond the site, and the possibility of locating dewatering equipment within the site.

Problem statement

The aim of this study is to investigate methods for protecting the underground portion of a new building from groundwater effects during the construction phase.

To achieve this goal, the following objectives have been defined: conducting engineering-geological and hydrogeological surveys of the site; identifying the filtration characteristics of the foundation soils; and performing calculations to determine the parameters of the dewatering system.

Basic material and results

The construction of underground parts of buildings and structures in difficult hydrogeological conditions requires additional and, therefore, complex and expensive work [5-6].

If the groundwater table is high, special measures should be taken to ensure safe conditions for the construction of underground structures and to prevent or reduce the impact on the surrounding area during such work.

This paper is based on the results of the design of a construction water drainage excavation pit for an administrative and production complex being built in the Podil district of Kyiv.

The site of the new building is located on the right bank of the Dnipro River, within the Eastern European Plain and is confined to the foot of the Kyiv Plateau slope in the historical Podil district of Kyiv. Kyiv. The site is located within the right-bank floodplain terrace of the Dnipro River. The territory of the project object is located in the central planning zone within the historical center of Kyiv. There are no objects of cultural heritage registered with the state among the surrounding buildings.

The site is located in a densely built-up area, which provides for the reconstruction and operation of the administrative and amenity complex in accordance with the requirements of DBN V.1.2-12-2008 [7].

The absolute elevation of 98.00 m, which corresponds to the level of the clean floor of the 1st floor, is taken as the conditional elevation of ±0.000 of the complex.

The foundations of the new building are made of ø620 mm diameter bored-injection piles. The length of the piles is 23 meters. The piles are united at the heads by a 900 mm thick reinforced concrete slab. The bottom of the excavation pit is located at -4.950 (absolute elevation 93.050 m) below the high-rise part. The retaining wall consists of bored-injection piles that are 7.65 to 10.35 m long and 420 mm in diameter, spaced 800 mm apart. Along the street, the excavation pit is excavated with a natural slope. Jet grouting piles are used for waterproofing the excavation perimeter.

According to DBN B.1.2-14-2018, the class of consequences for liability is CC3.

In geomorphological terms, the survey area is located within the right-bank floodplain of the Dnipro River, which was raised during economic development due to soil filling to absolute elevations of 96.56-98.32 m.

The geological section is composed of Holocene alluvial deposits, which are overlain by a thick man-made stratum from the surface (Fig. 1).

The following engineering geological elements (EGE) have been identified in the study area:

IHE-1 - Bulk soil - sandy loam with layers and lenses of dusty sand, with layers of loam, heterogeneous, sometimes with organic matter impurities in the base, from hard to plastic.

IGE-2 - Light, heavy, dusty loam, sometimes with an admixture of organic matter, soft-plastic.

IGE-2a - Light loam, dusty, slightly peaty, tightly laminated.

IGE-3 - Dusty and sandy loam, plastic.

IGE-3a - Sandy and sandy loam, medium peaty, sometimes strongly peaty, plastic.

IGE-4 - Fine, dense sand with medium density layers, saturated with water.

IGE-4a - Fine sand, medium density, with dense layers, saturated with water.

IGE-5 - Sand of medium size, dense, with separate layers of medium density, saturated with water.

IGE-6 - Light, heavy, dusty, tightly laminated loam.

IGE-7 - Fine, dense sand with some thin layers of medium density, saturated with water.

The hydrogeological conditions of the site are characterized by the presence of a Quaternary unconfined aquifer. Alluvial soils serve as water-bearing rocks. The groundwater mirror is recorded in the alluvial soils at the depths of 2.7...5.3 m at the absolute levels of 92.87...93.69 m. The aquifer is recharged by infiltration of precipitation, surface and groundwater runoff, leakage from water supply networks and hydraulic connection with the Dnipro River. The aquifer is discharged into the Dnipro River and the city's sewer system.

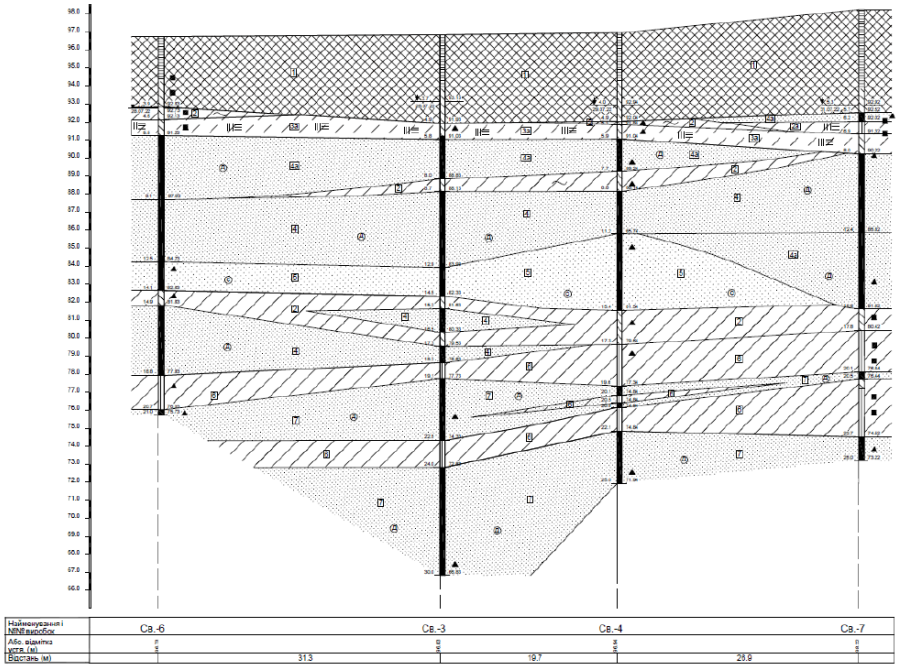

Figure. 1 - Characteristic geological section in the study area

During periods of seasonal heavy rains and snowmelt, the water table may rise, which is facilitated by the heterogeneity of the cut.

The projected rise in groundwater levels is related to the level regime of the Dnipro River. During spring floods, the estimated absolute water level in the Dnipro River is 96.7 m at the 1% flood (once every 100 years); 96.3 m at the 2% flood (once every 50 years); and 93.2 m at the 10% flood (once every 10 years). The maximum levels in the river persist on average for up to 2 weeks (sometimes more), during which the groundwater can become confined.

According to DBN V.1.1-25-2009 [1], the site is classified as naturally flooded.

The groundwater level within the survey area is not stable, which may indicate that the bulk soil has a heterogeneous composition and that there are periodic leaks from the water supply networks.

During excavation, the excavation pit will be flooded. To ensure normal conditions for zero-cycle operations during the construction period, it was decided to perform construction dewatering using needle filters.

Given the size of the excavation pit, it is possible to dewater it simultaneously or by dividing it into two excavations. In the project, water dewatering is performed from the entire area of the excavation pit.

Excavation works are carried out to develop the excavation pit to the -3.950 elevation (absolute elevation 94.050 m). After that, piles are drilled and water lowering equipment is installed.

Water lowering can be performed at one time from the entire area of the excavation pit or in two times (in 2 excavation zones). Dewatering is also performed at the site of the tower crane installation.

When performing dewatering, needle filters are installed in the excavation pit at a distance of 1.0 m from the retaining wall along its perimeter. For more efficient operation of the dewatering system, an additional branch of needle filters is installed in the central part of the excavation pit (Fig. 2). After excavating the pit to the -3.950 elevation (abscissa 94.050 m), needle filters are installed and a collector with needle filter connection is mounted.

A dewatering system is installed at the site of the tower crane. The excavation is carried out to the -3.550 elevation (absolute elevation 94.450 m). Needle filters are installed and a collector with needle filter connection is mounted.

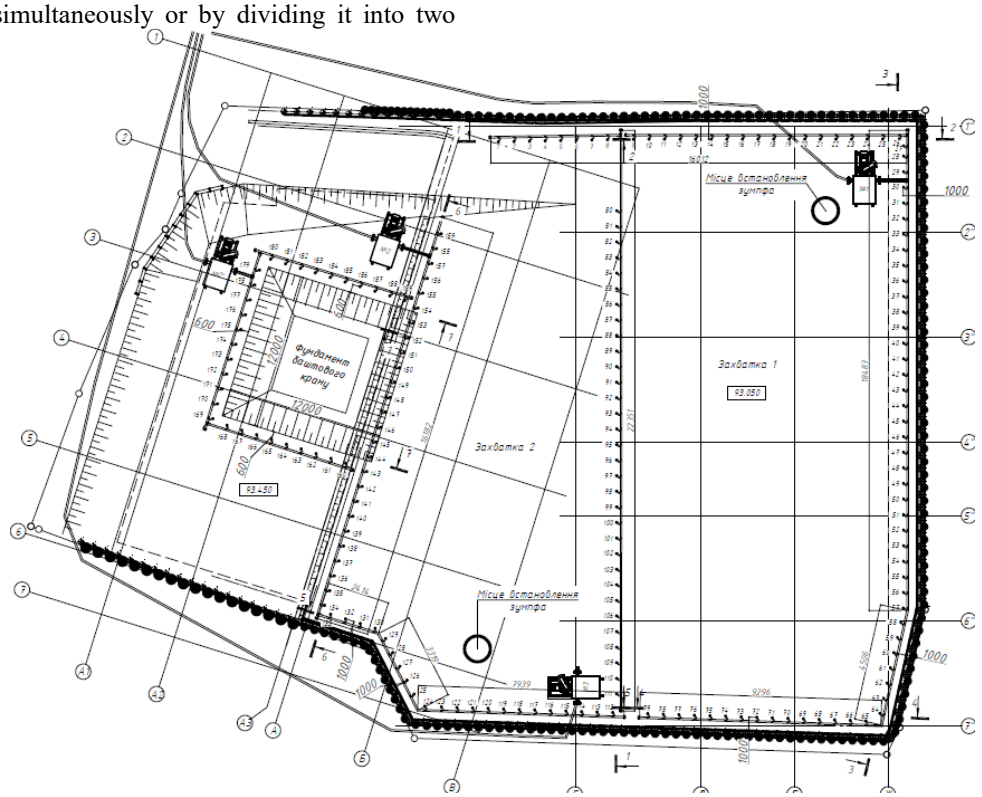

Figure 2 - Layout of needle filters in the excavation pit

After installation of the dewatering system, an as-built diagram of the actual arrangement of the system and its quantitative composition should be made.

The layout of dewatering systems may vary depending on the situation at the construction site.

Before starting construction dewatering, remove the soil to the level of the needle filters. This elevation should be at least 0.5 meters above the groundwater level. The temporary water supply system is laid out, coarse sand is brought in, temporary power supply is installed, and other preparatory work is carried out.

The dewatering procedure can be adjusted during construction and dewatering works.

After the water lowering system is launched, the second stage of excavation is carried out up to the bottom of the excavation pit.

Pumping units of the UVV-3A-6KM type are used for dewatering. Their number is determined by the results of calculations, and their installation locations are determined during their construction.

The collectors are fixed on supports or directly installed on the ground.

Install the needle filters with polymer sleeves Ø160 mm PVC160 SN4 to allow for concreting the foundation slab; after dismantling the needle filters, the holes should be concreted with concrete of the design class.

When arranging a suction collector with a diameter of 133 mm, it should be fixed to the structures of the retaining wall along the perimeter of the excavation pit.

Due to the fact that the groundwater level is on average ≈0.35 m above the bottom of the excavation pit, the water level should be lowered by 1.35...1.50 m. When determining the depth of lowering, it should be understood that the depth of lowering may vary, as the water level may change during the work, but these changes are not predictable, as they depend on many factors (time of work on the excavation sections, actual time of zero cycle work, the possibility of performing water lowering simultaneously or alternately, time of year, rainfall, etc.) The depth of groundwater lowering is determined if it is possible to achieve normal working conditions in the excavation pit, the depth of the minimum water lowering is ≥1.0 m below the bottom of the excavation pit.

The filtration coefficient of sand below the groundwater table was assumed to be 7.0 m/day in accordance with the data of engineering and geological surveys. The filtration coefficient of loam and sandy loam overlying the sand was assumed to be 0.5 m/day.

Dewatering is performed using a system of needle filters made of thin metal pipes that are immersed around the excavation pit. The lower ends of the pipes are equipped with filters, and the upper ends are connected to a suction manifold. The project envisages vacuum water lowering of the groundwater level using UVV-3A-6KM pumping units.

If the distance between the wells is less than two drawdown radii, then such wells interact when pumping water simultaneously. This leads to the closure of the drawdown curves and the formation of a common zone of groundwater level decline.

The UVV-3A-6-KM units are used for dewatering sandy soils and loams in various geological structures. The set includes needle filters (up to 100 pcs.), a water collector with a diameter of 133 mm and two centrifugal pumps, one of which is a backup, to ensure the uninterrupted operation of the plant.

The needle filter is a 38 mm diameter pipe, up to 8.5 m long (Fig. 3, 4), to the lower end of which is attached a filter link consisting of two pipes: an inner pipe, which is a continuation of the common 38 mm diameter pipe, and an outer pipe with a diameter of 60 mm with evenly distributed holes for water passage. The outer pipe is wrapped with 3 mm diameter wire and covered with filter and protective mesh. The filter link ends with a tip, inside which there are ball and ring valves.

The needle filters are submerged into the soil by hydraulic means.

Needle filters are installed along the perimeter of the dewatering excavation pit according to the set of working drawings.

Upon completion of the dewatering, all equipment is dismantled, and the dewatering wells are abandoned. Depending on the hydrogeological conditions, depth and location in relation to the nearest structures, abandonment grouting is performed in almost all rocks, except for loose and quicksand.

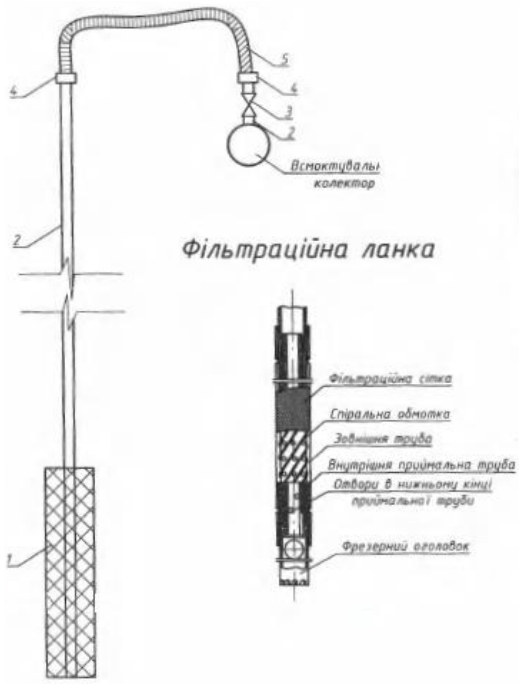

Figure 3. Needle filter designs
1 - tubular frame with slot perforation; 2 - lining longitudinal rods; 3 - water-receiving surface made of wire winding; 4 - lining spiral winding; 5 - water-receiving surface made of stainless mesh; 6 - water-receiving surface made of stamped sheet with holes.

Dewatering calculations are performed to determine the total flow rate (Q is the flow rate diverted from the site), the radii of influence of the adopted systems, and the actual decrease in groundwater levels, as well as to the selection (refinement) of the most effective measures of technological schemes of dewatering [8]. When determining the amount of groundwater inflow to the excavation pit, two groups of pits are distinguished: trenches and rectangular pits (width to length ratio 1 : 10); wide pits of square, rectangular, round and other shapes (width to length ratio more than 1 : 10). In this case, the pits that cannot be extended in length lead to an idealized equivalent circular area with radius r_0.

To calculate the dewatering, the natural conditions and the adopted dewatering system are schematized.

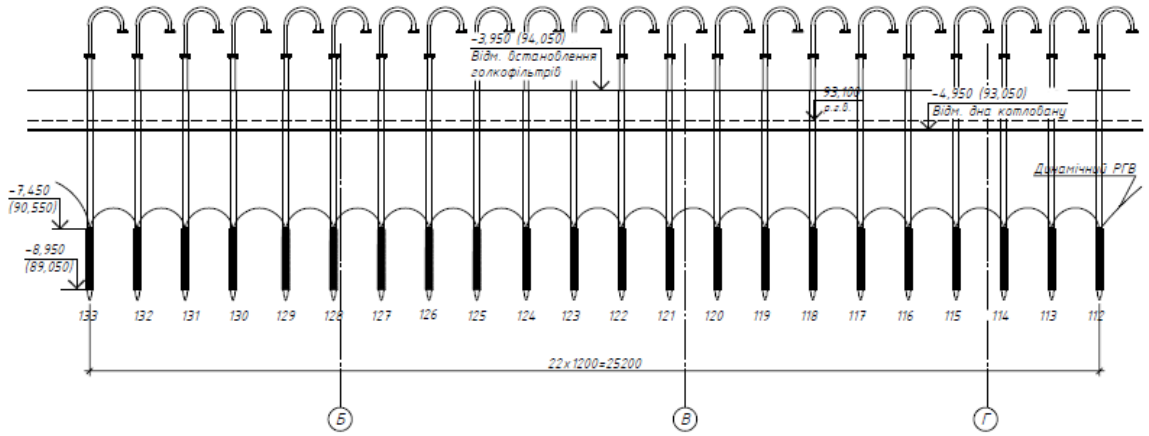

Figure 4. Cross section of the dewatering system

The general procedure for calculating a dewatering system is as follows:

- the necessary reduction in groundwater level is determined;
- the inflow to the dewatering system is determined;
- the parameters of the dewatering system are determined;
- selection of the necessary equipment.

According to the results of the calculations, it was found that when performing dewatering simultaneously over the entire area of the excavation pit, needle filters within the excavation pit are installed at elevation 94.050 m. The total length of the needle filters is 5.0 m. The dewatering area (pit) is serviced by three vacuum pumping units UVV-3A-6KM. Two sumps are installed in the excavation pit to collect and discharge surface water entering the pit.

According to the results of the calculations, the total groundwater extraction rate during dewatering over the entire area of the excavation pit will be:

949 m^3/day = 39.5 m^3/hour.

The drawdown curve is formed within 5 days. The radius of the drawdown curve is 120 m.

For the site where the crane is installed, it was obtained that the needle filters are made from the elevation of 94.450 m. The total length of the needle filters is 7.0 m. The dewatering section is serviced by 1 vacuum unit UVV-3A-6KM, which also serves as a backup for dewatering in the excavation pit.

According to the results of the calculations, it was obtained that the total water consumption during dewatering in the area where the crane is located will be 230 m^3/day = 10.5 m^3/hour. The formation of the drawdown curve occurs within 5 days. The radius of the drawdown curve is 120 m.

The total number of needle filters is 189.

The number of needle filters, their installation locations and length, and the location of the UVV-3A-6KM units are specified during the work.

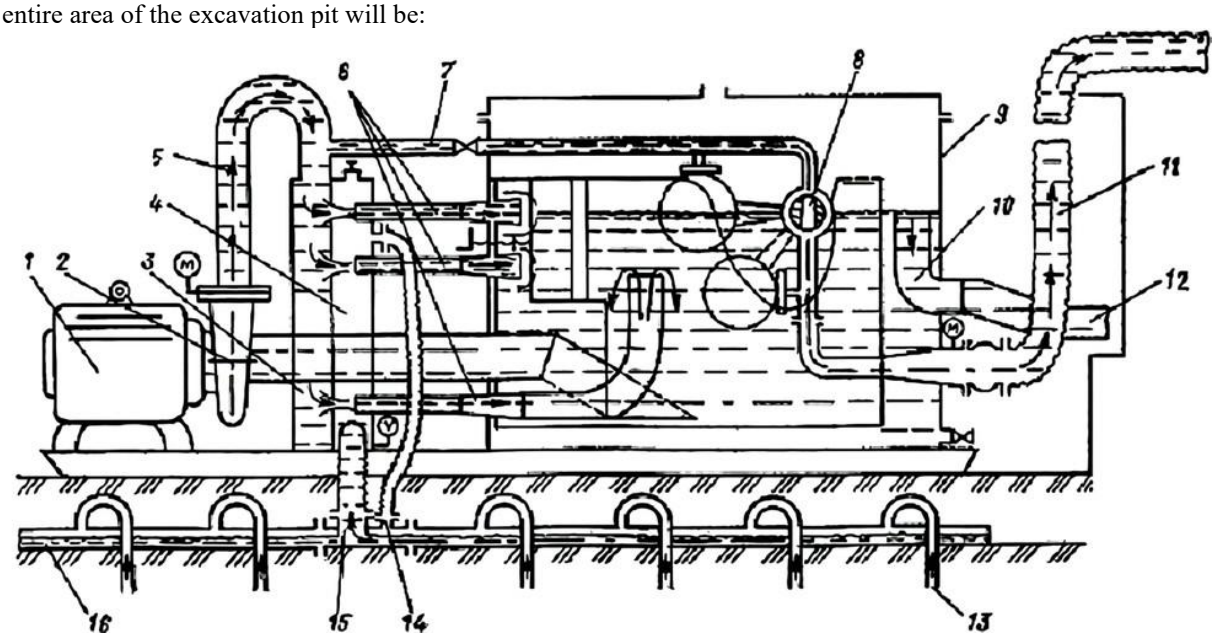

Figure 5 - Schematic diagram of the pumping unit UVV-3A-6KM:

1 - electric motor; 2 - centrifugal pump; 3, 4 - pressure and receiving chambers; 5 - pressure pipeline; 6 - ejectors; 7 - discharge pressure line; 8 - control valve with float; 9 - circulation tank; 10 - drain riser; 11 - discharge pressure pipeline; 12 - free drain line; 13 - needle filter; 14, 15 - air and water transition hoses; 16 - suction manifold.

In pumping units of the UVV-3 type (Fig. 5), two water-air ejectors are used to reproduce a stable vacuum in the cavities of the suction manifold and needle filters, which pump out the air released from the water-air mixture that enters the needle filters. With limited air flow to the water intake part of the needle filters, a vacuum of about 5 m Hg or more develops in their cavities. Water is pumped out by a water-water ejector. All three ejectors, which are part of the same module, are supplied with working water from a centrifugal pump. With a significant content of one of the components (water or air) in the water-air mixture, each of the ejectors is able to partially take over the functions of the other.

The unit ensures the lifting of water that is pumped to a height of up to 20.0 m. When protecting excavation pits, the unit is placed in a ring pattern.

During the excavation of the excavation pit and the installation of underground structures, dewatering was performed using needle filters, which ensured the necessary and safe conditions for construction work, confirming the correctness of the technical solutions adopted in the dewatering project.

Conclusions

The implementation of construction dewatering using needle filters under complex geotechnical and hydrogeological conditions ensures safe working conditions for excavation, provided current regulatory requirements are met.

The rational location of dewatering equipment ensures that optimal conditions are achieved for construction work. The construction conditions for each facility should be taken into account.

Considering the existing hydrological situation and substantiating the methods of protection of excavation pits with appropriate calculations and in compliance with the relevant requirements of regulatory documents at a high level of groundwater, effective methods of protection of construction sites can be developed for the construction of underground structures during the construction period.

At present, the performance of excavation protection works is regulated by regulatory documents developed in the USSR, so it is necessary to update the regulatory documents in this part to meet modern requirements.

References

1. ДБН В.1.1-25-2009 (2011) *Інженерний захист територій та споруд від підтоплення та затоплення.* Київ: Мінрегіонбуд України.

2. ДСТУ-Н Б В.1.1–38:2016. (2017) *Настанова щодо інженерного захисту територій, будівель і споруд від підтоплення та затоплення.* Київ: ДП УкрНДНЦ.

3. E. Forero-Ortiz, E. Martínez-Gomariz, M-C. Porcuna. (2020) A review of flood impact assessment approaches for underground infrastructures in urban areas: a focus on transport systems. *Hydrological Sciences Journal, 65:11,* 1943-1955.

4. Yong-sik Han, Eun Taek Shin, Tae Soo Eum, Chang Geun Song. (2019) A review of flood impact assessment approaches for underground infrastructures in urban areas: a focus on transport systems/ *Appl. Sci., № 9 (6),* 2–11.

5. Дмитрієв Д.А., Степанчук С.В., Кураш С.Ю. (2023) *Захист заглиблених конструкцій будівель та споруд від впливу підземних вод на будівельний та експлуатаційний періоди.* Науково-технічний журнал «Наука та будівництво», 35, 48-54.
DOI: 10.33644/2313-6679-1-2023-6.

6. Бамбура А.М., Ковальській Р.К., Дмитрієв Д.А., Дорогова О.В.. *Геотехнічні проблеми при проектуванні, будівництві та експлуатації відповідальних будівельних об'єктів.* Міжвідомчий науково-технічний збірник «Будівельні конструкції», 89 (2), 3-12

7. ДБН В.1.2.-12-2008 (2009) *Система надійності та безпеки в будівництві. Будівництво в умовах ущільненої забудови. Вимоги безпеки.* Київ: Міністерство регіонального розвитку та будівництва України.

8. ДБН В.2.1–10:2018.(2018) *Основи та фундаменти споруд. Основні положення*: Київ: Мінрегіон України.

1. DBN V.1.1-25-2009 (2011) *Engineering protection of territories and structures against flooding and submersion.* Kyiv: Ministry of Regional Development and Construction of Ukraine.

2. DSTU-N B V.1.1-38: 2016. (2017) *Guidelines for engineering protection of territories, buildings and structures from flooding and submersion.* Kyiv: UkrNDNC.

3. E. Forero-Ortiz, E. Martínez-Gomariz, M-C. Porcuna. (2020) A review of flood impact assessment approaches for underground infrastructures in urban areas: a focus on transport systems. *Hydrological Sciences Journal, 65:11,* 1943-1955.

4. Yong-sik Han, Eun Taek Shin, Tae Soo Eum, Chang Geun Song. (2019) A review of flood impact assessment approaches for underground infrastructures in urban areas: a focus on transport systems/ *Appl. Sci., № 9 (6),* 2–11.

5. Dmitriev D.A., Stepanchuk S.V., Kurash S.Y. (2023*) Protection of underground structures of buildings and structures from the impact of groundwater during construction* and *operational periods*. Scientific and Technical Journal "Science and Construction", 35, 48-54.
DOI: 10.33644/2313-6679-1-2023-6.

6. Bambura A.M., Kovalsky R.K., Dmitriev D.A., DorogovaO.V..*Geotechnical problems in the design, construction and operation of critical construction facilities.* Interdepartmental scientific and technical collection "Building structures", 89 (2), 3-12.

7. DBN B.1.2.-12-2008 (2009) *System of reliability and safety in construction. Construction in conditions of dense development. Safety requirements.* Kyiv: Ministry of Regional Development and Construction of Ukraine.

8. .DBN B.2.1-10:2018.(2018) *Bases and foundations of structures. Basic provisions*: Kyiv: Ministry of Regional Development of Ukraine.

Дмитрієв Д. А. *
Державне підприємство «Науково-дослідний інститут будівельних конструкцій
https://orcid.org/0000-0003-2993-1311

Перлова О. М.
Державне підприємство «Науково-дослідний інститут будівельних конструкцій
https://orcid.org/0000-0002-8751-1983

Будівельне водозниження в умовах щільної міської забудови

Проаналізовано особливості будівництва заглиблених конструкцій та споруд в складних гідрогеологічних умовах та в щільній забудові. Урбанізовані території є прикладом потужного і незбалансованого впливу на геологічне середовище техногенних факторів, які порушують гідрогеологічні та геоекологічні умови території. Спорудження фундаментів на палях, тунелів, інженерних мереж, а також підземних паркінгів в більшості випадків призводить до баражування потоку ґрунтових вод, та як наслідок, до підтоплення території. Підземний простір сучасного міста насичений водонесучими комунікаціями, які мають непередбачувані витоки. Витоки вод з комунікацій викликають значний підйом рівнів ґрунтових вод верхнього водоносного горизонту, які мають випадковий характер і важко піддаються прогнозуванню. В таких випадках основною вимогою є збереження, по можливості, існуючого гідрогеологічного режиму та недопущення виникнення додаткових деформацій споруд, що розташовані поруч. У разі необхідності виконання будівельного водозниження з ризиком значного зниження рівня ґрунтових вод період їх виконання повинен бути обґрунтованим та обмеженим в часі, при цьому повинні бути виконані умови для безпечного виконання робіт нульового циклу. Існують різні варіанти виконання захисту заглиблених споруд від негативного впливу ґрунтових вод. В статті розглянутий варіант виконання робіт з захисту заглиблених конструкцій за допомогою голкофільтрів. Такий варіант є найбільш доцільним при необхідності зниження рівня ґрунтових вод на 3...4 м. Як що слід понизити рівень ґрунтових вод нижче, можна виконати водозниження в декілька ярусів. На даний час виконання таких робіт не регламентується в повної мірі сучасними чинними в Україні нормативними документами. Використовуються норми, що були розроблені при СРСР, але на даний час вони є діючими в нашій країні. Тому необхідно вдосконалювати нормативну базу щодо захисту заглиблених споруд з урахуванням сучасних вимог.

Ключові слова: гідрогеологічні умови, рівень ґрунтових вод, будівельне водозниження, коефіцієнт фільтрації, голкофільтр.

*Адреса для листування E-mail: dmitrievgts71@gmail.com

Збірник наукових праць. Галузеве машинобудування, будівництво
Academic journal. Industrial Machine Building, Civil Engineering
http://journals.nupp.edu.ua/znp
https://doi.org/10.26906/znp.2024.63.3871

UDC 624.014:69.059.32:624.016

Andriy Reka
National University «Yuri Kondratyuk Poltava Polytechnic»
https://orcid.org/0009-0002-7136-8585

Tatiana Galinska *
National University «Yuri Kondratyuk Poltava Polytechnic»
https://orcid.org/0000-0002-6138-2757

Dmytro Ovsii
National University «Yuri Kondratyuk Poltava Polytechnic»
https://orcid.org/0000-0001-7007-1857

Mukhlis Hajiyev
Azerbaijan University of Architecture and Construction
https://orcid.org/0000-0001-6782-0941

Strengthening of the cross-section of steel i-beams in the tension zone: a review of scientific research

The article reviews scientific research on methods and means of strengthening steel beam structural elements by increasing (building up) cross-sections using additional elements made of steel rolled profiles, plates, reinforcing bars and plates made of polymeric materials. The main conclusions and directions of further scientific research on effective methods and means of strengthening steel beam structural elements by increasing (building up) their cross-sections, which have the potential for widespread use in the repair and reconstruction of buildings and structures, are substantiated.

Keywords: steel beam structural elements, repair and strengthening, cross-section increase, a review, scientific researchs

*Corresponding author E-mail: galinska@i.ua

Introduction

Currently, the long-term operation of construction facilities and the development of industrial production are inextricably linked with repair, reconstruction, expansion, and technical re-equipment of enterprises. Strengthening existing steel beam structures is a common approach to prevent failure due to significant physical deterioration, changes in functional purpose, or construction errors during design and manufacturing. Moreover, any reconstruction of an operational facility is typically accompanied by changes in the loads acting on building structures, and sometimes even by alterations to their original structural schemes. This necessitates an assessment of the technical condition of structural elements and an increase in their load-bearing capacity through rational strengthening.

Clause 8.3 of the national building code DBN B V.3.1-2:2016 [1] outlines the main methods and techniques for strengthening steel structures, one of which is the method of partially increasing the cross-sectional area. Reinforcing the cross-sections of steel beams by enlarging the tension zone with additional elements such as steel rolled profiles, plates, reinforcing bars, or polymer composite plates is one of the most commonly used methods. This is due to its practicality during installation, the homogeneous (isotropic) properties and ease of processing of the materials used, high tensile ductility, and excellent fatigue resistance. This method allows for the strengthening of steel beam structures in existing buildings and facilities either under load or with temporary unloading.

When choosing a method for strengthening steel beams, according to the requirements of clause 8.4.2 of DBN B V.3.1-2:2016 [1], the following factors must be considered: the support conditions of the floor or roof elements on the beam (whether on the upper or lower flanges); the possibility of increasing the constructional height of the beam and the availability of space to accommodate strengthening elements; the feasibility of performing the work without interrupting production or during natural technological pauses; and the technological capabilities for manufacturing and installing the strengthening components. To select the most effective method for strengthening steel beams by enlarging the cross-section in the tension zone, a comprehensive analysis of the full range of prior

scientific research conducted to date must be carried out.

Problem statement

The **aim of the work** is to conduct a review of scientific research devoted to theoretical developments and experimental testing of steel beam elements with symmetrical cross-sections, which are strengthened in the tension zone additional longitudinal elements made of steel rolled profiles, plates, reinforcing bars and plates made of polymeric materials.

Review and analysis of research sources and publications

The analysis of scientific research has shown that there is a wide range of methods for strengthening the bending strength of metal beams by increasing (augmenting) their cross-sections along the length. In recent years, in addition to traditional methods of reinforcing metal beams by augmenting their cross-sections with additional elements made of shaped and sheet rolled sections or reinforcement bars. Methods of reinforcement through cross-sectional increase using adaptive wire manufacturing have also been introduced (WAAM) and the installation (fixing, bonding) of additional elements made of carbon fiber (CFRP) to the lower tension zone of metal beams. In the studies [2], [3], researchers J. Yang, M.A. Wadee, and L. Gardner conducted experimental investigations to evaluate the bending strength of hot-rolled steel beams, which were reinforced along their length by increasing the I-shaped cross-section through arc-based additive wire manufacturing (WAAM). The beams were tested under four-point or three-point bending conditions. The results showed that as the mass of the specimens' cross-sections increased from 2,63% to 12,26%, the bending strength of the beams increased by 11,5%–33,2%.

In the work [4], researchers Ghafoori E. and Motavalli M. experimentally and numerically investigated the transverse-torsional bending of steel beams reinforced with a layered carbon fiber reinforced polymer (CFRP) material of normal modulus of elasticity (NM). The test results showed that reinforcing steel beams with layered carbon fiber materials almost equally increases the elastic stiffness of the specimens, both for bonded and unbonded systems, compared to the reference beam. Specimens reinforced with unbonded carbon fiber reinforced polymer (CFRP) laminates have higher strength than those reinforced with bonded carbon fiber reinforced polymer laminates. Pre-stressing of the carbon fiber reinforced polymer layered materials does not affect the elastic stiffness of the reinforced beams, but it significantly influences their bending strength. Higher levels of prestressing do not necessarily lead to an increase in bending strength in the retrofitted beams. [4]. The article by Omnia R. AbouEl-Hamd [5] presents the results of experimental and numerical studies on steel beams, which were reinforced along their length with hybrid fiber-reinforced polymers (HFRP) using steel bolts. Tests on 22 steel beams demonstrated their plastic behavior upon failure, with an increase in yield and ultimate bending strength by 15,1% and 22,2%, respectively [5]. The study of a structural solution for strengthening steel beams using adhesive strips made of shape memory alloy steel (also known as iron-based shape memory alloy, Fe-SMA) was conducted by Sizhe Wang and other researchers in work [6].

In the study [7], researchers Linghoff D., Al-Emrani M., and Kliger R. tested five beams under static four-point bending. The beams were fabricated from standard HEA180 steel profiles with a nominal span length of $L_u = 1.8$ m. The length of the carbon fiber-reinforced polymer (CFRP) laminate used to strengthen the beams at the level of the lower flange was 1600 mm, leaving an unreinforced gap of 100 mm between the ends of the CFRP laminate and the supports. Parametric studies were carried out to investigate how different parameters, such as the variation in thickness and elastic modulus of the laminates and the adhesive layer of different epoxy resins, would affect the strength and behavior of the strengthened beams. The CFRP laminate strips were bonded to the steel beam using epoxy resin over the entire surface with the help of a hard roller. To ensure a uniform thickness of epoxy resin along the bonding length, thin wooden strips were glued to the bottom flange of the beam. These strips, having a thickness of 2 mm plus the thickness of the CFRP laminate, served as supports during the placement of the laminate strips. Based on the test results, the ultimate loads of the strengthened beams were compared with that of the reference beam. The ultimate load for the reference beam was defined as the applied load level that resulted in a strain of 2% in the extreme tensile fiber of the beam, corresponding to a deflection of $f = 50$ mm. The ultimate load for the strengthened beams was defined as the load that caused rupture or delamination of the CFRP laminate. According to the data presented in Table 3 [7], the increase in ultimate load ΔP for the strengthened steel beams compared to the reference beam, depending on the strength characteristics of the CFRP laminate material used, ranged from 2% to 18%.

In research [8] Liu, Y. and Gannon, L. conducted experimental investigations on steel I-beams with cross-section W 310×100×28.3 and effective lengths of L_u=2.4 m and L_u=1.2 m. The beams were strengthened using conventional methods:

- by welding under load steel vertical cover plates with dimensions $t \times h$=9.5×320 mm along the length of the specimens symmetrically to the top and bottom flanges;
- by welding a horizontal cover plate with dimensions $t \times b$=9,5×137 mm along the length of the tensioned bottom flange of the I-section beam.

The experimental results [8] indicated that the degree of preloading influences the strength of the reinforced beams, which fail as a result of torsional bending of the vertical plane. Specifically, when the beams were strengthened under a preload level of 50–53% of the ultimate strength of the unstrengthen beam, the ultimate

strength of the reinforced beam under torsional buckling decreased by 13–14.2%.

In the study [9], Ridha, S., Abbood, A., and Atshan, A. conducted experimental investigations on three steel I-beams with IPE 100 cross-sections and a nominal span length of L_u=1.0 m. The beams were strengthened at mid-span by welding under load with inclined steel plates of dimensions $t \times b \times l = 3 \times 12.5 \times 250$ mm or $t \times b \times l = 3 \times 25 \times 250$ mm. Horizontal plates with dimensions $t \times b \times l = 3 \times 12.5 \times 500$ mm or $t \times b \times l = 3 \times 25 \times 500$ mm were also used for strengthening, symmetrically to the upper and lower flanges. As a result, the strength of the beam reinforced with 12.5 mm wide plates increased by 21.15% compared to the reference specimen under an ultimate load of F = 157.5 kN, while the beam reinforced with 25 mm wide plates increased its strength by 37.69% at F = 179 kN. Strengthening with additional plates and inclined stiffeners altered the failure mode from "lateral buckling" (as observed in the control specimen) to a "plastic hinge" formation at the point of concentrated load (mid-span). Additionally, reinforcing the beams with extra plates significantly reduced both vertical and horizontal deformations, as well as deflection and lateral bending, compared to the reference specimen.

In research [10], Yossef, N. conducted experimental tests on six steel I-beams with IPE 200 cross-sections and a nominal span of L_u = 1.8 m. The beams were strengthened at mid-span by welding, under load, by steel plates to the bottom flange with dimensions $t \times b = 6 \times 80$ mm and lengths of $l = 650$ mm or $l = 900$ mm. Additionally, horizontal plates of dimensions $t \times b \times l = 6 \times 80 \times 900$ mm and $t \times b \times l = 6 \times 80 \times 450$ mm were welded symmetrically to the bottom and top flanges, respectively. The test results indicated that the ultimate strength of the beams depends on the length of the welded reinforcement plate and the welding technology used under different load levels. Increasing the reinforcement plate length from 36% to 50% of the span led to an increase in beam strength ranging from 1% to 5%.

In the study [11], A. Al-Balhawi et al. carried out experimental tests on two steel I-beams with IPE 100 cross-sections and a nominal span length of L_u = 1.4 m. Beam B1 was strengthened at mid-span by welding a plate of dimensions $t \times b = 6 \times 65$ mm and length $l = 1250$ mm to the top flange. Beam B2 was reinforced by welding horizontal plates symmetrically to the top and bottom flanges with dimensions $t \times b \times l = 6 \times 65 \times 1250$ mm and $t \times b \times l = 3 \times 65 \times 1250$ mm, respectively. The additional bottom plate in beam B2 increased its flexural strength in the elastic stage twofold compared to beam B1.

In the study [12], Yu. Kushnir conducted experimental research on five steel I-beams fabricated from rolled I-section No. 16 with a nominal span length of L_u = 1.7 m. The beams were reinforced in the tensile zone by installing two additional reinforcing bars made of A500-grade steel with diameters of 10 mm, 16 mm, 20 mm, and 32 mm. The distance from the bottom flange to the longitudinal axis of the reinforcing bars was set at a = 25 mm for 10, 16, and 20 mm bars, and a = 30 mm for 32 mm bars. Experimental data on relative strains in the fibers of the I-section and comparisons with limiting stress values confirm the elastic-plastic behavior of the strengthened beams at the failure section. As the plastic zone at the failure section increased from 5% to 20%, the load-bearing capacity of the specimens also increased compared to the reference beam. The load-bearing capacity of beams reinforced with 10, 16, and 20 mm bars increased by 5–10%, while the beam reinforced with 32 mm bars showed a 51% increase in comparison to the reference specimen [12].

For the specimens that predominantly failed due to flexural bending about the horizontal plane, the level of preloading showed a negligible effect on the ultimate strength of the strengthened specimens. In article [13] and research work [14], researchers Mohammadzadeh, M. and Bhowmick, A. conducted finite element (FE) analyses to investigate the stress–strain behavior and flexural strength of steel I-beams with cross-sections strengthened under load by additional steel cover plates. A series of simply supported steel I-beams, reinforced with cover plates welded to the bottom tension flanges, was thoroughly analyzed. The finite element analysis shows that as the level of preloading increases, the load-bearing capacity of the I-beam strengthened under load decreases when the failure mode is lateral-torsional buckling (loss of stability from the vertical plane). On the other hand, variations in the level of preloading have a minimal effect on the behavior and ultimate strength of the strengthened beam when failure occurs in pure bending. In studies [15] and [16], Assaad Taoum, together with Jiao, H. and Holloway, D., investigated the effectiveness of the Local Prestressing Technique (LPT) for improving the repair of damaged steel beams. The studies demonstrated that the level of prestressing, the type of LPT method (internal or external), and the diameter of the reinforcing bars used had a significant impact on the stiffness of the beams and their ultimate load-bearing capacity [14], [15].

In article [17] Piotr Szewczyk and Maciej Szumigała presented the results of experimental investigations and numerical analysis on the strengthening of steel–concrete composite beams. The steel section of the IPE200 I-beam profile was strengthened along its length by welding additional steel plates with a thickness ranging from 6 to 22 mm to its bottom flange. One of the objectives was to find an optimal solution that minimizes costs while maximizing bending strength. To achieve this objective, the energy parameters available in numerical simulations were reviewed and analyzed. The proposed numerical models were experimentally validated using three specimens. The maximum deviation between the experimental and the average numerical bending

strength of the reinforced composite beams is approximately 2,5%.

The strengthening of composite steel–concrete beams using externally prestressed reinforcement bars has been the focus of studies by researchers such as El-Zohairy A. and Salim H. [18], M.Yu. Izbash [19], R.M. Shemet [20], as well as T.A. Halinska, V.F. Pentz, and Yu.O. Kushnir [21]. In article [18] El-Zohairy A. and Salim H. presented a numerical model for investigating the nonlinear behavior of composite beams reinforced with externally prestressed reinforcement bars (tie rods). The reliability of the developed numerical model was confirmed by comparing its results with available experimental data. Study [18] investigated the influence of various strengthening parameters, including inclined (triangular and trapezoidal profiles) and straight bars (tie elements); the length of the bars (ties); the effect of additional prestressing on restoring the bending performance of an overloaded beam; the eccentricity of stress application; and the degree of shear connection. A good agreement was obtained between the proposed model and the experimental data. The results indicate that, at the same stress application eccentricity, the trapezoidal profile demonstrates superior load-bearing capacity for reinforced beams compared to the horizontal strengthening element. In article [21], the authors present a classification of steel–concrete composite beams strengthened with prestressed horizontal elements (tie rods), based on the composite properties of their components and the cases of the ultimate stress–strain state.

Identification of unresolved issues

The analysis of research conducted by various scholars has demonstrated that the method of strengthening steel beams by partially increasing the cross-sectional area, particularly in the lower tension zone, can significantly enhance the load-bearing capacity (strength and stiffness) of the reinforced steel beams. In recent years, in addition to traditional strengthening or repair methods using welded or bolted plates and reinforcement bars, an alternative method involving the application of carbon fiber reinforced polymer (CFRP) laminate strips has been introduced and increasingly implemented in repair practice. These strips are either bonded or mechanically fastened to the flange sections of steel beams.

Experimental studies conducted by researchers have shown that the use of various strengthening systems enables partial or full restoration (or enhancement) of the load-carrying capacity of deteriorated beams. The increase in ultimate load capacity (ΔP) of the strengthened steel beams compared to the reference beam depends on numerous influencing factors. When strengthening the tension zone of steel beams using additional elements applied locally at mid-span, without extending to the support areas, several problems arise due to the altered cross-section. These include the non-uniform stress distribution, characterized by a stress intensity factor that varies at different stages of the stress-strain state of the strengthened beam, as well as the necessity of developing a constructive solution for anchoring the ends of the added strengthening element. The types and combinations of such connections present a wide range of possible configurations.

Conclusions

Thus, the conducted analysis of scientific studies has shown that an unresolved aspect of the broader issue concerning the development and improvement of strength calculation methods for strengthened structural elements is the lack of a clear (engineering) methodology for calculating the bending strength of metal beam structures (elements) strengthened by the addition of supplementary components in the tensile zone of their cross-section such a methodology should take into account the loading history, the strength characteristics of the materials, and the stages of their stress–strain state at the moment of failure.

The overall aim of the research is to develop an analytical method for calculating the bending strength of metal beams with symmetrical cross-sections that are strengthened under load by installing additional longitudinal reinforcement bars or other elements in their tensile zone, without prior prestressing.

References

1. ДБН Б В.3.1-2:2016. (2017). Ремонт і підсилення несучих і огороджувальних будівельних конструкцій та основ будівель і споруд: Наказ Мінрегіону від 24.06.2016 №182, чинний з 2017-04-01. Київ: ДП "УкрНДНЦ".
2. Yang, J., Wadee, M. A., & Gardner, L. (2025). Strengthening of steel I-section beams by wire arc additive manufacturing – Concept and experiments. Engineering Structures, 322, 119113. https://doi.org/10.1016/j.engstruct.2024.119113
3. Yang, J., Wadee, M. A., & Gardner, L. (2025). Residual stresses in steel I-section beams strengthened by wire arc additive manufacturing. Journal of Constructional Steel Research, 232, 109606. https://doi.org/10.1016/j.jcsr.2025.109606
4. Ghafoori, E., & Motavalli, M. (2015). Lateral-torsional buckling of steel I-beams retrofitted by bonded and un-

1. DBN B V.3.1-2:2016. (2017). Structures of buildings and structures. Steel-reinforced concrete structures. Basic provisions. Ministry of Regional Development of Ukraine. Kyiv: Minregion Ukraine. (in Ukrainian)
2. Yang, J., Wadee, M. A., & Gardner, L. (2025). Strengthening of steel I-section beams by wire arc additive manufacturing – Concept and experiments. *Engineering Structures, 322*, 119113. https://doi.org/10.1016/j.engstruct.2024.119113
3. Yang, J., Wadee, M. A., & Gardner, L. (2025). Residual stresses in steel I-section beams strengthened by wire arc additive manufacturing. Journal of Constructional Steel Research, 232, 109606. https://doi.org/10.1016/j.jcsr.2025.109606
4. Ghafoori, E., & Motavalli, M. (2015). Lateral-torsional buckling of steel I-beams retrofitted by bonded and un-

bonded CFRP laminates with different pre-stress levels: Experimental and numerical study. Construction and Building Materials, 76, 194–206. http://dx.doi.org/10.1016/j.conbuildmat.2014.11.070

5. AbouEl-Hamd, O. R., Sweedan, A. M. I., El-Ariss, B., & El-Sawy, K. M. (2023). Experimental and numerical investigation of the behavior of steel beams strengthened by bolted hybrid FRP composites. Buildings, 13(3), 824. https://doi.org/10.3390/buildings13030824

6. Wang, S., Li, L., Su, Q., Jiang, X., & Ghafoori, E. (2023). Strengthening of steel beams with adhesively bonded memory-steel strips. Thin-Walled Structures, 189, 110901. https://doi.org/10.1016/j.tws.2023.110901

7. Linghoff, D., Al-Emrani, M., & Kliger, R. (2010). Performance of steel beams strengthened with CFRP laminate – Part 1: Laboratory tests. Composites Part B: Engineering, 41(7), 509–515. https://doi.org/10.1016/j.compositesb.2009.05.008

8. Liu, Y., & Gannon, L. (2009). Experimental behavior and strength of steel beams strengthened while under load. Journal of Constructional Steel Research, 65(6), 1346–1354. https://doi.org/10.1016/j.jcsr.2009.01.008

9. Ridha, S., Abbood, A., & Atshan, A. (2020). Evaluating the efficiency of strengthening hot-rolled I-sectioned steel beams by using additional plates and inclined stiffeners with various widths. In IOP Conference Series: Materials Science and Engineering, 870(1). IOP Publishing. https://bit.ly/44S2dT2

10. Yossef, N. (2015). Strengthening steel I-beams by welding steel plates before or while loading. International Journal of Engineering Research & Technology, 4(07). https://bit.ly/44XiINw

11. Al-Balhawi, A., Shubber, A. N., Al-Asadi, L. S. M., Ibrahim, S. K., Hacheem, Z. A., Jassem, N. H., Dheyab, L. S., & AL-Ridha, A. S. D. (2022). Assessing the structural behavior of steel beams strengthening with additional plates. Materials Today: Proceedings, 62, 4562–4566. https://doi.org/10.1016/j.matpr.2022.05.304

12. Кушнір, Ю. О. (2012). Експериментальні дослідження міцності сталевих балок, що підсилені горизонтальними затяжками. Наук.-техн. зб. ХНАМГ: Комунальне господарство міст. Серія: Технічні науки та архітектура, 105, 168–179. https://khges.kname.edu.ua/index.php/khges/article/view/837/831

13. Mohammadzadeh, M., & Bhowmick, A. (2022). Behavior of steel I-beams reinforced while under load. In Lecture Notes in Civil Engineering (pp. 67–79). Singapore: Springer Singapore. https://doi.org/10.1007/978-981-19-0656-5_6

14. Mohammadzadeh, M. (2022). Behaviour of steel I-beams reinforced while under load (PhD thesis). Concordia University, Montreal, Canada. https://spectrum.library.concordia.ca/id/eprint/991496/1/Mohammadzadeh_PhD_S2023.pdf

15. Taoum, A., Jiao, H., & Holloway, D. (2015). Using locally pre-stressed reinforcing bars to restore the capacity of severely damaged steel beams. International Journal of Steel Structures, 15(1), 125–134. https://doi.org/10.1007/s13296-015-3009-1

16. Taoum, A., Jiao, H., & Holloway, D. (2015). Upgrading steel I-beams using local post-tensioning. Journal of Constructional Steel Research, 113, 127–134. https://doi.org/10.1016/j.jcsr.2015.06.012

17 Szewczyk, P., & Szumigała, M. (2021). Optimal design of steel–concrete composite beams strengthened under load. Materials, 14(16), 4715. https://doi.org/10.3390/ma14164715

bonded CFRP laminates with different pre-stress levels: Experimental and numerical study. Construction and Building Materials, 76, 194–206. http://dx.doi.org/10.1016/j.conbuildmat.2014.11.070

5. AbouEl-Hamd, O. R., Sweedan, A. M. I., El-Ariss, B., & El-Sawy, K. M. (2023). Experimental and numerical investigation of the behavior of steel beams strengthened by bolted hybrid FRP composites. Buildings, 13(3), 824. https://doi.org/10.3390/buildings13030824

6. Wang, S., Li, L., Su, Q., Jiang, X., & Ghafoori, E. (2023). Strengthening of steel beams with adhesively bonded memory-steel strips. Thin-Walled Structures, 189, 110901. https://doi.org/10.1016/j.tws.2023.110901

7. Linghoff, D., Al-Emrani, M., & Kliger, R. (2010). Performance of steel beams strengthened with CFRP laminate – Part 1: Laboratory tests. Composites Part B: Engineering, 41(7), 509–515. https://doi.org/10.1016/j.compositesb.2009.05.008

8. Liu, Y., & Gannon, L. (2009). Experimental behavior and strength of steel beams strengthened while under load. Journal of Constructional Steel Research, 65(6), 1346–1354. https://doi.org/10.1016/j.jcsr.2009.01.008

9. Ridha, S., Abbood, A., & Atshan, A. (2020). Evaluating the efficiency of strengthening hot-rolled I-sectioned steel beams by using additional plates and inclined stiffeners with various widths. In IOP Conference Series: Materials Science and Engineering, 870(1). IOP Publishing. https://bit.ly/44S2dT2

10. Yossef, N. (2015). Strengthening steel I-beams by welding steel plates before or while loading. International Journal of Engineering Research & Technology, 4(07). https://bit.ly/44XiINw

11. Al-Balhawi, A., Shubber, A. N., Al-Asadi, L. S. M., Ibrahim, S. K., Hacheem, Z. A., Jassem, N. H., Dheyab, L. S., & AL-Ridha, A. S. D. (2022). Assessing the structural behavior of steel beams strengthening with additional plates. Materials Today: Proceedings, 62, 4562–4566. https://doi.org/10.1016/j.matpr.2022.05.304

12. Kushnir, Yu. O. (2012). Experimental studies of the strength of steel beams strengthening with horizontal tightenings. Scientific and Technical Collection of KhNAMG: Municipal Utilities. Series: Technical Sciences and Architecture, 105, 168–179. https://khges.kname.edu.ua/index.php/khges/article/view/837/831

13. Mohammadzadeh, M., & Bhowmick, A. (2022). Behavior of steel I-beams reinforced while under load. In Lecture Notes in Civil Engineering (pp. 67–79). Singapore: Springer Singapore. https://doi.org/10.1007/978-981-19-0656-5_6

14. Mohammadzadeh, M. (2022). Behaviour of steel I-beams reinforced while under load (PhD thesis). Concordia University, Montreal, Canada. https://spectrum.library.concordia.ca/id/eprint/991496/1/Mohammadzadeh_PhD_S2023.pdf

15. Taoum, A., Jiao, H., & Holloway, D. (2015). Using locally pre-stressed reinforcing bars to restore the capacity of severely damaged steel beams. International Journal of Steel Structures, 15(1), 125–134. https://doi.org/10.1007/s13296-015-3009-1

16. Taoum, A., Jiao, H., & Holloway, D. (2015). Upgrading steel I-beams using local post-tensioning. Journal of Constructional Steel Research, 113, 127–134. https://doi.org/10.1016/j.jcsr.2015.06.012

17. Szewczyk, P., & Szumigała, M. (2021). Optimal design of steel–concrete composite beams strengthened under load. Materials, 14(16), 4715. https://doi.org/10.3390/ma14164715

18. El-Zohairy, A., & Salim, H. (2017). Parametric study for post-tensioned composite beams with external tendons. Advances in Structural Engineering, 20(10), 1433–1450. https://doi.org/10.1177/1369433216684352
19. Ізбаш, М. Ю. (2008). Локально попередньо напружені сталезалізобетонні конструкції для нового будівництва та реконструкції (Автореф. дис. д-ра техн. наук, спец. 05.23.01). ХДАБА. http://lib.kart.edu.ua/bitstream/123456789/05985/1/aref_Izbash.pdf
20. Shemet, R. (2007). Steel-reinforced concrete continuous locally prestressed beams (Candidate of Technical Sciences thesis). Technical University of Construction and Architecture, Kharkiv, Ukraine. http://lib.kart.edu.ua/handle/123456789/6866
21. Галінська, Т. А., Пенц, В. Ф., та Кушнір, Ю. О. (2014). Підсилення сталебетонних балок попередньо-напруженими затяжками при реконструкції будівель і споруд. Матеріали IV міжнар. конф. "Будівництво, реконструкція та реставрація муніципальних будівель", листопад–грудень 2014 р., 24–27. https://eprints.kname.edu.ua/38928/1/КНИГА%20по%20конференции2014.pdf

18 El-Zohairy, A., & Salim, H. (2017). Parametric study for post-tensioned composite beams with external tendons. Advances in Structural Engineering, 20(10), 1433–1450. https://doi.org/10.1177/1369433216684352
19. Izbash, M. (2008). Locally prestressed steel-reinforced concrete structures for new construction and reconstruction (Abstract of the Doctoral thesis). Kharkiv, Ukraine. http://lib.kart.edu.ua/bitstream/123456789/05985/1/aref_Izbash.pdf

20. Shemet, R. (2007). Steel-reinforced concrete continuous locally prestressed beams (Candidate of Technical Sciences thesis). Technical University of Construction and Architecture, Kharkiv, Ukraine. http://lib.kart.edu.ua/handle/123456789/6866
21. Galinska, T., Pents, V., & Kushnir, Y. (2014). Strengthening of steel-concrete beams with prestressed tensioning during the reconstruction of buildings and structures. In Proceedings of the IV International Conference "Construction, Reconstruction and Restoration of Municipal Buildings" (pp. 24–27). https://eprints.kname.edu.ua/38928/1/КНИГА%20по%20конференции2014.pdf

Река А.В.
Національний університет «Полтавська політехніка імені Юрія Кондратюка»
https://orcid.org/0009-0002-7136-8585

Галінська Т.А.*
Національний університет «Полтавська політехніка імені Юрія Кондратюка»
https://orcid.org/0000-0002-6138-2757

Овсій Д.М.
Національний університет «Полтавська політехніка імені Юрія Кондратюка»
https://orcid.org/0000-0001-7007-1857

Мухліс Гаджієв
Азербайджанський архітектурно-будівельний університет
https://orcid.org/0000-0001-6782-0941

Підсилення поперечних перерізів сталевих двутаврових балок в зоні розтягу: огляд наукових досліджень

В результаті довготривалої експлуатації сталеві балкові конструкції в існуючих будівлях і спорудах зазнають фізичного зношення, часткового чи повного руйнування під впливом агресивного середовища, статичних і динамічних навантажень вибухового типу. Під впливом агресивного середовища з підвищеною вологістю і перепадом температур, який характеризується циклічним заморожуванням та відтаюванням, наявністю хімічно активних сполук в рідині і повітрі, які безпосередньо контактують з конструкцією, в стальних балкових елементах виникають пошкодження у вигляді: появи і розвитку поверхневої корозії різної глибини на визначених ділянках чи по всій їх поверхні. Випадкова або непередбачена дія позапроектного статичного чи динамічного навантаження вибухового типу, також можуть призвести до перевантаження і появи ознак значного фізичного зносу і зрілої форми видимого руйнування сталевих балкових конструктивних елементів, таких як: залишкові деформації у вигляді прогинів, величина яких перевищує гранично допустиме значення; поява і розвиток тріщин різної орієнтації в полицях і стінці перерізу балки у зонах її згину і зрізу, особливо у місцях поблизу зварних швів чи місць зміни площі перерізу, де виникають локальні зміни структури матеріалу чи додаткові внутрішні напруження різної інтенсивності; наявність загального вигину поздовжньої осі балкового елементу із вертикальної площини, величина якого перевищує гранично допустиме значення; точкові чи локальні вминання полиці в стиснутій зоні чи вертикальної стінки, ребер жорсткості в перерізі балки на величину, що перевищує гранично допустиме значення.
В статті проведено огляд наукових досліджень, які присвячені методам і способам підсилення сталевих балкових конструктивних елементів шляхом збільшення (нарощування) поперечних перерізів за допомогою додаткових елементів із сталевих прокатних профілів, пластин, арматурних стержнів та пластин із полімерних матеріалів. Обгрунтовані основні висновки і напрямки подальших наукових досліджень ефективних методів і способів підсилення сталевих балкових конструктивних елементів, що здійснюються шляхом збільшення (нарощування) їх поперечних перерізів, які маємо можливість застосувати при ремонті та реконструкції будівель і споруд.

Ключові слова: сталеві балкові конструктивні елементи, ремонт та підсилення, збільшення поперечного перерізу, огляд, наукові дослідження

*Адреса для листування E-mail: galinska@i.ua

Збірник наукових праць. Галузеве машинобудування, будівництво
Academic journal. Industrial Machine Building, Civil Engineering
http://journals.nupp.edu.ua/znp
https://doi.org/10.26906/znp.2024.63.3886

UDC 624.016:624.042.65

Anton Hasenko
National University «Yuri Kondratyuk Poltava Polytechnic»
https://orcid.org/00000-0003-1045-8077

Kostiantyn Shtanko *
National University «Yuri Kondratyuk Poltava Polytechnic»
https://orcid.org/0009-0008-2070-1628

Results of experimental studies of civil defense structures self-weight pre-stressed continuous three-span steel-reinforced concrete slabs

The paper presents results of experimentally tested samples of resource-saving non-cut three-span steel-reinforced concrete slabs that can be used for the construction of floors of civil defense structures. The specimens differed in the lengths of the concreting grips, which made it possible to study the development of deflections in the extreme and middle spans due to changes in the stiffness of the section at the supports. The length of the concreting section is determined by the points of zero bending moments. During the first stage of concreting, the middle span of the steel structure bends downward due to the concrete mix's own weight, which causes the extreme sections that are not under load to bend upward. After the concrete of the first stage reaches the design strength, the concrete of the outer spans is concreted. At the same time, the extreme spans bend downward due to the weight of the concrete mixture, forcing the middle span, which already has a steel-reinforced concrete section, to bend upward.

Keywords: experiment, continuous scheme, steel-reinforced concrete slabs, resource-saving manufacturing technology.

*Corresponding author E-mail: gasentk@gmail.com

Introduction

The problem of ensuring a uniform stress distribution in continuous steel–concrete composite slabs remains a pressing issue in modern construction. The application of prestressing technologies helps to reduce stress irregularities; however, the question of effectively inducing prestressing in experimental specimens of such slabs has not yet been sufficiently investigated. The study of this process is essential for improving the service performance of structures and enhancing their load-bearing capacity.

Review of the research sources and publications

Steel–concrete composite structures are employed both in new construction and in the reconstruction of buildings and facilities, achieved through the effective combination of predominantly bar-type steel elements and cast-in-place concrete [1]. Multi-span flexural steel–concrete composite structures, in which the cast-in-place reinforced concrete slab serves as the compressed planar component of the cross-section and the profiled steel member functions as the tensioned bar component, have proven their effectiveness due to the high constructability of their installation and their substantial load-bearing capacity in both civil and industrial construction [2; 3]. In addition, the cast-in-place reinforced concrete slab provides a rigid diaphragm for the floor system and enables the subdivision of the building's internal space into multiple storeys [4].

Quite often, in order to improve the constructability of such floor systems and reduce construction time, the cast-in-place reinforced concrete slab is arranged on permanent formwork made of profiled sheeting [5]. When composite action between the cast-in-place slab and the profiled steel sheeting of the permanent formwork is ensured through the ribbed surface of the decking, such slabs become comparable to reinforced concrete floor systems in terms of material consumption, since the profiled sheeting functions not only as formwork but also as external reinforcement of the slab [6].

The aforementioned advantages of steel–concrete composite slabs—namely, increased load-bearing capacity and high installation efficiency—enable their application in the construction of floor systems for protective structures of civil defense facilities [7]. However, the wide implementation of this structural solution in practice is limited by the absence of ribbed profiled sheeting on the building materials market, due to the more complex rolling technology required, as

well as by the low fire and corrosion resistance of the exposed bottom surface of the profiled steel sheeting.

With equal support spacing of continuous steel–concrete composite slabs, the profiled sheeting of the middle spans, when employed as the working reinforcement of the slab, is subjected to lower stresses than that of the end spans [8]. To achieve uniform utilization of the load-bearing capacity of the profiled sheeting in continuous steel–concrete composite slabs, it is advisable to design the end spans longer than the central span [9].

Definition of unsolved aspects of the problem

In modern construction, it is essential to ensure the stability and durability of structures. One approach to enhancing these performance indicators is the identification of effective technologies and methods for inducing prestressing in structural elements, which contribute to achieving an optimal stress distribution within them [10]. The study of this process enables the identification of best practices applied in construction and their subsequent implementation in production.

Problem statement

The aim of this study is to present the results of experimental investigations of resource-efficient, continuous three-span prestressed steel–concrete composite slab specimens, which may be utilized in the construction of floor systems for protective structures of civil defense facilities.

Basic material and results

The tests of the steel–concrete composite slab specimens were conducted when the concrete had reached an age of more than 28 days. The loading was applied using small-sized artificial weights—hollow ceramic bricks. To determine the weight of the bricks, a selective weighing procedure was performed: 5 bricks were weighed from each batch of 50 used bricks (i.e., approximately 1/10 of the total number of bricks employed for loading).

As a result of the experimental investigations of the two continuous steel–concrete composite slab specimens, data from measuring instruments installed according to the developed schemes provided information on both the slab deflections (deformability) and longitudinal strains in the extreme fibers. These measurements allowed for the subsequent determination of stresses and load-bearing capacity.

The experimental studies of the slab specimens were extended over time due to the period required for the cast-in-place reinforced concrete slab to attain its design strength. As previously noted, the fabrication—specifically, the concreting—of the slab specimens was performed in two stages. Therefore, the overall fabrication period for the steel–concrete composite slab specimens was approximately two months. During each concreting stage, deflections at characteristic cross-sections of the specimen, caused by the weight of the freshly placed concrete, were measured. An analysis was conducted on the variation of deflections along the length of the specimen and on the strains of the normal cross-section throughout the two fabrication stages and during the application of the service load.

Figure 1 shows the general view of one of the specimens under loading with small-sized weights (hollow ceramic bricks).

Figure 1 – General view of specimen 1.7–2.3–1.7 SCCS 0.53 × 6.0 under maximum loading.

Figure 2 presents the graphs of the maximum deflections along the length of the steel–concrete composite slab specimens at the end of the two concreting stages and under the maximum applied service load with small-sized weights. For a clearer analysis of the influence of concreting segment width on the deformability of the three-span slabs, the general view of each tested specimen is shown above the corresponding deflection graph.

Figure 3 illustrates the development of deflections in the end and central spans at each stage of the steel–concrete composite slab fabrication and during loading with bricks. As can be seen from the deflection variation graphs in Figure 3, extending the first concreting stage beyond the intermediate supports results in more limited adjustment of internal forces during the second concreting stage, compared to concreting the first stage up to the intermediate supports. Consequently, the load-bearing capacity of the continuous slab is exhausted in the central span, where, at the moment of failure, deflections are 32% greater than in the end spans.

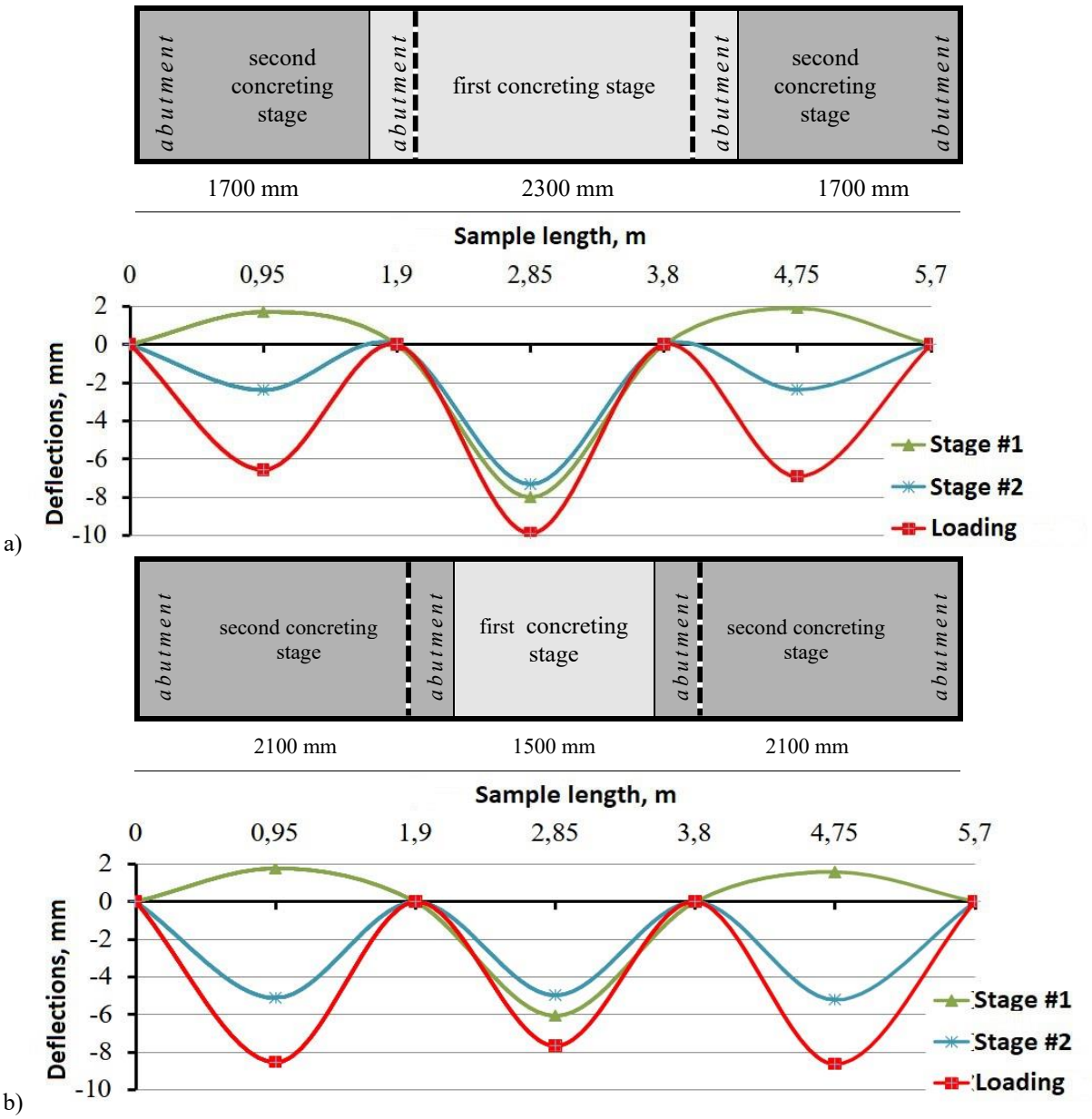

Figure 2 – Deflection variations of the specimens at the end of the two concreting stages and under maximum applied load: (a) 1.7–2.3–1.7 SCCS (0.53 × 6.0 m); (b) 2.1–1.5–2.1 SCCS (0.53 × 6.0 m).

For the slab with the first segment concreted up to the intermediate supports (specimen 2.1–1.5–2.1 SCCS 0.53 × 6.0), uniform deformability was achieved across all three spans (Figure 3b), with a deflection difference of 11.2% under maximum load.

Figure 4 shows the development of relative strains in the bottom and top fibers of the cross-sections at the midpoints of the left, central, and right spans of the steel–concrete composite slab specimens as the load in the cross-sections increased. The vertical axis represents the total load applied to the specimen, including its self-weight.

From the strain distribution diagrams in Figure 4, it can be observed that, for the specimen with a steel–concrete cross-section at the intermediate supports, at the moment of the second concreting stage and under the maximum applied load, the strain in the most tensioned fiber of the central span is 12.5% higher than in the end spans. For the second specimen, the corresponding strain difference in these cross-sections is 4.1%. Moreover, the maximum tensile strains in the second specimen under the same load level decreased by 44.7%.

Thus, based on the measurements of relative strains, the same conclusion regarding the segment lengths in two-stage concreting can be drawn as from the analysis of deflection development: for the investigated continuous three-span slabs with an external reinforcement ratio of 1.7% provided by the profiled sheeting, the first concreting stage should not extend to the intermediate supports by 1/10 of the span. Under this condition, the exhaustion of load-bearing capacity and deformability across all three spans occurs at the same level of applied external load. In this case, the steel decking in the span areas acts solely in tension, and the load-bearing capacity is governed by the attainment of yield stresses in the bottom flanges of the profiled sheeting.

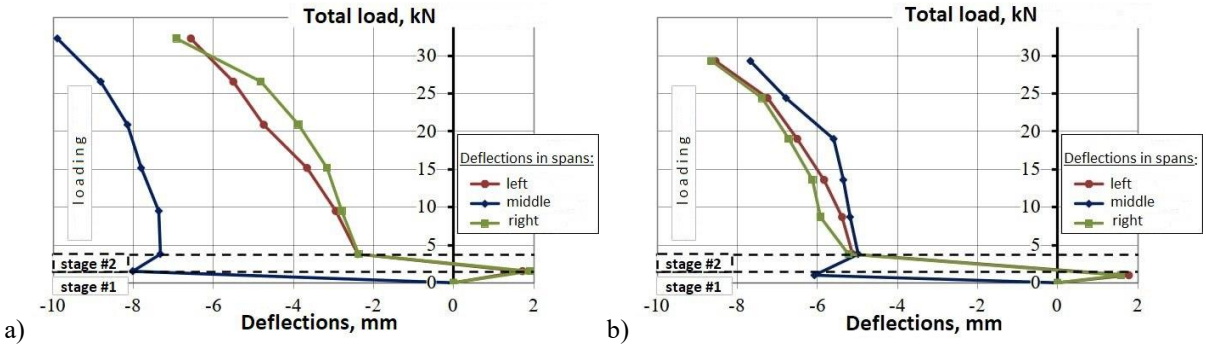

Figure 3 – Deflection development in the spans of steel–concrete composite slab specimens during each fabrication stage and under applied loading: (a) 1.7–2.3–1.7 SCCS (0.53 × 6.0 m); (b) 2.1–1.5–2.1 SCCS (0.53 × 6.0 m).

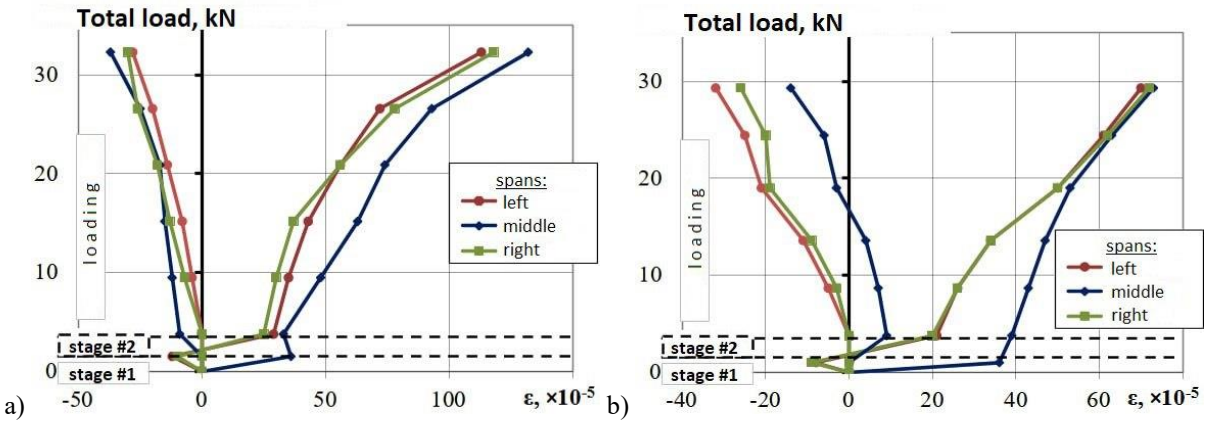

Figure 4 – Increments of relative strains in the bottom and top fibers of the cross-sections of the steel-concrete composite slab specimens: a) 1.7–2.3–1.7 SCCS (0.53 × 6.0 m); b) 2.1–1.5–2.1 SCCS (0.53 × 6.0 m)

Failure of the steel–concrete composite slabs occurred suddenly due to the formation of cracks in the top concrete zone at the intermediate supports (on the support face closer to the central span; see Figure 5), in the region of maximum bending moment within the tensile zone of the top fibers of the cross-section. No relative slip between the concrete slab and the steel decking was observed.

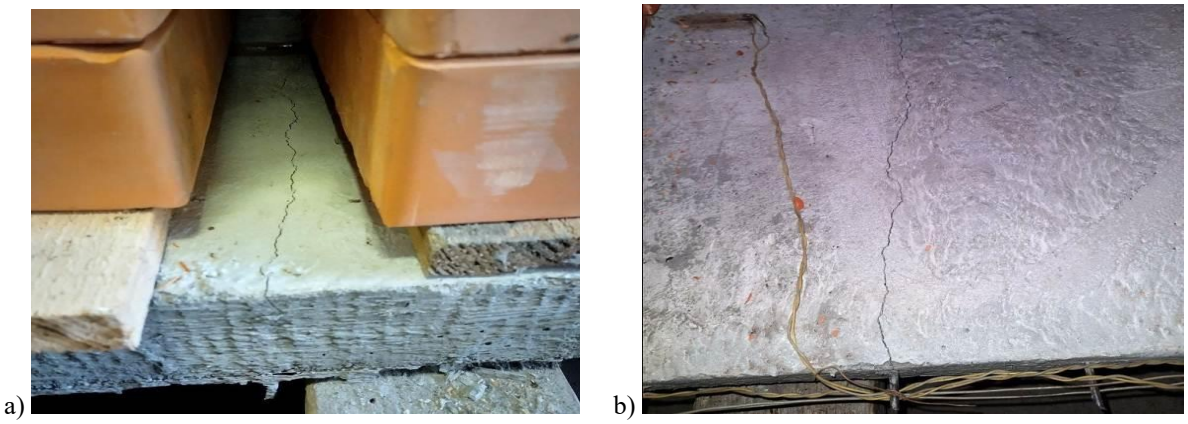

Figure 5 – Crack formation at the central support during the failure of the steel–concrete composite slabs

The proposed and experimentally investigated two-stage concreting technology for continuous cast-in-place steel–concrete floor slabs was implemented during the construction of a three-story superstructure atop a three-story public building in Poltava. Figure 6 shows the general view prior to casting the cast-in-place reinforced concrete slab of the steel beam framework, with the profiled permanent formwork in place and flexible anchors made of reinforcing bars welded in position. Figure 7 shows the overall arrangement of the supports — secondary steel beams — and the continuous cast-in-place reinforced concrete floor slab.

The application of this cast-in-place slab using the two-stage concreting technology allowed a reduction in steel consumption of up to 5% per square meter of the floor slab.

a)

b)

Figure 6 – General view prior to casting the cast-in-place reinforced concrete slab of the steel beam framework with the profiled permanent formwork in place (a) and flexible reinforcing bar anchors welded in position (b)

a)

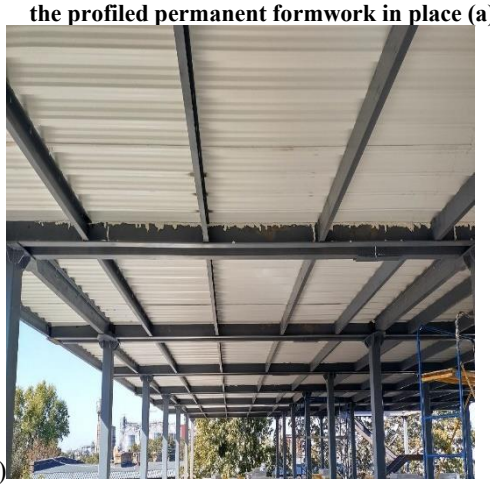

b)

Figure 7 – General view of the support arrangement – the secondary steel beams – of the continuous cast-in-place reinforced concrete floor slab from below

Conclusions

Pre-stressing of bent steel–concrete composite structures, taking into account material nonlinearity, was studied using continuous three-span floor slabs as an example. The effectiveness of the two-stage fabrication technology for slabs prestressed by their self-weight, as well as the method for inducing initial camber, was experimentally demonstrated on two continuous three-span steel–concrete composite slab specimens, 6 m in length, cast on permanent profiled-sheet formwork. It was established that, for the investigated slabs with an external reinforcement ratio of 1.7%, the concreting of the central span during the first stage should not extend to the intermediate supports by 1/10 of the span. Under this condition, the exhaustion of load-bearing capacity and deformability in all three spans occurs at the same level of applied external load.

References

1. Стороженко Л.І. (2013). Проблеми створення та проектування сталезалізобетонних конструкцій. *Зб. наук. пр. НДІБК: Будівельні конструкції*, 78(1), 129-136.

2. Storozhenko L., Yermolenko D., Gasii G. (2018). Investigation of the Deformation State of a Composite Cable Space Frame Structures with a Photogrammetric Method. *Intern. Journal of Engineering & Technology*. *7* (3.2), 442-446.
http://doi.org/10.14419/ijet.v7i3.2.14568

3. Ватуля Г.Л., Орел Е.Ф. (2012). Вплив параметрів перерізу на несучу здатність сталебетонних конструкцій. *Зб. наук. пр. Галузеве машинобудування, будівництво, 3* (33), 30-34.

4. Гасенко А.В., Новицький О.П., Пенц В.Ф. (2021). Реконструкція багатоповерхових промислових будівель під доступне житло із використанням ресурсозбережувальних конструктивних рішень. *Зб. наук. пр. Вісник НУВГП, серія Технічні науки, 2 (94),* 27-40.
https://doi.org/10.31713/vt220214

5. Стороженко Л.І., Лапенко О.І. (2008). *Залізобетонні конструкції в незнімній опалубці*: *монографія*, 312 с.

6. Бобало Т.В. (2012). Порівняння результатів експериментального дослідження сталебетонних балок із комбінованим армуванням з результатами розрахунку за діючими національними нормами. *Архітектура і сільськогосподарське будівництво: Вісник НАУ, 13,* 34-43.

7. ДБН В.2.2-5:2023. Захисні споруди цивільного захисту. [Чинний з 01-11-2023]. К.: Міністерство розвитку громад, територій та інфраструктури України, 115 с.

8. Семко О.В. Гасенко А.В., Фенко О.Г., Дарієнко В.В. (2022). Раціональне використання несучої здатності сталевих профільованих листів незнімної опалубки сталезалізобетонних перекриттів. *Зб. наук. пр. КНТУ: Центральноукраїнський науковий вісник. Серія: Технічні науки*, *5* (36), Ч. 2, 153-161.
https://doi.org/10.32515/2664-262X.2022.5(36).153-161

9. Семко О.В., Гасенко А.В. (17-20 травня 2022 р.) Оптимізація кроку опор нерозрізних балок сталезалізобетонного самонапруженого перекриття. *Тези доповідей IX Міжн. конф. «Актуальні проблеми інженерної механіки»*. 153-154.

10. Hasenko A.V. (2021). Previous self-stresses creation methods review in bent steel reinforced concrete structures with solid cross section. *Academic journal. Series: Industrial Machine Building, Civil Engineering*, *2* (57), 82-89.
https://doi.org/10.26906/znp.2021.57.2589

1. Storozhenko, L. I. (2013). Problems of creation and design of steel–concrete composite structures. *Collection of Scientific Works of the Research Institute of Building Structures: Building Structures*, 78(1), 129–136.

2. Storozhenko L., Yermolenko D., Gasii G. (2018). Investigation of the Deformation State of a Composite Cable Space Frame Structures with a Photogrammetric Method. *Intern. Journal of Engineering & Technology*. *7* (3.2), 442-446.
http://doi.org/10.14419/ijet.v7i3.2.14568

3. Vatulia, H. L., & Orel, E. F. (2012). Influence of cross-section parameters on the load-bearing capacity of steel–concrete structures. *Collection of Scientific Works: Industrial Engineering, Construction*, 3(33), 30–34.

4. Hasenko, A. V., Novytskyi, O. P., & Pents, V. F. (2021). Reconstruction of multi-story industrial buildings into affordable housing using resource-saving structural solutions. *Bulletin of NUVGP, Technical Sciences Series*, 2(94), 27–40.
https://doi.org/10.31713/vt220214

5. Storozhenko, L. I., & Lapenko, O. I. (2008). *Reinforced concrete structures in permanent formwork: Monograph* (312 pp.).

6. Bobalo, T. V. (2012). Comparison of experimental results for steel–concrete beams with combined reinforcement with calculations according to current national standards. *Architecture and Agricultural Construction: Bulletin of NAU*, 13, 34–43.

7. DBN V.2.2-5:2023. (2023). *Civil protection shelters* [Effective from 01-11-2023]. Kyiv: Ministry for Communities, Territories and Infrastructure Development of Ukraine, 115 pp.

8. Semko, O. V., Hasenko, A. V., Fenko, O. H., & Darienko, V. V. (2022). Rational use of the load-bearing capacity of steel profiled sheets of permanent formwork in steel–concrete composite floor slabs. *Collection of Scientific Works of KNTU: Central Ukrainian Scientific Bulletin, Technical Sciences Series*, 5(36), Part 2, 153–161.
https://doi.org/10.32515/2664-262X.2022.5(36).153-161

9. Semko, O. V., & Hasenko, A. V. (2022, May 17–20). Optimization of support spacing for continuous steel–concrete prestressed floor beams. In *Proceedings of the IX International Conference "Current Issues of Engineering Mechanics"* (pp. 153–154).

10. Hasenko A.V. (2021). Previous self-stresses creation methods review in bent steel reinforced concrete structures with solid cross section. *Academic journal. Series: Industrial Machine Building, Civil Engineering*, *2* (57), 82-89.
https://doi.org/10.26906/znp.2021.57.2589

Гасенко А.В.
Національний університет «Полтавська політехніка імені Юрія Кондратюка»
https://orcid.org/00000-0003-1045-8077

Штанько К.Г.*
Національний університет «Полтавська політехніка імені Юрія Кондратюка»
https://orcid.org/0009-0008-2070-1628

Результати експериментальних досліджень попередньо напружених власною вагою нерозрізних трипролітних сталезалізобетонних плит споруд цивільного захисту

Проблема забезпечення рівномірного розподілу напружень у нерозрізних сталезалізобетонних плитах є актуальною для сучасного будівництва. Використання технологій попереднього напруження дозволяє зменшити нерівномірний розподіл напружень у перерізах таких плит. У статті представлені результати експериментальних випробувань зразків ресурсозберігаючих нерозрізних трипрогонових сталезалізобетонних плит, які можуть бути використані для будівництва перекрить споруд цивільного захисту. Зразки відрізнялися довжинами бетонувальних ділянок, що дозволило дослідити розвиток прогинів у крайніх та середніх прольотах через зміну жорсткості перерізу на опорах. Довжина бетонуючої ділянки визначається точками нульових згинальних моментів. Під час першого етапу бетонування середній проліт сталевої конструкції згинається вниз під дією власної ваги бетонної суміші, що призводить до згину крайніх ділянок, які не перебувають під навантаженням, вгору. Після досягнення бетоном першого етапу проектної міцності бетонують бетон зовнішніх прольотів. Водночас крайні прольоти під дією ваги бетонної суміші згинаються вниз, змушуючи середній проліт, який вже має сталезалізобетонний переріз, згинатися вгору. Експериментально доведено ефективність двостадійної технології виготовлення попередньо напружених від власної ваги й технології створення, за допомогою яких створюють попередні вигини, двох зразків нерозрізних трипролітних сталезалізобетонних плит довжиною 6 м, виконаних по незнімній опалубці із профільованого настилу. Встановлено, що для досліджених плит із коефіцієнтом зовнішнього армування 1,7%, бетонування середнього прольоту в першому етапі слід не доводити до середніх опор на 1/10 прольоту. За такої умови вичерпування несучої здатності та деформативності в трьох прольотах буде при однаковому рівні зовнішнього навантаження.

Ключові слова: експеримент, нерозрізна схема, сталезалізобетонні плити, ресурсоощадна технологія виготовлення.

*Адреса для листування E-mail: gasentk@gmail.com

Збірник наукових праць. Галузеве машинобудування, будівництво
Academic journal. Industrial Machine Building, Civil Engineering
http://journals.nupp.edu.ua/znp
https://doi.org/10.26906/znp.2024.63.3872

UDC: 624.154:624.138.2

Oleksandr Novytskyi
Sumy National Agrarian University
https://orcid.org/0000-0001-5923-9524

Yevhenii Skrypka *
Sumy National Agrarian University
https://orcid.org/0009-0003-1405-8115

Technological Features of Foundation Construction Using Vibro-Reinforced Soil-Cement Piles

The article examines the technological features of foundation construction using vibro-reinforced soil-cement piles. The technology is based on the bore-mixing method, which allows for pile formation without soil excavation, utilizing the existing soil as the main component of the soil-cement mixture. The use of vibro-reinforced soil-cement piles significantly increases the load-bearing capacity of foundations, reduces labor intensity in the construction process, and ensures the stable performance of the foundation in complex engineering and geological conditions. The article explores the specifics of the technological process of manufacturing vibro-reinforced soil-cement piles, particularly their formation, vibro-compaction, and the use of a high-frequency vibrator when embedding the reinforcement cage. It has been proven that the physical and mechanical properties of soil-cement piles, such as compressive strength, improve when deep vibrators are used in pile installation. A comparative analysis of vibro-reinforced and conventional soil-cement piles has demonstrated a significant increase in the load-bearing capacity of vibro-reinforced piles, which allows for a reduction in their number within foundation structures and leads to lower construction costs. Additionally, the article compares the soil cementation methods Jet Grouting, Pressure Grouting, and Deep Soil Mixing, which are used to improve soil bearing capacity and reduce deformations. Each of these technologies has its own characteristics that determine their effectiveness under different conditions. The advantages and disadvantages of each method are examined, including the ability to reach great depths, cost-effectiveness, and localized application.

Keywords: soil-cement piles, foundations, vibration reinforcement, vibration compaction, manufacturing technology.

*Corresponding author E-mail: e.skrypka.gs@snau.edu.ua

Introduction

Modern construction requires the use of reliable and efficient foundation technologies that ensure the stability of buildings and structures in challenging geotechnical conditions. With the advancement of construction technologies, there is a growing need for methods that strengthen weak soils and improve their physical and mechanical properties. One of the most effective solutions is soil-cement piles, which combine the advantages of the deep mixing method and deep vibro-compaction.

Soil-cement piles are widely used for building foundations in areas with low soil-bearing capacity. Their construction methodology significantly reduces settlement, enhances foundation stability, and minimizes the risks of uneven deformations. The core principle of this technology involves deep mixing of soil with a cement slurry without removing the soil, ensuring a uniform distribution of material and forming a strong soil-cement element.

Beyond improving the physical and mechanical properties of the soil, this technology offers several other significant advantages. It reduces the time and cost of foundation works, minimizes environmental impact by limiting earthworks, and increases the durability of structures. Additionally, the deep mixing method effectively prevents void formation and soil subsidence, making it particularly relevant for construction in seismically active regions or on unstable terrains.

This article examines the features of soil-cement pile technology, its main stages, quality control methods, and comparative efficiency in relation to other foundation construction techniques.

The design and calculation of foundations on soil-cement piles are based on modern regulatory documents, such as Eurocode 7 [1], which defines the general principles of geotechnical design.

Review of the research sources and publications.

Modern scientific studies in the field of soil-cement pile installation using deep mixing and vibro-compaction methods focus on increasing technological efficiency, reducing material consumption, and ensuring structural reliability under weak soil conditions. In particular, works [10,11] analyze the economic feasibility and design features of vibro-reinforced soil-cement piles, demonstrating their advantages in reducing the number of foundation elements without compromising load-bearing capacity.

Monographs [7,8] provide a detailed examination of the deep mixing method and its application under various engineering and geological conditions, including loess and sandy soils. Study [9] emphasizes the role of vibro-reinforcement in ensuring pile integrity and base stability.

The regulatory framework, including Eurocode 7 [1], Eurocode 2 [2], and standard EN 1536 [5], sets the requirements for the design and execution of special geotechnical works, defining technical criteria for quality control and structural reliability assessment.

Study [13] presents international experience with the Deep Mixing method for ground improvement, summarizing research findings and practical implementation across different countries.

Definition of unsolved aspects of the problem

Currently, there are no clearly defined standards for the installation technology of vibro-reinforced soil-cement piles in construction practice. As a result, various technical solutions are employed, leading to inconsistencies in the execution of works. This variability complicates quality control and reduces the predictability of results. Moreover, inconsistencies in the selection of process parameters-such as mixing speed or reinforcement insertion method-can negatively affect the strength and stability of the piles. Consequently, this may reduce foundation reliability, which is particularly critical in complex soil conditions or under high loads.

Therefore, there is a pressing need to develop a unified construction methodology that ensures consistent quality, adequate load-bearing capacity, and long-term durability of foundations.

Problem statement

Considering the identified lack of standardized approaches to the construction of soil-cement piles, the main objective of this research is to analyze and improve the technological process of their installation.To achieve this objective, the following tasks were set within the scope of the study:

- to describe the main stages of the technological process of deep mixing and insertion of the reinforcement cage using a deep vibrator;
- to present a sequence of quality control operations at all stages of the technological cycle.

Basic material and results

The essence of the deep mixing technology for soil-cement production lies in the fact that during the drilling of a borehole, the natural soil is loosened without being removed from the borehole. A water-cement slurry is pumped through a swivel equipped on the drilling rig into the zone of loosened soil, where it is thoroughly mixed with the soil using a working nozzle. The loosening of the soil, the supply of the cement slurry, and its mixing with the soil are carried out along the entire length of the soil-cement pile. Once the mixture hardens, a strong soil-cement element is formed, which functions as a pile in the soil. The compressive strength of the soil-cement pile usually reaches up to 10 MPa.

The process of vibratory reinforcement of the pile with a reinforcement cage is carried out immediately after mixing. A deep vibrator is inserted into the cage and secured. The cage is lifted, centered, and then gradually lowered. High-frequency vibrations facilitate the immersion of the cage to the design depth. Deep vibratory compaction of soil-cement piles is performed immediately after the reinforcement cage is installed. The high-frequency deep vibrator, submerged to the design depth, is gradually raised to ensure reverse compaction. The vibration process continues until the entire pile shaft material is fully compacted.

The main stages of soil-cement pile construction, from preparatory work to quality control, will be examined in detail below.

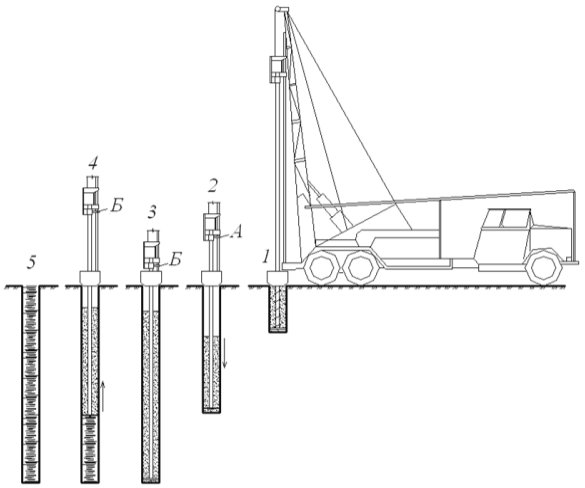

Figure 1. Technological scheme for the construction of soil-cement piles using the Deep Soil Mixing method: 1 – creation of a shallow pit; 2 – penetration of the mixing auger and conversion of the soil into a fluid state; 3 – cavity filled with soil of a fluid consistency; 4 – lifting of the mixing auger and injection of the water-cement grout; 5 –pile ready for reinforcement cage installation: А – water; Б – grout.

Before installing soil-cement piles, it is recommended to conduct field test trials on the adjacent construction site. The test should monitor the rotational speed and penetration rate of the auger. A trial installation of a soil-cement pile in field conditions should be conducted to verify that its physical and mechanical properties meet the specified design requirements.

The use of cement slurries and reinforcement of foundation elements must comply with Eurocode 2 [2], which regulates the design of concrete and reinforced concrete structures.

Various types of sands, loess, loess-like carbonate loams, and sandy loams are suitable for the production of vibratory-reinforced soil-cement piles. The content of water-soluble salts should not exceed 3%, including sulfate salts, which should be no more than 2%. The optimal pH level for soil-cement formation should be between 6 and 8.

Drilling begins by positioning the nozzle at the designated drilling point and lowering it into the soil through rotation. The water-cement slurry is supplied only after the nozzle is fully embedded in the soil. The design depth is achieved by continuous slurry supply using the deep mixing method. The mixing of soil-cement within the pile shaft continues until the material reaches a homogeneous state. Borehole drilling with auger extension starts with the first drill rod, which is equipped with a nozzle for breaking up the soil and mixing it with the cement slurry. The design depth of the borehole is achieved through the gradual addition of rods, which are connected with special couplings. During auger extraction, additional mixing is performed with the introduction of cement suspension. Several mixing cycles can be conducted per auger height to achieve a more uniform soil-cement composition.

Fig. 2. – **Reinforcement Cage Immersion Scheme: 1 – reinforcement cage; 2 – deep vibrator.**

When passing through loess sandy loams and loams above the groundwater level, water should be injected first instead of the water-cement slurry to create a homogeneous fluidized soil mass. The water-cement slurry is supplied during auger extraction. When drilling through water-saturated sands and clayey soils, the water-cement slurry is supplied immediately upon auger penetration.

The mixing efficiency of soil-cement depends on the rotation speed of the loosening tool. Higher rotational speeds improve the mixing process. The quality of soil-cement mixing is also influenced by the auger penetration speed. A lower penetration speed with a constant auger rotation rate results in finer soil loosening, which enhances the homogeneity of the mixture. During forward movement (penetration), the auger should operate at the following speeds:

- In sandy soils: 0.5 m/min, with 60 rotations per minute;
- In clayey soils: 0.3 m/min, with 60 rotations per minute.

The reverse movement of the auger and repeated penetration cycles should be performed at a speed not exceeding 1.0 m/min, ensuring vertical displacement per auger rotation of 16 mm at 60 rotations per minute.

A freshly installed soil-cement pile undergoes vibratory reinforcement immediately. The reinforcement cage is inserted into the soil-cement mixture while it is still in a fluid state. Initially, the cage is embedded under its own weight, and later it is driven further into the pile using vibratory action.

High-frequency vibrations enable the reinforcement cage to be embedded to the design depth. Deep vibro-compaction of soil-cement piles is carried out immediately after the completion of the reinforcement cage installation. A high-frequency deep vibrator, having been lowered to the design depth after the cage insertion, is gradually raised to perform reverse compaction. After the project-specified time, the vibrator is lifted by a distance equal to the sum of the working element length and twice the radius of influence. The vibration process continues until full compaction of the entire pile shaft material is achieved.

Reinforcement cages are manufactured from ribbed reinforcement bars of class A400C. The circular cross-section diameter of the cage must be 150 mm smaller than the pile diameter. The cage is installed immediately after the formation of the pile in soil-cement, which remains in a fluid consistency. At the initial stage, the cage is embedded under its own weight, and subsequently, under the influence of vibration.

During winter installation, when the ambient temperature is below 0°C, antifreeze additives should be added to the slurry to prevent freezing. The additive is mixed with water before preparing the water-cement slurry. At temperatures below -5°C, the water should be preheated. After pile installation in freezing conditions, insulation with thermal materials (such as dry sawdust, fiberglass, mineral wool, or polystyrene foam) is

required for a curing period of seven days. Before foundation preparation, all insulation materials must be completely removed down to the undisturbed soil level.

Quality Control of Reinforced Soil-Cement Piles Since the production of soil-cement piles using the deep mixing method and their vibratory reinforcement are essentially concealed construction processes, quality control measures must be strictly observed to ensure the reliability of the produced soil-cement elements.

After construction, the quality of the soil-cement piles must be verified to confirm their compliance with parameters such as material homogeneity, strength, and dimensions. Quality control of piles installed by the deep mixing method is performed no earlier than seven days after installation, according to national construction standards [3,4], using core drilling of the pile body at 1-meter intervals along its depth, followed by strength testing of extracted cores. The number of control boreholes for core sampling should be at least 5% of the total number of piles.

The normative and calculated characteristics of soil-cement are determined in laboratory conditions and based on field studies, which include the adopted production technology for soil-cement.

The deep mixing method for soil-cement pile production complies with standard EN 1536 [5], which regulates the execution of specialized geotechnical works. Ensuring the quality of vibratory-reinforced soil-cement piles constructed using deep mixing technology is achieved through monitoring:

- Compliance of the cement type and grade with the project specifications;
- Accurate adherence to the design composition and consumption of the water-cement slurry;
- Operating parameters of the grout pump;
- Performance parameters of the deep mixer (rotation frequency, linear penetration speed, and number of passes);
- Operating parameters of the deep vibrator and the vibratory compaction regime;
- The vibratory embedding process of the reinforcement cage;
- The quality of the soil-cement mass and, if necessary, the load-bearing capacity of the soil-cement pile.

Let us consider the three most common soil cementation technologies: Jet Grouting, Pressure Grouting, and Deep Soil Mixing (DSM). All of these methods share a common purpose-improving the bearing capacity of the foundation and reducing its deformations. However, each method has its own specific features that determine its effectiveness under different conditions. Below is a comparison of these methods, highlighting their advantages and disadvantages.

Jet Grouting uses a high-pressure jet of cement grout to break up and mix the soil. This method is highly effective in clayey and sandy soils. Its main advantage is the ability to reach significant depths (up to 50 m or more) and form large-diameter piles. However, it requires complex equipment and involves high cement consumption due to significant grout losses. When piles are installed at great depths, reinforcement with cages is only carried out in the upper part of the pile.

Deep Soil Mixing (DSM) involves mechanically mixing the soil with cement grout, making it more economical compared to Jet Grouting. It is best suited for weak water-saturated soils, ensuring uniform strengthening at depths of up to 30 m. Although it produces a smaller diameter of the treated zone compared to Jet Grouting, this method ensures more stable cement usage with minimal losses.

Pressure Grouting involves injecting cement or another binding grout into the pores and cracks of the soil. This method is most effective when voids need to be filled locally or when fractured rock formations require stabilisation. Its main drawback is the slow execution speed, as the injection grout gradually permeates the soil, requiring additional monitoring.

Thus, it can be concluded that Jet Grouting is the most powerful and versatile method but requires complex equipment for high-pressure grout injection and leads to excess cement consumption due to the nature of the technology, where part of the cement mixture remains outside the pile body.

Additionally, if the soil layers along the pile depth vary in their physical and mechanical properties, the pile diameter may not be maintained consistently and can differ according to the soil parameters. In turn, Deep Soil Mixing is a more accessible and economical option for weak water-saturated soils, whereas Pressure Grouting is used for local applications, strengthening existing buildings and structures, and filling voids in the foundation.

Conclusions

The efficiency of soil-cement foundations primarily lies in the simplicity of their construction technology. The Deep Soil Mixing method benefits from the absence of heavy machinery, reduced transportation costs, and no dependency on the timely delivery of concrete mix.

An analysis of the technological process demonstrates that a proper approach to each stage of work significantly influences the quality of the final result. The application of modern soil stabilization methods contributes to the optimization of construction processes and enhances the reliability of structures.

The key stages of the soil-cement pile formation technology that affect the final outcome include:

1. Preparation stage – Analysis of the geotechnical conditions of the construction site, conduction of engineering and geological investigations, and selection of the optimal pile formation technology. Execution of trial testing and equipment inspection. Verification of the need to comply with special installation requirements, such as performing work in low temperatures.

2. Drilling boreholes – Execution of drilling operations to the specified depth, considering soil characteristics.

3. Injection of cement slurry – Pumping cement slurry under pressure into the borehole and mixing it with the soil to create a homogeneous mixture.

4. Mixing and compaction – Even distribution of the cement-soil mixture and its compaction to achieve the required mechanical properties.

5. Quality control – Testing the strength, homogeneity, and compliance of the piles with technical requirements.

6. Vibro-reinforcement – The process of inserting a steel reinforcement cage and compacting the soil-cement pile.

7. Hardening and curing – The process of the pile gaining strength up to the designed parameters.

Compliance with these technological processes ensures the reliability and durability of soil-cement piles.

References

1. British Standards Institution. (2004). BS EN 1997-1: Eurocode 7 – Geotechnical design – Part 1: General rules. BSI.

2. British Standards Institution. (2004). BS EN 1992-1: Eurocode 2 – Design of concrete structures – Part 1-1: General rules and rules for buildings. BSI.

3. Мінрегіонбуд України. (2012). ДБН В.2.1-10-2009. Зміна №2. Основи та фундаменти споруд ,20 с..

4. Мінрегіонбуд України. (2012). ДБН В.2.1-10-2009. Основи та фундаменти споруд, 107 с.

5. British Standards Institution. (1994). EN 1536: Execution of special geotechnical work – Bored piles. BSI.

6. Reliability and durability of railway transport engineering structure and buildings, 17–19 November 2021, Kharkiv, Ukraine. (2021). AIP Conference Proceedings, 2684(1), 030045. https://pubs.aip.org/aip/acp/article-abstract/2684/1/030045/2893627/Methods-of-soils-cementation?redirectedFrom=fulltext

7. Зоценко, М. Л., Винников, Ю. Л., & Зоценко, В. М. (2016). Бурові ґрунтоцементні палі, які виготовляються за бурозмішувальним методом: Монографія. Друкарня Мадрид.

8. Зоценко, М. Л., Сухоросов, І. М., & Зоценко, Л. М. (2007). Порівняльна характеристика фундаментів будівель і споруд із паль та на армованій основі. *Міжвідомчий науково-технічний збірник наукових праць (Будівництво)*, (66), 405–409. Київ: НДІБК.

9. Нестеренко, Т., Новицький, О., & Воскобійник, С. (2018). Вібровані ґрунтоцементні палі. International Journal of Engineering & Technology, 7(3.2), 269–274.

10. Зоценко, М., & Новицький, О. (2023). Методи цементації ґрунтів. AIP Conference Proceedings, 2684(1), 030045. https://doi.org/10.1063/5.0119941

11. Крисан В.І. Дослідження напружено-деформованого стану грунтового масиву, армованого грунтоцементними елементами, що виготовлені по струминно-змішувальній методиці: дис. ... канд. техн. наук : 05.23.02 / В.І. Крисан ; Полтав. нац. техн. ун-т ім. Ю.Кондратюка. — Полтава, 2010. — 23 с. — укр.

12. Ларцева І.І. Економічна ефективність використання ґрунтоцементних паль як фундаментів будівель і споруд / І.І. Ларцева, Р.В. Петраш, С.С. Петраш // Економіка і регіони. – Полтава: ПолтНТУ, 2006. – №1 (8). – С. 118–121.

13. Denies, N., & Van Lysebetten, G. (2012). General report. Session 4 – Soil mixing 2 – Deep mixing. In International Symposium on Ground Improvement IS-GI (ISSMGE, Brussels).

1. British Standards Institution. (2004). BS EN 1997-1: Eurocode 7 – Geotechnical design – Part 1: General rules. BSI.

2. British Standards Institution. (2004). BS EN 1992-1: Eurocode 2 – Design of concrete structures – Part 1-1: General rules and rules for buildings. BSI.

3. Ministry of Regional Development of Ukraine. (2012). DBN V.2.1-10-2009. Amendment No. 2. Bases and foundations of structures (20 p.). [In Ukrainian].

4. Ministry of Regional Development of Ukraine. (2012). DBN V.2.1-10-2009. Bases and foundations of structures (107 p.). [In Ukrainian].

5. British Standards Institution. (1994). EN 1536: Execution of special geotechnical work – Bored piles. BSI.

6. Reliability and durability of railway transport engineering structure and buildings, 17–19 November 2021, Kharkiv, Ukraine. (2021). AIP Conference Proceedings, 2684(1), 030045. https://pubs.aip.org/aip/acp/article-abstract/2684/1/030045/2893627/Methods-of-soils-cementation?redirectedFrom=fulltext

7. Zotsenko, M. L., Vynnykov, YU. L., & Zotsenko, V. M. (2016). Burovi gruntotsementni pali, yaki vyhotovlyayut′sya za burozmishuval′nym metodom: Monohrafiya [Drilling soil-cement piles manufactured by mixing method: Monograph]. Drukarnya Madryd.

8. Zotsenko, M. L., Sukhorosov, I. M., & Zotsenko, L. M. (2007). Porivnyal′na kharakterystyka fundamentiv budivel′ i sporud iz pal′ ta na armovaniy osnovi. NDIBK, (66), 405–409.

9. Nesterenko, T., Novytskyi, O., & Voskobiynyk, S. (2018). Vibrated soilcement piles. International Journal of Engineering & Technology, 7(3.2), 269–274.

10. Mykola Zotsenko, Oleksandr Novytskyi; Methods of soils cementation. AIP Conf. Proc. 31 May 2023; 2684 (1): 030045. https://doi.org/10.1063/5.0119941

11. Krysan, V. I. (2010). Doslidzhennya napruzheno-deformovanoho stanu hruntovoho masyvu, armovanoho hruntotsementnymy elementamy, shcho vyhotovleni po strumynno-zmishuval′niy metodytsi [Ph.D. thesis, Poltava National Technical University named after Yuriy Kondratyuk].

12. Lartseva, I., Petrash, R. V., & Petrash, S. S. (2006). Ekonomichna efektyvnist′ vykorystannya gruntotsementnykh pal′ yak fundamentiv budivel′ i sporud. Ekonomika i rehiony, (1)8, 118–121.

13. Denies, N., & Van Lysebetten, G. (2012). General report. Session 4 – Soil mixing 2 – Deep mixing. In International Symposium on Ground Improvement IS-GI (ISSMGE, Brussels).

Новицький О.П.
Сумський Національний Аграрний Університет
https://orcid.org/0000-0001-5923-9524

Скрипка Є.О.*
Сумський Національний Аграрний Університет
https://orcid.org/0009-0003-1405-8115

Технологічні особливості влаштування фундаментів із використанням віброармованих ґрунтоцементних паль

У статті розглянуто технологічні особливості влаштування фундаментів із використанням віброармованих ґрунтоцементних паль. Технологія базується на методі бурозмішування, який дозволяє формувати палі без вилучення ґрунту, використовуючи наявний ґрунт як основний компонент ґрунтоцементної суміші. Використання віброармованих ґрунтоцементних паль суттєво підвищує несучу здатність фундаментів, зменшує трудомісткість будівельного процесу та забезпечує стабільну роботу фундаменту в складних інженерно-геологічних умовах. У статті досліджено особливості технологічного процесу виготовлення віброармованих ґрунтоцементних паль, зокрема етапи їх формування, віброущільнення та застосування високочастотного вібратора під час заглиблення арматурного каркасу. Доведено, що фізико-механічні властивості ґрунтоцементних паль, зокрема міцність на стиск, покращуються при використанні глибинних вібраторів під час встановлення паль. Порівняльний аналіз віброармованих і звичайних ґрунтоцементних паль показав суттєве зростання несучої здатності віброармованих паль, що дозволяє зменшити їх кількість у конструкції фундаменту та знизити загальні витрати на будівництво. Крім того, у статті проведено порівняння методів цементації ґрунтів - Jet Grouting, Pressure Grouting і Deep Soil Mixing, які застосовуються для покращення несучої здатності ґрунтів та зменшення деформацій. Кожна з цих технологій має свої особливості, які визначають ефективність їх застосування за різних умов. Розглянуто переваги та недоліки кожного методу, зокрема здатність досягати значних глибин, економічність та можливість локального застосування.

Ключові слова: ґрунтоцементні палі, фундаменти, віброармування, віброущільнення, технологія виготовлення.

*Адреса для листування E-mail: e.skrypka.gs@snau.edu.ua

Збірник наукових праць. Галузеве машинобудування, будівництво
Academic journal. Industrial Machine Building, Civil Engineering
http://journals.nupp.edu.ua/znp
https://doi.org/10.26906/znp.2024.63.3873

UDC 67.15.55 : 67.09.55 : 67.09.91 : 67.29.59

Oleksandr Dryuchko *
National University «Yuri Kondratyuk Poltava Polytechnic»
https://orcid.org/0000-0002-2157-0526

Natalia Bunyakina
National University «Yuri Kondratyuk Poltava Polytechnic»
https://orcid.org/0000-0003-4241-5127

Vasyl Halai
National University «Yuri Kondratyuk Poltava Polytechnic»
https://orcid.org/0000-0002-1205-7923

Bohdan Boriak
National University «Yuri Kondratyuk Poltava Polytechnic»
https://orcid.org/0000-0002-8114-7930

Andrii Tretiak
National University «Yuri Kondratyuk Poltava Polytechnic»
https://orcid.org/0000-0003-3971-3078

Dmytro Kyslytsia
National University «Yuri Kondratyuk Poltava Polytechnic»
https://orcid.org/0009-0005-2007-4220

Elucidation of the technological conditions for the formation of alkali silicates heat-insulating products based on ash-removal of thermal power plants and liquid glass

The raw material mixture from the silicon-like techno genic component the ash-removal of thermal power plants and the preparation methods of waterproof porous heat-insulated materials wide usage for raw mass hot foaming powdered two-stage technology are developed. The development uses the polyfunctional properties of liquid glass as a) the binder component; c) breeder; c) the speed regulator of the clamping mass hardening. Its optimized version begins to solidify at its usual temperature from the moment its "reproduction" is soluble glass and forms a paste-shaped cake with a set of properties necessary for the next fragmentation. The proposed formulation allows compositions processing in various ways, with the formation of granular heat-insulating fillers, materials for thermal insulation in complex structures, slab and shell-like types of thermal insulation materials. The task is set, depending on the goals and features of the tasks being solved; it is possible to conduct several different methods at the final stages of their obtaining. Two stages of the recycling process determine the character and behavior of the rare-glass composite systems constituent components during heat treatment, their strong adhesion to most structural materials and the need to solve billets easy removal problem from the molding unit. Study results can be used in the field of building materials production, in particular porous artificial products, in obtaining granular insulating material and light aggregate for concrete industrial and civil construction, in thermal engineering as thermal insulation, etc.

Keywords: alkaline-silicate heat-insulation composite materials; ash removal; liquid glass; thermal foaming.

*Corresponding author E-mail: dog.chemistry@gmail.com

Introduction

Alkali-silicate porous materials obtained by means of thermal or cold foaming of alkali metals silicates aqueous solutions (soluble glass) or solid alkali silicate hydrogels [1 – 6], are referred to the present-day, efficient inorganic insulates, promising due to the ability to achieve low values of the relative density and thermal conductivity while maintaining sufficient structure strength and easy handling of foaming and induration processes within a wide range of composition formulations. The above benefits are based on the equilibrium and homogeneity of the main raw mixture component: soluble glass and hydrogels based on it.

Composite alkaline-silicate porous thermal-insulating materials, both granulated and block type, contain significant amounts of the gas phase. There are various technological approaches to obtaining such materials at gas development directly in the strata of the formed composition. Moreover, the process of gas development at high temperatures can be based both on the special additives reactions, and on the crystallization and chemically bound water vapors liberation.

Identification of Previously Unsettled Parts of the General Problem

Analysis of the existing suggested raw mixtures formulations and methods of obtaining thermal insulating materials proves that introducing a significant gel formers amount has a serious drawback: the gelling agent breaks the soluble glass structure to form hydro silicic acid gel, which is capable of retaining less water than soluble glass. This adversely affects the porosity of the resulting rare glass compositions. Therefore, there is a need to introduce such substances that are inert to soluble glass at the normal temperature.

In addition, a significant drawback of the known methods is performing air-entrainment at fixed temperatures in the furnace within the range of 300 – 700 °C. Such a mode of heat treatment reveals several contradictory trends. At relatively low temperatures, the air entrainment process is complicated due to the low warming up rate of the raw mass internal areas, resulting in the increased duration of its air-entrainment process. At the same time, the slow warming up of rare-glass mixtures also leads to significant losses of chemically bound water, due to which air-entrainment of the mixtures occurs. The high rate and unevenness of their heating is manifested in the size, regularity of the pores and the strength of the entire porous structure, in the internal ten-sons of the products. Therefore, an important prerequisite for obtaining the expanded material possessing a set of required properties and their reproduction, is compliance with the principle of correspondence between the rate of crystallization and chemically bound water isolation and the rate of new solid silicate structures formation.

In all of the above-described methods, the first stage is to obtain a solid or plastic composition from soluble glass which can then be subjected to heat treatment. At the same time it is not necessary to use different additives that cause coagulation of silicates. It is possible to obtain a plastic composition using soluble glass simply by means of adding an inert disperse component.

The purpose of the Work

The study performed is aimed at the search and development of an optimized raw material mixture variant of the silicon oxide containing techno genic component: fly ash of thermal power plants and methods of obtaining the fly ash based porous alkaline-silicate composite thermal insulating materials of extended application, differing from the analogues by their composition, the content of the starting raw mass, the sequence and modes of the target product formation, the applied technological equipment.

Experimental part

Raw Materials and Regulations for Composite Alkaline-Silicate Insulation Materials Preparation Development

The proposed development is an option for interconnected, interdependent choice of composition combining and complex practical implementation, content of raw material based on techno genic origin liquid glass and a method for utilization an ash-making coal-energy complex by creating wide usage water-resistant, porous, thermal-insulating material.

In the raw mixture, the industrial soluble glass, thermal power plants fly ash of the mixed chemical composition (see Table 1), sticky Portland cement and, additionally, a thickener (pre-staged partially dehydrated hardened “dry glass”) are used.

Table 1- Chemical composition of the thermal power plants fly ash, mass. %

SiO_2	Al_2O_3	Fe_2O_3	MgO	CaO	Na_2O	K_2O	TiO_2	SO_3
51,68	16,75	14,47	0,88	4,38	0,35	2,58	0,86	4,24

In the prepared samples, the fly ash is manifesting good reinforcing properties, high thermal stability, sufficient resistance to aggressive media, has a small bulk density.

At the same time, the results of the authors’ studies [5, 6] (on the ability of alkaline-silicate systems with Al_2O_3 in alkaline media to form insoluble products of $Na_2O{\cdot}Al_2O_3{\cdot}2Si_2O_3{\cdot}nH_2O$) permit to consider aluminum oxide contained in ash to be a modifying component that provides the raw mix with the properties necessary for the targeted product formation.

In forming the raw mix, the results were taken into account on improving the water resistance of alkali silicate composition by means of replacing the two-calcium silicate (belt) hydrophobia components with the sticky Portland cement; the results are presented in [6].

The “setting” rate control of the suggested raw mix during the formation of hydro silicic acid aerogel (depending on the executed tasks purposes) was performed by means of varying properties of the thickener used and by means of regulating the hardened processed mass fragmentation in the further processes and its subsequent hot foaming.

In the present project, the set task of making the targeted porous thermal insulating material is achieved by means of the raw mass hot foaming technology, which procedure includes the four main stages:

1) preparation of the starting raw mixture components and homogenization of the latter;

2) the composite system “gaging” by soluble glass and formation of a persistent gel; fragmentation of the hardened raw mass and placement of the granulate into lined dismountable molds;

3) heating and transferring of the work pieces’ substance into the pyro plastic state (110 – 115 °C); 4)

further hot foaming and reproduction of the regular porous macrostructure of composite systems (130 – 220 °C) and formation of the targeted processed product's properties (500 – 550 °C).

The blowing agent in this case is water (mainly silanol or molecular, strongly bound by hydrogen bonds with unbridged oxygen atoms), which is released during heat treatment of composite systems.

Study Results and Their Discussion

The raw mix prepared according to the optimized formulation, in contrast to the previously considered analogues, starts hardening at the usual temperature from the moment of its "gaging" with soluble glass and forms a plastic cake with the properties necessary for further fragmentation.

The suggested raw mix also permits to overcome the difficulties associated with drying of viscous rare-glass mix to remove a large output amount of water (56 – 62 %) to the water content of 33 – 38 % needed to obtain a rigid hydrogel capable of thermal blowing.

The optimized formulation of the raw mix allows processing of the compositions in various ways, with the formation of thermal insulating materials of extended application. An important prerequisite for their reproduction with the necessary properties system is strict compliance with the regulatory requirements established by the previous empirical studies.

In parallel with the formulation development, the technology of samples manufacturing was being tried. Thereat, the decisive factor, in contrast to the regulations [4], the exclusion of the raw mix granulation stage after heat treatment 110 – 115 °C and the use of sealed closed forms at their temperature annealing.

The suggested hot air entrainment of the silicate compositions structure "blowing" of the systems in a aerogel form passes quickly, avoiding the viscous-adhesive state. The determining factor in the process of the systems thermal activation was the technical performing of their heating reproduced rate [see 7].

The conscious choice of its optimal mode is motivated by empirical data to determine the thermal foaming features of composite systems obtained by the method of differential-thermal analysis (DTA) presented in Fig. 1.

The air entrainment process includes the three main stages, the duration and nature of which depends on the type and amount of water containing the raw mix: – within the range of 100 – 110 °C, the hardened composite system partially transforms into the pseudopyroplastic state and begins to deform with increasing volume;

– within the range of 130 – 147 °C, an intensive release of free and adsorbed water and intensive air entrainment of the sample mass occurs;

– at the temperature values above 147 °C, the removal of constitutional moisture, the completion of restructuring, physical and chemical transformations of composite systems are observed.

Based on the analysis of the thermo graphic data and the macrostructure of the samples obtained, it can be concluded that the greatest contribution to the formation of the product's structure with maximum homogeneity is made by the constitutional water, while removal of the excess adsorption moisture at the initial stages leads to the formation of large through pores and capillary channels in the raw mass. Therefore, the initial rare-glass composition should contain a minimum amount of free and adsorbed water.

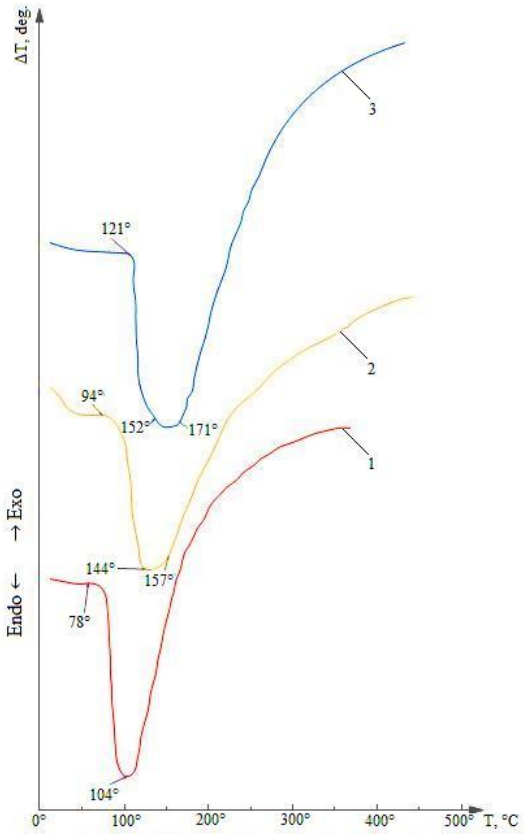

Figure 1 - DTA thermo grams of sodium rare-glass composites aerogels in coordinates ΔT – T, recorded at heating the samples in adequate conditions at different rates: curve 1 – 4 deg. / min.; curve 2 – 7 deg. / min.; curve 3 – 20 deg. / min.

As the efficient ways to reduce the free water's effects, the following ones can be recommended:

– direct thermal dehydration and transformation of soluble glass into aerogel (the basis of the present variant of the suggested technical solution);

– liquid granulation of composite systems (for example, in Al, Ca, Zn, Mg chlorides solutions or their mixtures);

– introducing of mineral fillers or chemical additives into the rare-glass composite system, which leads to the development of gelation processes.

According to the results of the study [6], alkaline-silicate compositions in solutions at heating form a number of hydrated associates with differing properties (see Fig. 2). This permits modifying the properties of the raw mix thickener - grated "dry glass" – by means of the partial unwatering of the purchased product in a liquid state at different temperature values, in the conditions of the technological cycle for the target product formation, simultaneously with the same equipment, without the use of additional equipment.

Meanwhile, the empirically determined physicochemical behavior of composite silicate systems, the features of unwatering and the viscosity state passing, strong adhesion of the intermediate transformation products to

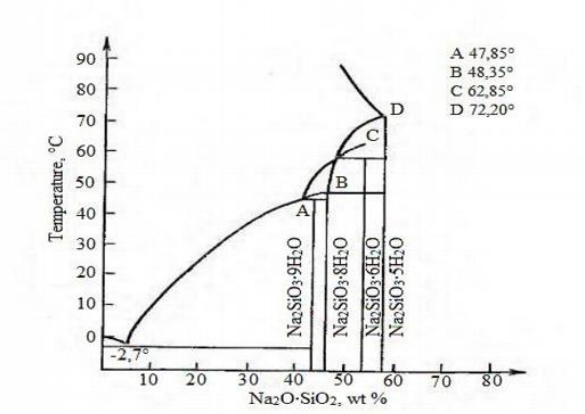

Figure 2 - Solubility in the $Na_2O – SiO_2 – H_2O$ system

metals, ceramics, glass allow to suggest technological regulations, stages, sequence of operations during processing, development and selection of the equipment materials, variations in the methods of obtaining and using porous targeted composites.

Laboratory practice proves that the excess amount of the soluble glass introduced in a liquid state during the "gaging", on the one hand improves the rheological properties, the plasticity of the treated raw mix, and on the other hand, during the subsequent heat treatment, causes additional viscosity of the system, deteriorates the heat transfer conditions, requires more prolonged temperature holding at higher temperature values and leads to the increased energy costs. Therefore, a necessity arises to find an efficient way of regulating the rate of gelling, using the method of shifting the equilibrium of physical and chemical processes of the disperse systems dehydration by adding less hydrated forms of the dried soluble glass; with the degree of the grated "dry glass" dispersion, with its dosage and regulating the processes of the hardened processed mix fragmentation during the granulate formation and the subsequent hot air entrainment.

The improved formulation of the raw mix preparing allows processing compositions in various ways with the formation of insulating materials of extended application: granular insulating filler (Fig. 3, [8]), materials for thermal insulation for the structures complicated in the form (Fig. 4, [9]), the plate and film-like types of insulating materials (Fig. 5, [10]). This task (depending on the purpose and features of the performed tasks) is solved by the capability of performing the final stages by means of several different ways of the products obtaining.

The use of the two stages procedure of the suggested renovation in the technology of preparing the porous thermal insulating materials determines:

1) the nature and the behavior peculiarities of the rare-glass composite systems components during the heat treatment, their strong adhesion manifestation related to most structural materials;
2) the necessity to solve the problem of easy work pieces removal from the formation molds;
3) the choice of the method for lining the internal surfaces of dismountable equipment molds;
4) thermo physical and chemical properties of the used lining material.

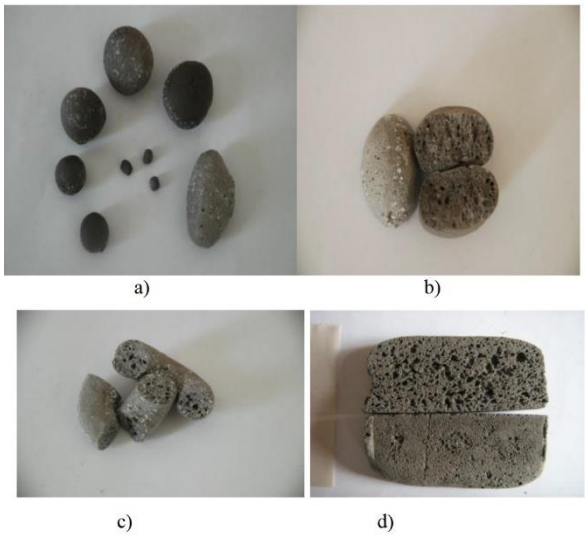

Figure 3 - Illustration of the granular thermal insulating fillers' samples, obtained in the lined molds without limitation of formation volume: a), b) - cutting of iso-sized elements; c) - cutting elements of plastic hardened raw cake of the set preformed thickness; d) –of work pieces, formed in separate dismountable molds.

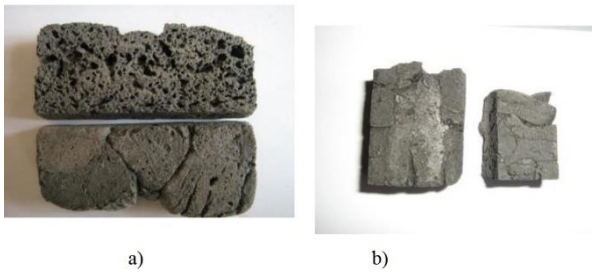

Figure 4 - Illustration of fragments of thermal insulation zones sections in complicated form structures performed by the working zone filling with fragmented elements and the subsequent heat treatment in dismountable equipment of varying complexity: a) - without limiting the free volume of formation; b) - with restriction of formation space

Figure 5 - Illustration of the items fragments formed: a) – in the form of plates; b) – in the form of films

Developed step by step circuit forming composite alkaline silicate porous insulating materials based on soluble glass and fly ash thermal power plants include:

1) the preparation of initial components of raw mix grinding, milling sifting through a sieve (80-315 microns), fly ash thermal power plants, sticky Portland cement, partially dehydrated "dry glass", dried at the given temperature, in accordance with the proposed regulations for the processing of the composition system (105, 190 °C);
2) preparation constituent raw powder components and dosed amount of soluble glass according to proven recipes optimized;
3) homogenization of the of the raw material mixture powder components by thorough mixing (for example, using a mixer);
4) "formation" of raw material by soluble glass and mixing to thickening of the stable gel composition and formation under standard conditions;
5) mechanical fragmentation hardened plastic cake into individual elements (rolling perforated thorn, punching, cut-ting, cutting and other methods) defined size, shape and configuration of the coefficient swelling (depending on the characteristics of tasks,
6) placing the fragmented elements in lined shape with unlimited volume on a heat-resistant pallet separately, without touching the neighbors;
7) heating at a speed of 4-7 degrees. / min and transferring granular material blanks in pyro plastic state (110-115 °C, 15 min exposure, may seal) followed by a two-stage heat treatment hot foaming and play regular porous structure of the body pellet (130-220 °C, 20 min exposure) non sticky carrying blanks to form resistant lined pan and then heating to 500-550 °C and their exposure (to give them satisfactory water and vapor resistance), cooling and receiving the end products.

The features of the suggested project are:

– ease and availability of obtaining components and preparing the raw mix;

– formation of the raw mix directly at its “gaging” with soluble glass under the normal conditions;

– the thermal insulation method is fast;

– the possibility of easy formation and fragmentation of the raw work pieces, their inherent properties makes it possible to spread in time and space separate stages of thermal insulation: the stage of preparation, formation of granulate (possibly, in a specialized site); storage; transportation; technological packing in the working area complying with the increased resistance requirements to the heat transfer (possibly, in the construction site);

– processing of complicated working areas: selection of the raw mix cake thickness, the size and shape of the starting fragmented elements (depending on the target task and in order to provide more tight packing);

– the versatility of the thermal insulation method (based on the manifestation of significant adhesion ability of alkaline-silicate composite systems in relation to most structural materials: metals, ceramics, glass, wood);

– low shrinkage with the suggested formulation of the raw mix and the method of treatment;

– indifference to most components and stability of the thermal insulation material properties, high thermal and chemical resistance, no combustibility, ability to withstand significant temperatures;

– combination of the valuable properties set: low thermal conductivity factor, thermal stability, incombustibility, durability, low cost.

Conclusions

The raw mix of silica-containing techno genic component - fly ash of thermal power plants - and the methods of preparing waterproof porous thermal insulating materials of extended application on its base according to the powder low-temperature technology has been developed using multifunctional properties of soluble glass as: a) a binding component; b) blowing agent; c) the raw mix hardening rate regulator. The physical and chemical, technological aspects of obtaining and using the suggested alkaline-silicate compositions have been considered.

References

1. Рижков І. В. Фізико-хімічні основи формування властивостей розчинної скломісткої суміші / І. В. Рижков, В. С. Толстой. – Харків : Вища школа, 1975. – 139 с.

2. Леонович С. Н. Особливості отримання лужно-силікатних теплоізоляційних матеріалів / С. Н. Леонович, Г. Л. Щукін, А. Л. Беланович та ін. // Наука і техніка. – 2012. – № 6. – С. 45–50.

3. Shi F., Wang L., Liu J., Zeng M. Effect of heat treatment on silica aerogels prepared via ambient drying // Journal of Materials Science and Technology. – 2007. – Vol. 23, No. 3. – P. 402–406.

4. Малявський Н. І. Аероскло – новий лужно-силікатний піноматеріал / Н. І. Малявський, Б. В. Покідько, Л. І. Шумаков // Покрівельні та ізоляційні матеріали. – 2007. – № 1. – С. 28–30.

5. Figovsky O., Borisov Yu., Beilin D. Nanostructured binder for acid-resisting building materials // Scientific Israel – Technological Advantages. – 2012. – Vol. 14, No. 1. – P. 7–12.

1. Ryzhkov I. V., Tolstoy V. S. Physical and chemical fundamentals of forming the soluble glass containing mix properties. Kharkiv : Higher School, 1975. 139 p.

2. Leonovich S. N., Shchukin G. L., Belanovich A. L., et al. Features of obtaining alkaline-silicate heat-insulating materials // Science and Technology. 2012. No. 6. P. 45–50.

3. Shi F., Wang L., Liu J., Zeng M. Effect of heat treatment on silica aerogels prepared via ambient drying // Journal of Materials Science and Technology. 2007. Vol. 23, No. 3. P. 402–406

4. Malyavsky N. I., Pokidko B. V., Shumakov L. I. Aero-glass – a new alkaline-silicate foam material // Roofing and Insulating Materials. 2007. No. 1. P. 28–30.

5. Figovsky O., Borisov Yu., Beilin D. Nanostructured binder for acid-resisting building materials // Scientific Israel – Technological Advantages. 2012. Vol. 14, No. 1. P. 7–12.

6. Фіговський О. Л., Бейлін Д. А., Пономарьов А. Н. Успіхи застосування нанотехнологій у будівельних матеріалах // Нанотехнології в будівництві. – 2012. – № 3. – С. 6–21.

7. Дрючко О. Г., Стороженко Д. О., Бунякіна Н. В., Іваницька І. О. Спосіб програмованого формування лінійного закону зміни температури нагрівача : пат. 43549 Україна. МПК G05D 23/00 / заявник та власник О. Г. Дрючко та ін. – № u 2009 01783; заявл. 02.03.2009; опубл. 25.08.2009, Бюл. № 16. – 10 с.

8. Павленко А. М., Стороженко Д. О., Дручко О. Г., Бунякіна Н. В., Іваницька І. О. Спосіб виробництва роздутого гранульованого теплоізоляційного наповнювача : пат. на корисну модель № 121407 Україна. МПК (2006.01) C04B 28/26 / заявл. 21.04.2017; опубл. 11.12.2017, Бюл. № 23. – 9 с.

9. Стороженко Д. О., Дручко О. Г., Бунякіна Н. В., Іваницька І. О. Спосіб теплоізоляції в складних формах конструкцій : пат. на корисну модель № 121408 Україна. МПК (2006.01) C04B 28/26 / заявл. 21.04.2017; опубл. 11.12.2017, Бюл. № 23. – 9 с.

10. Стороженко Д. О., Дручко О. Г., Бунякіна Н. В., Іваницька І. О. Спосіб виробництва теплоізоляційних матеріалів пластинчастого та оболонкового типу : пат. на корисну модель № 121406 Україна. МПК (2006.01) C04B 28/26 / заявл. 21.04.2017; опубл. 11.12.2017, Бюл. № 23. – 8 с..

6. Figovsky O. L., Beilin D. A., Ponomarev A. N. Successes in the application of nanotechnology in building materials // Nanotechnology in Construction. 2012. No. 3. P. 6–21

7. Dryuchko O. G., Storozhenko D. O., Bunyakina N. V., Ivanytska I. O. Method of programmable formation of the linear law of the heater's temperature change : patent 43549 Ukraine. IPC G05D 23/00. Appl. u 2009 01783; appl. 02.03.2009; publ. 25.08.2009, Bul. No. 16. 10 p..

8. Pavlenko A. M., Storozhenko D. O., Druchko O. G., Bunyakina N. V., Ivanytska I. O. Inflated granulated thermal insulating filler production method : utility model patent 121407 Ukraine. IPC (2006.01) C04B 28/26. Appl. u 2017 03934; appl. 21.04.2017; publ. 11.12.2017, Bul. No. 23. 9 p.

9. Storozhenko D. O., Druchko O. G., Bunyakina N. V., Ivanytska I. O. Thermal insulation method in complex construction forms : utility model patent 121408 Ukraine. IPC (2006.01) C04B 28/26. Appl. u 2017 03935; appl. 21.04.2017; publ. 11.12.2017, Bul. No. 23. 9 p.

10. Storozhenko D. O., Druchko O. G., Bunyakina N. V., Ivanytska I. O. Thermal insulation materials plate and shell-like types production method : utility model patent 121406 Ukraine. IPC (2006.01) C04B 28/26. Appl. u 2017 03932; appl. 21.04.2017; publ. 11.12.2017, Bul. No. 23. 8 p.

Дрючко О.Г.*
Національний університет «Полтавська політехніка імені Юрія Кондратюка»
https://orcid.org/0000-0002-2157-0526

Бунякіна Н.В.
Національний університет «Полтавська політехніка імені Юрія Кондратюка»
https://orcid.org/0000-0003-4241-5127

Галай В.М.
Національний університет «Полтавська політехніка імені Юрія Кондратюка»
https://orcid.org/0000-0002-1205-7923

Боряк Б.Р.
Національний університет «Полтавська політехніка імені Юрія Кондратюка»
https://orcid.org/0000-0002-8114-7930

Трет′як А.В.
Національний університет «Полтавська політехніка імені Юрія Кондратюка»
https://orcid.org/0000-0003-3971-3078

Кислиця Д.В.
Національний університет «Полтавська політехніка імені Юрія Кондратюка»
https://orcid.org/0009-0005-2007-4220

З′ясування технологічних умов для формування лужно-силікатних теплоізоляційних виробів на основі золи-винесення теплових електростанцій і рідкого скла

Розроблено сировинну суміш із кремнеземвмісної техногенної складової – золи-винесення теплових електростанцій та способи приготування водостійких пористих теплоізоляційних матеріалів широкого призначення за двостадійною технологією гарячого спінювання порошкоподібної сировини. У розробці використовуються полі функціональні властивості рідкого скла як а) зв'язуючого компонента; б) пороутворювача; в) регулятора швидкості твердіння сирцевої маси. Сирцева маса, приготовлена за оптимізованою рецептурою, починає тверднути за звичайної температури вже з моменту її «за творення» розчинним склом й утворює пастоподібний корж з набором властивостей, необхідних для наступної фрагментації. Оптимізована рецептура приготування сирцевої суміші дозволяє перероблення композицій різними способами з формуванням термоізоляційних матеріалів широкого призначення: гранульованих теплоізоляційних наповнювачів, матеріалів для термоізолювання у складних за формою конструкціях,

плитного і оболонко подібного видів термоізоляційних матеріалів. Така поставлена задача в залежності від цілей і особливостей вирішуваних завдань досягається можливістю проведення декількома відмінними способами завершальних стадій їх отримання. Двох стадійність процесу перероблення визначають характер і поведінка складових компонентів рідко-скляної композитної системи під час термічної обробки, їх міцна адгезію до більшості конструкційних матеріалів і необхідність вирішення проблеми легкого видалення заготовок із розбірних форм оснащення. Результати досліджень можуть бути використані у галузі виробництва будівельних матеріалів, зокрема пористих штучних виробів, при отриманні зернистого ізоляційного матеріалу та легкого заповнювача для бетону промислового та цивільного будівництва, у теплотехніці як теплоізоляція тощо.

Ключові слова: лужно-силікатні теплоізоляційні композиційні матеріали; видалення золи; рідке скло; термічне спінювання.

*Адреса для листування E-mail: dog.chemistry@gmail.com

Збірник наукових праць. Галузеве машинобудування, будівництво
Academic journal. Industrial Machine Building, Civil Engineering
http://journals.nupp.edu.ua/znp
https://doi.org/10.26906/znp.2024.63.3877

UDC 502.3.06:504.32

Mykola Halaktionov *
National University «Yuri Kondratyuk Poltava Polytechnic»
https://orcid.org/0009-0006-7949-5713

Viktor Bredun
National University «Yuri Kondratyuk Poltava Polytechnic»
https://orcid.org/0000-0002-8214-3878

Determining the impact of motor vehicles on atmospheric air using existing predictive models

Motor vehicle emissions have become a significant air pollution problem, especially in cities with high industrial concentrations like Kryvyi Rih. Despite ongoing air quality monitoring, assessing the direct impact of vehicles is challenging. Vehicle emissions, primarily released in the lower atmosphere, affect areas where human activity is most concentrated. To evaluate the impact of motor vehicles on air pollution, mathematical models are used to estimate pollutant concentrations based on traffic volume, intensity, fuel type, and other factors. In Kryvyi Rih, areas with the highest traffic intensity were identified, and CO and NO_2 dispersion models were developed. The CALRoads View software, using the CALINE4 model, and "EOL Plus," based on the OND-86 methodology, were applied. A comparison of the results helped determine the suitable applications of each model for analyzing vehicle emissions in large urban areas.

Keywords: motor vehicles, air pollution, pollutant emissions, forecasting models, mathematical models

*Corresponding author E-mail: nikolay@galaktionov.com

Introduction

Atmospheric air is a critical component of human life, and its degradation due to anthropogenic factors adversely affects both quality of life and public health. In industrial cities such as Kryvyi Rih, air quality often fails to meet established permissible concentration limits due to emissions from industrial enterprises and motor vehicles.

With the continual increase in the number of vehicles in urban areas, emissions from road transport have become the dominant source of air pollution. Moreover, the rising vehicle count intensifies the load on urban infrastructure, resulting in traffic congestion at interchanges and intersections, which in turn leads to increased emissions. Therefore, it is crucial to conduct emission forecasting to develop effective strategies aimed at reducing air pollution.

Review of Recent Studies and Publications

Modeling the environmental impact of road transport is a vital tool for forecasting ecological consequences, and it is extensively explored in numerous scientific studies. Various methodological approaches and models are employed to address different objectives, including the prediction of transport emission levels. These models often comprise complex, multifactorial mathematical solutions that account for a multitude of variables [1,2].

Special attention is given to the development of mathematical models for assessing the dispersion of pollutants in the air. Regression models analyzing the impact of motor vehicles on atmospheric air pollution not only assess the current situation but also offer effective tools for forecasting emission trends, taking into account traffic intensity, vehicle type, and operational conditions [2,3].

Several studies actively utilize statistical forecasting methods to identify general emission trends and their correlation with transport flow parameters. Additionally, software packages for simulating the dispersion of pollutants in the atmosphere are widely applied. These tools allow for accurate evaluation of the impact of transport emissions on air quality in specific urban settings [4].

Given the continuous growth of the vehicle fleet and the heterogeneous structure of traffic flows, integrating such models into environmental monitoring systems is essential for formulating strategies to mitigate environmental harm.

Identification of Gaps in Existing Research

The heavy industrial burden in Kryvyi Rih places

significant pressure on the local environment, and emissions from motor vehicles further exacerbate air pollution. The concentration of pollutants frequently exceeds regulatory limits for individual substances emitted by both industrial facilities and vehicles. However, accurately quantifying the contribution of motor transport to overall pollution levels is challenging due to the mixed nature of emission sources.

In this context, it is imperative to conduct comprehensive research and develop predictive emission models that enable precise assessment of transport-related environmental impacts. The development of integrated environmental protection measures, the establishment of monitoring systems for vehicle emissions, and appropriate legal regulation are essential steps toward reducing ecological risks and safeguarding public health.

Furthermore, the introduction of modern technologies into the transportation infrastructure—such as electric vehicles and advanced emission control systems—can substantially improve environmental conditions and contribute to sustainable urban development.

Problem Statement

The aim of this study is to analyze the contribution of motor transport to the overall air pollution levels in Kryvyi Rih and to develop a predictive model for assessing this impact, along with measures to mitigate its negative environmental effects.

Research Objectives:

- analyze air pollution sources in Kryvyi Rih, with a specific focus on categorizing motor transport as a separate emission source.
- develop a model for forecasting the impact of road transport on air quality in various city zones, considering traffic flows and operational conditions.
- formulate recommendations for comprehensive environmental measures aimed at reducing the negative impact of motor transport on air quality.

Main Content and Results

Motor transport is one of the primary contributors to environmental pollution, particularly of the atmospheric environment. Various predictive modeling approaches are widely used to assess its impact on air quality. The primary methods for evaluating transport emissions include:

- *emission modeling* and *statistical methods* – involving specialized software tools to estimate the volume of pollutants emitted by vehicles.
- *emission models* – designed to quantify emissions of pollutants from vehicles, aiming to calculate the total mass of harmful substances released over a given period, depending on input parameters.
- *dispersion models* – used to determine the distribution of pollutants in the atmosphere based on meteorological conditions and emission source characteristics.
- *traffic models* – focus on analyzing traffic flow and forecasting future changes in transport systems, incorporating data on traffic, road infrastructure, and urban planning.
- *field research methods* – involve direct measurements of pollutant concentrations on-site.

These approaches allow for accurate evaluation of the scope and nature of transport-related environmental impacts.

Transport Emission Modeling. Emission modeling involves calculating the amount of pollutants released by vehicles into the atmosphere during operation. Specialized software solutions employ emission models that account for factors such as:

- vehicle type – different vehicle categories (passenger cars, trucks, buses) exhibit varied emission profiles.
- engine technologies and fuel type – diesel, gasoline, and electric vehicles differ in their environmental impacts.
- road conditions and traffic regimes – speed, stops, congestion, and other factors influence emission volumes.
- vehicle count – traffic intensity directly affects total emissions in a specific area.

Specialized transport emission modeling tools, such as MOVES, EMFAC, and COPERT, facilitate calculations that support the development of transport policies aimed at reducing air pollution. These tools are used to assess the environmental impact of motor vehicles, including the estimation of emissions of pollutants and greenhouse gases. Each model has specific features and is used in different regions and contexts.

- *MOVES* (Motor Vehicle Emission Simulator) – developed by the U.S. Environmental Protection Agency (EPA), it is used for calculating emissions from motor vehicles [5].
- *EMFAC* (Emission Factor Model) – developed by the California Air Resources Board (CARB), it is employed exclusively within the state of California for evaluating vehicle emissions and air quality management [6].
- *COPERT* (Computer Programme to Calculate Emissions from Road Transport) – a European model created under the auspices of the European Environment Agency to assess road transport emissions in EU countries [7].

COPERT uses data from the EMEP/EEA Emission Inventory Guidebook (2019 edition) [8], which outlines standards and methodologies for emission calculations based on European environmental regulations and EMEP research findings. This enables EU countries to effectively evaluate transport systems' environmental impact and develop sound environmental policies.

EMEP is a program established under the Convention on Long-Range Transboundary Air Pollution (CLRTAP) and coordinated by the United Nations Economic Commission for Europe (UNECE). It focuses on air quality monitoring and assessment across Europe, supporting international efforts to reduce air pollution.

The results of vehicle emission impact assessments obtained using the *COPERT* software are available via the interactive Emisia emission map [9] (Fig. 1).

Figure 1 – Interactive emissions map "Emisia" from the COPERT software tool

Various approaches and methods are employed to determine the concentrations of pollutants in the atmosphere, including field measurements and mathematical modeling.

Field measurements are conducted using networks of stationary and mobile monitoring stations, which directly measure the concentrations of pollutants in the air. These systems provide real-time data on pollution levels but may be limited in terms of spatial coverage and typically account for emissions from all sources, such as industrial discharges and motor vehicle emissions.

Dispersion models are mathematical tools used to simulate how pollutants released into the atmosphere are transported and dispersed in space. These models allow estimation of pollutant concentrations at various distances from emission sources, taking into account several factors, including:

- *meteorological conditions* – wind speed and direction, temperature, humidity, and precipitation influence the dispersion of pollutants;
- *topography* – terrain features (mountains, hills, plains) affect airflow and the movement of pollutants;
- *type of emission source* – different sources (e.g., point or line sources, such as roadways) produce different dispersion patterns.

Examples of dispersion models include *CALRoads View* (Lakes Environmental), *CALINE4, AERMOD* (Lakes Environmental), *ADMS*, and *EOL+*, which are commonly used to assess the impact of road transport on air quality in specific areas. These models enable the prediction of pollutant concentration levels at defined locations, which is essential for planning environmentally sustainable infrastructure and minimizing health risks to the population.

- *CALRoads View* is used for modeling the impact of vehicular emissions on air quality. The software integrates the *CALINE4, CAL3QHC*, and *CAL3QHCR* models.
- *CALINE4* is specifically designed to estimate pollutant concentrations from roadway traffic and considers various road types and meteorological factors. The *CAL3QHC* and *CAL3QHCR* models are enhanced versions of *CALINE3*, incorporating the ability to simulate traffic queue effects on pollutant concentrations and account for temporal variations in meteorological conditions and traffic volumes.
- *AERMOD* is an atmospheric dispersion model developed by the United States Environmental Protection Agency (EPA) for regulatory purposes.
- *ADMS-Roads* is used for modeling vehicular emissions on urban roads and highways.
- *EOL+* is based on the *OND-86* regulatory methodology ("Organizational Normative Document 1986"), which provides a framework for calculating pollutant dispersion in the atmosphere from both industrial and vehicular sources. The *OND-86* method remains a foundational guideline for estimating ground-level concentrations from industrial emissions, although its outdated nature may limit compliance with modern environmental standards and requirements.

To investigate the impact of motor vehicles on atmospheric air pollution, we identified areas with the highest traffic intensity within the city of Kryvyi Rih and developed pollutant dispersion models for those locations.

Three high-traffic intersections were selected for detailed analysis:

- 95th Quarter Roundabout, one of the busiest traffic hubs in Kryvyi Rih, recorded a traffic volume of 1,258 vehicles in 20 minutes, equivalent to 3,855 vehicles per hour. Traffic flow was nearly uniform from all directions, with a high proportion of public transportation.
- Vilna Ichkeria Street recorded a traffic volume of 1,548 vehicles in 20 minutes, or 4,641 vehicles per hour, also featuring evenly distributed flow and significant public transport presence.
- Intersection of Metallurgiv Avenue and Nikopolske Highway recorded 1,204 vehicles in 20 minutes, or 3,609 vehicles per hour, with similarly balanced traffic from all directions and heavy public transportation use.

For further modeling, nitrogen dioxide (NO_2) and carbon monoxide (CO) were selected as the most common and representative pollutants. Emission power values (g/s) were determined for these substances based on daily traffic intensity, and a graphical representation of their dependence was developed [12].

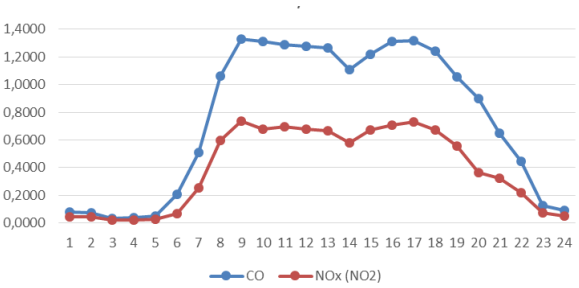

Figure 2 – Pollutant emissions during the day g/s

The graph (Fig. 2) shows that traffic intensity begins to increase from 6:00 a.m. to 9:00 a.m., after which it gradually decreases throughout the day. Between 2:00 p.m. and 6:00 p.m., traffic intensity rises again, followed by a subsequent decline. Peak traffic hours are observed at 9:00 a.m. and 6:00 p.m., corresponding to the periods of population mobility from home to work

and from work to home. As traffic volume increases, emissions of air pollutants also rise accordingly.

To assess the impact of motor vehicle emissions, the *CALRoads View* software suite was used, employing the *CALINE4* dispersion model. This model was selected for its high accuracy in simulating the dispersion of pollutants emitted by motor vehicles within urban road networks. *CALINE4* enables the estimation of pollutant emissions and their concentrations while accounting for various influencing factors, including wind speed, local topography, meteorological conditions, and traffic intensity.

The model was configured to simulate dispersion under worst-case wind direction conditions, where the software automatically identifies the direction that results in the maximum pollutant concentration.

The modeling domain was defined as a square area measuring 3,000 × 3,000 meters.

The road type was categorized as urban, with a surface roughness length of 400 cm, which reflects the local turbulence of the air and affects pollutant dispersion.

The wind speed was assumed to be 3 m/s across all sections of the study area, with an air temperature of 20°C.

At the selected site, the roadway consists of three traffic lanes in each direction, amounting to a total width of 22 meters, with an additional 3 meters on each side. Thus, the total mixing zone width was set to 28 meters.

Based on these parameters, dispersion models were constructed for carbon monoxide (CO) and nitrogen dioxide (NO_2) emissions. The highest predicted concentrations were found within the 95th Quarter roundabout, Vilna Ichkeria Street, the intersection of Metallurgiv Avenue and Nikopolske Highway, as well as at other nearby intersections within the vicinity of the study area.

The 95th Quarter roundabout, a large circular intersection, is not equipped with traffic lights and connects major city avenues, each comprising three lanes in both directions. This location experiences high traffic density, including a significant volume of private vehicles and public transport.

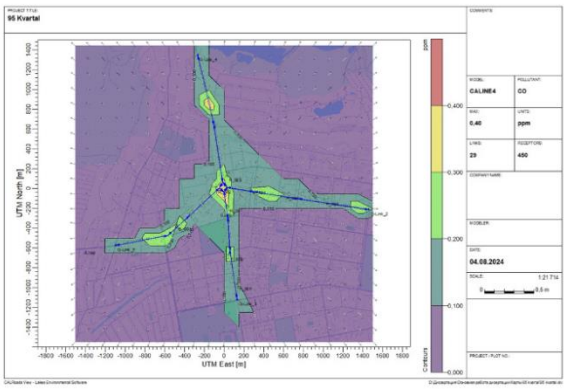

Figure 3 – CO distribution model 95 quarter.

As we can see (Fig. 3), according to the results of calculations, CO emissions do not exceed the established MPC values. Within the limits of highways, the maximum value for this section is 0.458 mg/m3 (0.4 ppm) or 0.09 MPC.

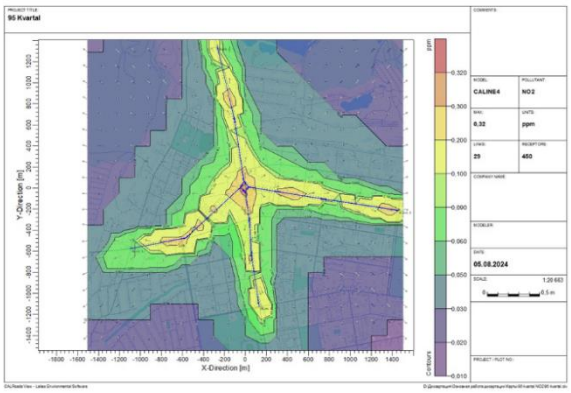

Figure 4 – Distribution model NO2 95 quarter.

The results of NO_2 emission calculations (Fig. 4) indicate that the concentration values exceed the established maximum permissible concentrations (MPC) within the intersection area under investigation. The maximum concentration recorded for this section is 0.61 mg/m³ (0.32 ppm), which corresponds to 3.04 MPC.

A pollutant dispersion model was also developed for the section of V. Ichkeria Street. This street originates in the vicinity of the 95th Quarter and terminates at a Y-shaped intersection near Artem 1 mine, Volodymyr Velykyi Street, and Mariyska Street. The primary research focus was on the intersection with Darwin Street, which functions as a bypass route for heavy-duty vehicles and is characterized by high traffic volumes, including public, passenger, and freight transport.

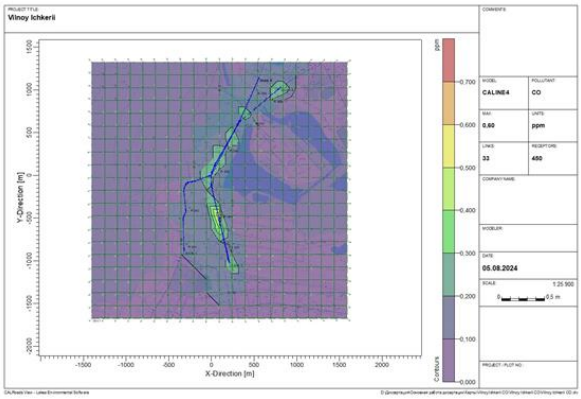

Figure 5 – CO distribution model on Vilna Ichkeria Street

In this section (Fig. 5), CO emissions do not exceed the established MPC values along the roadways. The maximum value recorded for this location is 0.687 mg/m³ (0.6 ppm), or 0.14 MPC.

The results of NO_2 emission calculations (Fig. 6) again indicate that concentration values exceed the established MPC within the intersection where the study was conducted. The maximum recorded concentration for this site is 1.2 mg/m³ (0.64 ppm), which is equivalent to 6.02 MPC.

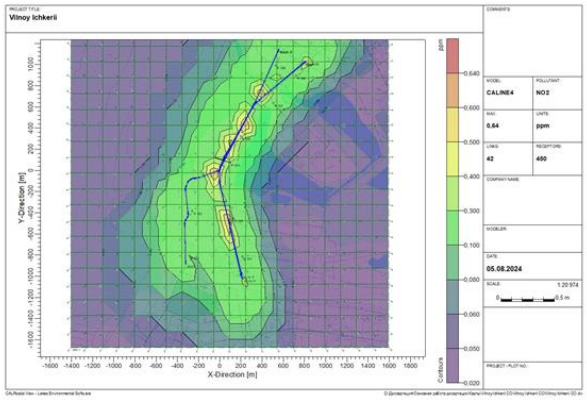

Figure 6 – Distribution model NO_2 Vilnoi Ichkerii Street

The intersection of Metalurhiv Avenue and Nikopolske Highway represents a location where one of the city's central avenues intersects with a bypass route that carries major transit highways H23, H11, and P74. This area is characterized by heavy traffic flow, including public, passenger, and heavy-duty transport.

As shown in the **CO emissions calculation results (Fig. 7)**, the values do not exceed the established MPC along the roadways. The maximum concentration observed for this section is 0.573 mg/m³ (0.5 ppm), or 0.115 MPC.

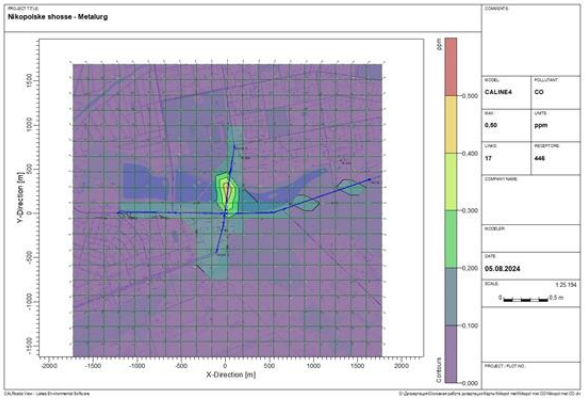

Figure 7 – CO distribution model Intersection of Metallurg Avenue and Nikopol Highway

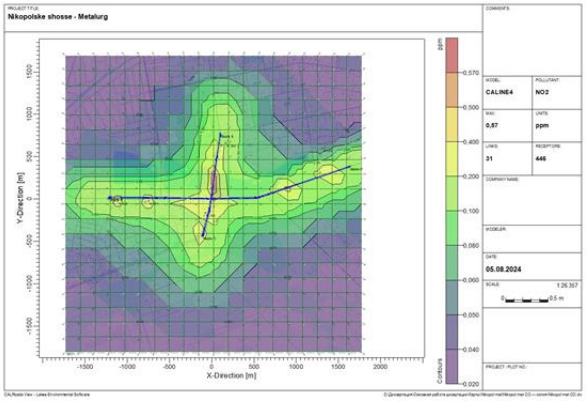

Figure 8 – NO_2 Distribution Model Intersection of Metallurg Avenue and Nikopol Highway

The NO_2 emission results (Fig. 8) show that concentration levels once again exceed the MPC at the studied intersection. The highest value recorded for this section is 1.07 mg/m³ (0.64 ppm), or 5.36 MPC.

Additionally, dispersion calculations for pollutants in the ground-level atmospheric layer were conducted for the analyzed areas using the "EOL Plus" software package, which implements the OND-86 methodology *("Method for Calculating the Concentrations of Harmful Substances in Ambient Air Emitted by Industrial Facilities")*.

The maximum concentration values based on the calculations for the investigated sections are summarized in Table 1.

Analysis of the results of ground-level pollutant dispersion calculations revealed that nitrogen dioxide (NO_2) concentrations exceed the established environmental safety standards (maximum permissible concentrations – MPC). For other substances present in vehicular emissions within the studied sections, no exceedances of MPC were recorded.

It should be noted that the pollutant dispersion calculations in the atmospheric air were performed under the worst-case meteorological conditions for each calculation point and for each pollutant, taking into account the simultaneous maximum possible emission values.

Table 1 Maximum concentration values

Research area	A polluting substance	Concen-tration mg/m3	Concen-tration, portion of MPC
95th Quarter Ring	CO	1,9	0,38
	NO_2	1,09	5,49
Vilnoi Ichkerii St.	CO	2,21	0,44
	NO_2	1,15	5,75
Intersection of Metallurgists Ave. and Nikopol Highway	CO	2,21	0,44
	NO_2	1,16	5,78

When comparing the two pollutant dispersion models, it is observed that the results for carbon monoxide (CO) differ, while nitrogen dioxide (NO_2) emissions are highly similar. This discrepancy may be attributed to differences in the calculation algorithms and emission input parameters of the respective models. Nevertheless, the general trends observed in both models remain consistent.

Conclusions.

The conducted study has established that road transport has a significant impact on the ambient air quality in the city of Kryvyi Rih. The developed models show that CO emissions do not exceed the MPC values along roadways, though they still contribute to overall air pollution. In contrast, NO_2 emissions exceed the MPC values at intersections across all studied sites.

Both dispersion modeling methods—based on the OND-86 methodology and the CALINE4 model—can be applied in future studies. However, CALINE4 offers a key advantage due to its ability to account for complex meteorological conditions and road geometries, which is particularly important in urbanized areas such as Kryvyi Rih, where numerous roads are located in close proximity to residential areas. Furthermore, the model effectively handles various types of pollutants, such as nitrogen oxides (NO_x) and carbon monoxide (CO), making it a versatile tool for analyzing the impact of road transport on air quality.

Due to its accuracy and adaptability to local conditions, CALINE4 not only supports assessment of current pollution levels but also enables the development of predictive models for designing effective environmental protection measures.

In contrast, the OND-86 model is better suited for simulating emissions from stationary sources, such as industrial facilities. While it can also be applied to assess the impact of road transport by treating it as a linear emission source, this approach limits its accuracy because vehicular emissions have dynamic characteristics influenced by changes in vehicle speed, type, and other factors.

Unlike CALINE4, which is specifically designed to model linear pollution sources such as roadways, OND-86 does not consistently account for the specific features of vehicular movement and meteorological conditions that influence pollutant dispersion along transport corridors. Therefore, although OND-86 remains useful for general pollution analysis, its precision in evaluating the environmental impact of road transport is lower compared to more specialized models like CALINE4.

Thus, the modeling of vehicular emissions provides a valuable tool for assessing the current road infrastructure, developing predictive models for the expansion or construction of new roads and transport interchanges.

The importance of predictive models lies in their ability to evaluate future environmental consequences under various scenarios of transportation infrastructure development and traffic dynamics. These models help forecast how changes in traffic volume, vehicle types, or regulatory measures may affect air pollution levels. This, in turn, enables the timely development of strategies to reduce emissions, improve the effectiveness of urban environmental initiatives, and minimize health risks for the population.

References

1. Бабков В. С. Анализ математических моделей распространения примесей от точечных источников / В. С. Бабков, Т. Ю. Ткаченко // Наукові праці Донецького національного технічного університету. Серія : Інформатика, кібернетика та обчислювальна техніка. - 2011. - Вип. 13. - С. 147-155
2. Петросян А. А., Маремуха Т. П., Моргульова В. В. Порівняльний аналіз моделювання усереднених концентрацій забруднюючих речовин у приземному шарі атмосфери LAYER // Молодий вчений. – 2020. – № 7(83). – URL: https://doi.org/10.32839/2304-5809/2020-7-83-2.
3. Wang X., et al. Apportionment of Vehicle Fleet Emissions by Linear Regression, Positive Matrix Factorization, and Emission Modeling // Atmosphere. – 2022. – Vol. 13, no. 7. – P. 1066. – URL: https://doi.org/10.3390/atmos13071066.
4. Татарченко Г. Теоретичні аспекти моделювання розсіювання забруднюючих речовин в атмосфері // Містобудування та територіальне планування. – 2022. – № 79. – С. 381–395. – URL: https://doi.org/10.32347/2076-815x.2022.79.381-395.
5. MOVES and Related Models. EPA. – URL: https://www.epa.gov/moves/latest-version-motor-vehicle-emission-simulator-moves.
6. On-Road (EMFAC). California Air Resources Board. – URL: https://ww2.arb.ca.gov/our-work/programs/msei/on-road-emfac.
7. COPERT The Industry Standard Emissions Calculator. COPERT. – URL: https://copert.emisia.com/.
8. EMEP/EEA Air Pollutant Emission Inventory Guidebook 2019: Technical Guidance to Prepare National Emission Inventories. European Environment Agency. – 2019. – URL: https://www.eea.europa.eu/www/ru/publications/rukovodstvo-emep-eaos-po-inventarizaciivybrosov-2019.
9. Emissions Report Overview. EMISIA. – URL: https://emissions-map.emisia.com/.

1. Babkov V. S., Tkachenko T. Yu. Analysis of mathematical models for the dispersion of impurities from point sources / V. S. Babkov, T. Yu. Tkachenko // Scientific Works of Donetsk National Technical University. Series: Informatics, Cybernetics and Computer Technology. – 2011. – Iss. 13. – P. 147–155.
2. Petrosyan A. A., Maremukha T. P., Morgulova V. V. Comparative analysis of modeling the average concentrations of pollutants in the atmospheric surface layer using LAYER // Young Scientist. – 2020. – Vol. 7, No. 83. – URL: https://doi.org/10.32839/2304-5809/2020-7-83-2.
3. Wang X., et al. Apportionment of vehicle fleet emissions by linear regression, positive matrix factorization, and emission modeling / X. Wang et al. // Atmosphere. – 2022. – Vol. 13, No. 7. – P. 1066. – URL: https://doi.org/10.3390/atmos13071066.
4. Tatarchenko H. Theoretical aspects of modeling the dispersion of pollutants in the atmosphere / H. Tatarchenko // Urban Development and Spatial Planning. – 2022. – No. 79. – P. 381–395. – URL: https://doi.org/10.32347/2076-815x.2022.79.381-395.
5. MOVES and Related Models. EPA. – URL: https://www.epa.gov/moves/latest-version-motor-vehicle-emission-simulator-moves.
6. On-Road (EMFAC). California Air Resources Board. – URL: https://ww2.arb.ca.gov/our-work/programs/msei/on-road-emfac.
7. COPERT The Industry Standard Emissions Calculator. COPERT. – URL: https://copert.emisia.com/.
8. EMEP/EEA Air Pollutant Emission Inventory Guidebook 2019: Technical Guidance to Prepare National Emission Inventories. European Environment Agency. – 2019. – URL: https://www.eea.europa.eu/www/ru/publications/rukovodstvo-emep-eaos-po-inventarizaciivybrosov-2019.
9. Emissions Report Overview. EMISIA. – URL: https://emissions-map.emisia.com/.

10. Software Products. Lakes Software. – URL: https://www.weblakes.com/software/.

11. ОНД-86. Методика розрахунку концентрацій в атмосферному повітрі шкідливих речовин, що містяться у викидах підприємств. - 68 С.

12. Галактіонов М. С., Бредун В. І. Інфраструктурні особливості міста Кривий Ріг як додатковий фактор впливу автотранспорту на навколишнє середовище // Herald of Khmelnytskyi National University. Technical sciences. – 2024. – Т. 339, № 4.

10. Software Products. Lakes Software. – URL: https://www.weblakes.com/software/.

11. OND-86: Methodology for calculating concentrations of harmful substances in ambient air from industrial emissions. - 68 P.

12. Halaktionov M. S., Bredun V. I. Infrastructure features of the city of Kryvyi Rih as an additional factor of road transport impact on the environment / M. S. Halaktionov, V. I. Bredun // Herald of Khmelnytskyi National University. Technical Sciences. – 2024. – Vol. 339, No. 4.

Галактіонов М.С. *
Національний університет «Полтавська політехніка імені Юрія Кондратюка»
https://orcid.org/0009-0006-7949-5713

Бредун В.І.
Національний університет «Полтавська політехніка імені Юрія Кондратюка»
https://orcid.org/0000-0002-8214-3878

Визначення впливу автотранспорту на атмосферне повітря за допомогою існуючих прогнозних моделей

Останнім часом викиди від автотранспорту стають дедалі серйознішою проблемою забруднення атмосферного повітря, особливо в містах із високою концентрацією промислових підприємств, таких як Кривий Ріг. Хоча в таких містах постійно здійснюється моніторинг якості повітря, визначити безпосередній вплив автотранспорту залишається складним завданням. Особливістю автомобільного забруднення є те, що шкідливі викиди, що містяться у відпрацьованих газах, потрапляють у найнижчі, приземні шари атмосфери – саме там, де відбувається основна життєдіяльність людини. Для оцінки впливу автотранспорту на забруднення повітря використовують різні методи прогнозування, які ґрунтуються на математичних моделях. Ці моделі дозволяють оцінити концентрації забруднювальних речовин у повітрі в залежності від кількості транспортних засобів, інтенсивності руху, типу палива та інших факторів.

Для проведення дослідження в пливу автотранспорту на стан забруднення атмосферного повітря міста Кривий Ріг визначено ділянки з найбільшою інтенсивністю руху та побудовані моделі розповсюдження CO та NO2. Для визначення впливу автотранспорту використано програмний комплекс CALRoads View із застосуванням моделі CALINE4 та програмний комплекс «ЕОЛ Плюс», який реалізує методику ОНД-86. На основі співставлення результатів розрахунків встановлено можливі сфери застосування кожної з моделей для аналізу викидів автомобільного транспорту в умовах крупних міських агломерацій.

Ключові слова: автотранспорт, атмосферне повітря, викиди забруднюючих речовин, прогнозні моделі математичні моделі.

*Адреса для листування E-mail: nikolay@galaktionov.com

Збірник наукових праць. Галузеве машинобудування, будівництво
Academic journal. Industrial Machine Building, Civil Engineering
http://journals.nupp.edu.ua/znp
https://doi.org/10.26906/znp.2024.63.3875

UDC 66.067:004.94

Ruslan Toister *
National University «Yuri Kondratyuk Poltava Polytechnic»
https://orcid.org/0009-0006-6201-7811

Anton Khrapach
National University «Yuri Kondratyuk Poltava Polytechnic»
https://orcid.org/0009-0005-2763-4542

Computer modelling of the flow structure in a combined mixer for aqueous suspensions with solid and gas phases

Computer modeling of multiphase flows in mixers for aqueous suspensions with solid and gas phases opens up new opportunities for optimizing mixing processes in industry. The creation of CFD-DEM models allows taking into account the interaction of liquid, solid and gas phases, fixing the features of circulation, mass transfer and rheological behavior of the medium. The article considers the features of the formation of the flow structure in a combined-type mixing chamber, analyzes the nature of changes in turbulent and convective processes in the presence of a gas phase and solid inclusions, and also substantiates approaches to building effective mixing modes.

Keywords: CFD-DEM modeling, multiphase flows, combined mixer, mass transfer, gas bubbles, circulation structures.

*Corresponding author E-mail: rtoister.cv@gmail.com

Introduction

Computer modeling of flow structures in mixers for aqueous suspensions containing solid and gas phases remains one of the priority areas of applied hydrodynamics and mechanical engineering.

The formation of an optimal multiphase flow structure directly determines the energy efficiency of mixing processes, the quality of the final product, and the resource load on the equipment.

The issue of improving the efficiency of mixing systems is highly relevant in the fields of water treatment, chemical technology, and mineral processing, where liquid-solid-gas media with complex rheological behavior dominate [1].

Analytical approaches based on simplified flow models do not fully capture the dynamics of multiphase systems.

Computational fluid dynamics (CFD) and discrete element modeling (DEM) methods offer opportunities for analyzing local flow characteristics, phase interactions, mixing regimes, and the development of boundary structures [2].

Computer modeling enables consideration of the multifactorial nature of processes in which mechanical, hydrodynamic, and thermal effects are realized simultaneously.

Analysis of Recent Research and Publications

The problem of numerical modeling of multiphase flows in mixing systems has evolved gradually, as the challenges of applied hydrodynamics became more complex.

O. Kasat, A.R. Khopkar, V.V. Ranade, and A.B. Pandit [1] laid the foundation for describing the processes of solid phase mixing in liquid media, using computational fluid dynamics (CFD) combined with discrete element modeling (DEM).

Their calculations made it possible to identify patterns of solid inclusion transport in mechanical mixers and to formulate criteria for evaluating mixing efficiency.

The challenges of modeling dense multiparticle flows were systematized by S. Van and Y. Shen [2], who emphasized the complexity of describing multiphase interactions in conditions of high discrete element concentration.

Their approaches aim to expand the capabilities of CFD-DEM modeling by integrating multiphysical models of mass transfer, heat transfer, and chemical reactions.

Local aspects of mixing processes were examined by S. Duan, S. Feng, C. Peng, C. Yang, and Z. Mao [3], who analyzed the micro-level structure of mixing in gas-liquid and solid-liquid media.

Their application of the CFD-E approach made it possible to trace the relationship between local concentration fluctuations and the macroscopic efficiency of mass transfer.

A.M. Zapata Rivera and his colleagues [4] demonstrated that without considering empirical observations, it is impossible to achieve a high correlation between simulation results and real three-dimensional flows in mixing tanks.

Understanding the spatial variability of multiphase medium properties was advanced by V.S. Biletskyi [5], who emphasized the need to adapt numerical algorithms to changes in phase density and viscosity during flow.

Based on his findings, a new concept for constructing CFD models for complex technological systems has been formulated.

In discussions about transitions between different flow regimes, D.A. Alaita [6] made a notable contribution by highlighting the critical importance of accounting for laminar-to-turbulent transitions in particle-laden flows.

His approach established new requirements for models aiming to accurately reproduce regime dynamics under real-world conditions.

High-speed multiphase processes were explored by D. Friso [8], who demonstrated how the structure of momentum and heat transfer changes with increasing Reynolds number.

V.M.S. Vullenweber and his colleagues [9], studying the micro-level behavior of solid particles in turbulent flows, showed that particles not only passively move with the flow but also actively influence its local characteristics, altering the structure of turbulent fluctuations.

The combination of approaches proposed by the aforementioned researchers indicates that numerical modeling of multiphase flows is entering a new stage of multiphysical integration.

The description of phase interactions, consideration of changing rheological properties, and the incorporation of turbulent effects are increasingly being combined within unified computational models, opening new prospects for solving complex engineering challenges.

Identification of Previously Unresolved Aspects of the General Problem

In recent years, computer modeling of multiphase flows has made significant progress; however, certain aspects related to mixing systems with complex configurations remain insufficiently studied.

Most existing models focus on describing two-phase media, which creates difficulties in accurately reproducing real processes involving the presence of a gas phase [2; 4].

The presence of gas alters circulation contours, modifies local velocity fields, and affects mass transfer efficiency, thus requiring more sophisticated numerical analysis approaches and a transition to three-phase models.

In studies dedicated to CFD-DEM modeling, the issue of accounting for turbulent effects during the interaction of discrete solid particles with liquid and gas phases remains relevant [3; 9].

Simplifications in modeling these processes limit the ability to accurately describe real mixing phenomena, where flow fluctuations and micro-level interactions significantly influence suspension stability and mass transfer efficiency.

The lack of consideration of these features complicates the application of numerical models in practical tasks where high accuracy in reproducing multiphase dynamics is required.

Finally, for combined-type mixers, where local high-velocity flows, recirculation zones, and phase segregation coexist, there are no universal numerical models capable of capturing both the macro- and micro-level flow structures during interactions between all phases [1; 5].

Thus, the scientific task lies in developing a comprehensive CFD-DEM model of the flow structure in a combined mixer for aqueous suspensions containing solid and gas phases, taking into account the effects of turbulence, interphase interactions, and multiphase instability.

Problem Statement

The aim of this article is to develop a conceptual CFD-DEM model of the flow structure in a combined mixer for aqueous suspensions containing solid and gas phases.

In line with this objective, the research focuses on identifying the patterns of hydrodynamic structure formation in a multiphase environment, analyzing the influence of the mixer's geometric parameters on the dynamics of phase interactions, and substantiating criteria for optimizing the mixing process.

Achieving this goal involves the application of computer modelling using computational fluid dynamics (CFD) methods to describe the flow of the liquid and gas phases, discrete element modelling (DEM) to simulate the dynamics of solid particles within the multiphase flow, as well as a multiphysics approach to integrate models of turbulence, mass transfer, and phase interactions.

Main Material and Results

The flow of the medium in combined mixers is not formed as a simple phase combination, but as a complex interaction process, where the liquid, solid, and gas components simultaneously contribute to the construction of a dynamic, changing system.

The mutual penetration of phases creates a dynamic structure in which local circulations, convective transfers, and turbulent fluctuations continuously influence each other, leaving no space for the establishment of stable regimes.

The formation of the flow is accompanied by constant changes in velocity, density, and viscosity in different areas of the mixer, leading to the appearance of temporary zones of order or, conversely, local disruptions of circulation loops.

Each disturbance in the flow initiates a wave of subsequent changes that alter the overall picture even at the macrostructural level.

This dynamic nature makes it impossible to describe the process through fixed instantaneous states and requires an approach that accounts for the continuous temporal evolution of the environment.

In complex mixing systems, no characteristic—whether velocity, concentration, or flow structure—remains constant, but instead continuously evolves in a chain of self-transformation, which defines the primary challenges in numerical modelling of multiphase flows.

The geometry of the mixer determines the architecture of the flow at a fundamental level. A cylindrical chamber with a rotor of combined blade shape installed at the center creates conditions for the development of two main types of motion: axial lifting of the mixture due to the mechanical rotation of the rotor and secondary circulatory currents resulting from the injection of gas through nozzles (Fig. 1).

The interaction of these two mechanisms defines the primary nature of the multiphase environment, where solid particles do not merely follow the flow but constantly alter their trajectories in response to local changes in velocity, pressure, and turbulent stresses.

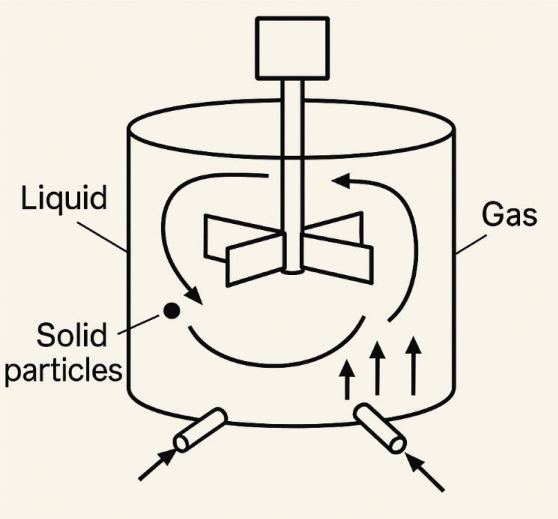

Figure 1 – Schematic of a combined mixer for aqueous suspensions with solid and gas phases

At approximately half the height of the mixing chamber, the zone of most intensive mixing forms. In this area, turbulent energy reaches its highest levels, which ensures active mass transfer between the liquid phase, gas bubbles, and solid inclusions [8]. The upper layers of the chamber and the regions near its bottom are characterized by a reduced level of turbulent fluctuations, where the accumulation of solid particles and gas bubbles occurs, creating the risk of forming zones with reduced mass transfer.

The dynamics of these processes depend not only on the structural parameters of the mixer but also on the operating characteristics of the system – rotor speed, gas flow intensity, liquid phase viscosity, and solid component concentration (Fig. 2). It is the complex interaction of these factors that determines the possibility of maintaining a homogeneous flow state over time.

The stratification of the medium, revealed during the simulation, is not a random phenomenon. It reflects the natural balance of forces in the mixing system: mechanical activation, gravitational settling, and the buoyant force of gas bubbles. An increase in the concentration of the solid phase in the peripheral zones of the chamber indicates insufficient efficiency of local convective mechanisms.

The discovery of the spiral logic of particle movement allows for a better understanding of not only the mechanisms of their movement but also the nature of the formation of zones of active and passive mass exchange.

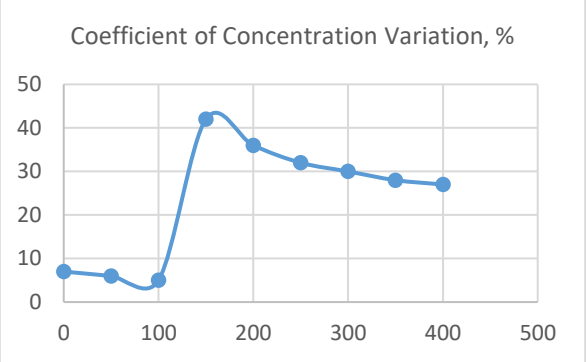

Figure 2 – Dependence of the solid phase concentration variation coefficient on rotor speed

Computer modelling of discrete trajectories shows that solid particles move from the central axis to the periphery and return back through the formed recirculating flows (Fig. 3). The delay of particles in stagnant zones near the walls is related to the combination of turbulent dispersion, gravitational settling, and local velocity gradients [3; 9].

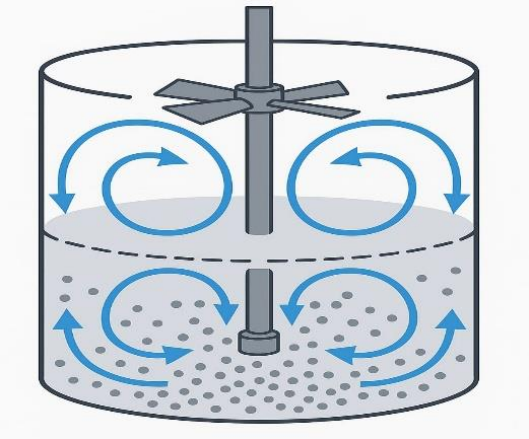

Figure 3 – Circulation contours and particle trajectory movement in the mixer.

In a multiphase environment of a combined mixer, no process exists in isolation: energy transfer between different scales, phase interactions, and continuous fluctuations in structure form a complex network of changes, where the state of one element directly influences the behavior of the entire flow. Disturbances in local flow, changes in concentration or velocity in a

particular zone, immediately affect other levels, creating a dynamic system of interdependent reactions that constantly evolve over time.

The integration of the gas phase into the overall flow structure changes not only the local parameters but also the principle of organizing the circulation processes. When gas bubbles are introduced through nozzles at the lower part of the mixing chamber, they create lifting forces that alter the direction of primary convective flows and simultaneously restructure the internal flow structure. The formation of vertical circulation contours based on gas bubbles increases mass transfer intensity and prevents the formation of horizontal layers with increased solid-phase concentration, which often occur in systems without aeration.

The distribution of gas bubbles in the chamber shows stratification by size, adding another level of complexity to the dynamics of the environment. Larger bubbles concentrate near the axis, where the axial flow has the highest velocity, while smaller bubbles more evenly spread across the radius, forming a network of micro-flows. These small-scale structures enhance the exchange of substances between phases and ensure the expansion of the spatial region of effective interaction, maintaining the system's dynamic activity even in regimes with reduced primary flow intensity.

Such a multi-level distribution of the gas phase changes the overall structure of circulation: where small bubbles dominate, there is higher mixing efficiency due to the increased interfacial surface area. The enhanced mass transfer mechanism is realized through small bubbles, which cannot be achieved by mechanical mixing alone.

The turbulent flow structure, formed by the simultaneous influence of mechanical and gas activation, is not homogeneous across the height of the mixer. In the upper part, horizontal flows prevail, flowing around the walls of the chamber and reducing axial circulation. In the lower part, however, the upward movement along the axis dominates, caused by the lifting force of the bubbles and mechanical drag from the rotor.

The formation of a multiphase flow in the mixing chamber is a continuous process of phase interaction, where no movement develops autonomously. Energy transfer between different movement scales, constant fluctuations in the internal structure, and the mutual penetration of liquid, solid, and gas phases change both the instantaneous flow characteristics and the overall stability of the system over time. In an environment that is constantly in a state of dynamic equilibrium, small-scale disturbances can alter large-scale circulation contours, while the general direction of primary flows determines the development of microstructural elements.

The gas phase, introduced through nozzles at the bottom of the chamber, actively participates in these processes. As noted by A.M. Sapata Rivera and colleagues, gas bubbles passing through the liquid medium not only create lifting forces that promote vertical movement of the mixture but also initiate the formation of convective contours that restructure the overall circulation structure. Such incorporation of gas into the internal dynamics of the flow enhances vertical mass transfer and prevents the formation of horizontal zones with high solid-phase concentrations, which are characteristic of mixers without aeration.

The structure of the distribution of gas bubbles in the chamber shows stratification by size, which forms additional levels of organization of the flow. As D. Frizo points out, large bubbles concentrate near the axis of the mixer, where the axial rise speed of the liquid is maximal, while smaller ones are distributed mainly in the radial direction, forming a network of micro-flows. These structures support effective mass exchange between phases and contribute to maintaining dynamic activity even in regimes of reduced turbulent energy in the primary flow.

The presence of such a dual distribution—large bubbles dominating along the axis and small bubbles scattered throughout the volume—provides a unique mass transfer dynamics: a combination of rapid vertical convective currents and slow horizontal micro-movements. This interaction of structures determines the mixer’s ability to maintain suspension homogeneity and the stability of the hydrodynamic regime across a wide range of technological loads.

The structure of the multiphase flow in the mixer is in a constant state of change. The formation and destruction of local convective contours, the accumulation and dispersion of solid particles, and the shifting position of gas bubbles—all these processes occur continuously, altering the configuration of the system in the time dimension. Such non-stationarity makes numerical modelling challenging and explains the sensitivity of mixing processes to even slight changes in external parameters.

Increasing the intensity of gas aeration changes the nature of mixing not only by increasing the lifting force in the liquid medium but also through a profound restructuring of the internal flow structure. As the gas flow rate increases, the upward velocity in the center of the chamber strengthens, shifting the zone of maximum mixing toward the upper part of the mixer. At the same time, excessive gas lift intensity can generate unstable regimes: large bubbles push solid particles to the periphery, creating areas with local oversaturation near the walls and reducing the overall efficiency of mass transfer.

The mixing regime in a combined mixer is determined by the relationship between the rotor’s rotational speed and the intensity of gas injection. Optimal working parameters allow for maintaining a uniform distribution of the solid phase throughout the chamber volume, preventing the formation of stagnant zones or areas with uneven concentration. Shifting this balance—toward excessive aeration or insufficient mechanical activation—changes the flow nature, leading to phase stratification and a gradual reduction in mixing efficiency.

Numerical modelling of multiphase processes offers the opportunity not only to describe the changing flow regimes but also to track the critical conditions at which the flow structure loses stability. Analyzing turbulent

energy distribution, velocity fields, and solid inclusion concentrations in mixing chambers helps identify threshold values of operational parameters, beyond which the circulation character changes and the system's dynamic equilibrium is disrupted. Crossing these boundaries leads to a transformation of the flow, which directly impacts mixing efficiency.

In combined mixers, even small changes in rotor speed or gas flow rate lead to a restructuring of circulation contours. These changes are not limited to local zones but spread throughout the flow structure, altering velocity profiles and mass transfer processes. Establishing a new regime depends not only on the initial intensity of the disturbance but also on the system's ability to quickly return to a stable state without significant fluctuations.

Disruptions in the mixing regime in production conditions often lead to local aggregation of solid particles, the appearance of zones with reduced mass transfer, and a decrease in overall process efficiency. Such deviations can affect not only product properties but also the productivity of the production line, as even short-term disruptions in the flow structure change the kinetic parameters of reactions or the physico-chemical properties of the suspension. Using numerical modelling to create regime maps for mixers enables planning the system's operation within safe regimes and reducing the likelihood of unstable conditions in real operational conditions.

The formation of stagnant zones in the mixing volume is a result not only of decreased local turbulent energy but also of the complex interaction of phases on a micro level. The accumulation of solid particles near the chamber walls is the result of a combination of mechanical drag by turbulent eddies, gravitational settling, and insufficient compensation of these effects by the lifting force of gas bubbles. In cases of excessive bubble coalescence and a decrease in the total interfacial surface area, the efficiency of mass transfer is noticeably reduced.

Using CFD-DEM models allows not only visualizing the overall flows but also tracking individual particle trajectories, determining their average residence time in zones of active mixing, and identifying local concentration fluctuations. Under optimal working conditions, the average residence time of solid particles in the active turbulence zone is about 70–80% of the total movement time, indicating high mixing efficiency. A decrease in this figure signals the appearance of stagnant zones, which can significantly impact the final quality of the technological product.

Energy analysis of the mixer's operation shows that combining mechanical rotor rotation with gas aeration allows for reducing specific energy consumption without losing process efficiency. Gas bubbles, by aiding the rise of the liquid phase, partially compensate for the required mechanical energy, reducing the overall load on the rotor drive. This opens up the possibility for creating energy-efficient mixing systems capable of operating at high productivity with reduced energy consumption.

Parametric studies of the mixing chamber show that changes in its geometric proportions, without corresponding adjustment of operational characteristics, can significantly affect the flow structure. Reducing the chamber height or increasing its diameter without proper adjustment of rotor speed leads to weakening of vertical circulation and disruption of the force balance in the multiphase environment. Under these conditions, the risk of phase stratification increases: solid particles and gas bubbles accumulate in peripheral or bottom zones, and the mass transfer efficiency between phases decreases noticeably.

The flow structure in multiphase mixing systems is determined by the ratio between the chamber height, rotor diameter, and rotational speed. As D.A. Alaita notes, this relationship forms the stability of circulation contours and determines the nature of mass transfer within the mixing volume. Within the range of optimal parameters, the flow maintains phase uniformity and stability of the circulation structure without significant increases in energy costs, ensuring the necessary technological conditions over long periods.

Exceeding this balance, even to a small degree, alters the course of the process. Local zones with low mass transfer intensity form, where solid particles accumulate, and the gas phase forms clusters that fall out of the general circulation pattern. The development of such isolated structures leads to a gradual loss of multiphase flow uniformity, changing not only the mixing efficiency but also the rheological properties of the environment, affecting the stability of the technological process.

Understanding these relationships is not only of theoretical value. In the practice of designing mixing systems, the alignment of geometric and operational parameters determines the equipment's service life, energy efficiency level, and the stability of the suspension's technological characteristics.

At the general level, combined mixing of aqueous suspensions with solid and gas phases appears as a multi-level system of interactions. At each level—from the movement of individual particles to macroscopic circulation—specific mechanisms of mutual influence between phases are realized. Understanding these mechanisms through computational modelling not only allows for reconstructing the actual behavior of the flow but also for developing effective strategies to optimize technological processes in industry, focusing on increasing homogeneity, maintaining regime stability, and reducing energy consumption.

Conclusions

Computer simulation of the flow structure in a combined mixer for aqueous suspensions with solid and gas phases has made it possible to identify the patterns of multiphase flow formation in complex technological systems. The built CFD-DEM model reproduced the main physical processes accompanying mixing, including circulation loops, phase segregation, and the formation of recirculation zones.

The scientific novelty of the study lies in determining the critical parameters of the rotor rotation regime and

the intensity of gas aeration, which ensure optimal homogenization of the solid and gas phases with minimal energy consumption. For mixers of this type, the relationship between the structure of turbulent characteristics and the spatial arrangement of gas bubbles and the local concentration of solid particles in different zones of the mixing chamber was established.

The practical significance of the obtained results lies in the possibility of using the built model for optimizing the structural parameters of mixers, calculating regime characteristics, and developing recommendations for improving suspension preparation systems in water treatment, chemical, and mining industries. Taking into account the peculiarities of phase circulation, turbulent energy distribution, and the behavior of solid particles in a multiphase environment allows for enhancing the energy efficiency of mixing processes and the stability of the final technological characteristics of the product.

Modelling multiphase flows is gradually moving beyond standard approaches and requires considering the deformation of gas bubbles in the flow dynamics. The change in the shape of the bubbles and their behavior under the influence of local conditions affects not only the microstructure of the medium but also determines the character of mass transfer processes across the entire mixing system. In regimes with high circulation intensity, where the properties of the medium change over time and space, such effects gain particular significance.

Along with bubble deformation, significant roles are played by processes of bubble coalescence and breakage, as well as the aggregation of solid particles. The change in the number of phase transitions and the appearance of new areas of non-uniformity in the suspension alters the mass transfer trajectories, which requires new approaches to numerical description. The development of models capable of integrating hydrodynamic and microstructural phenomena into a single computational picture is a logical direction for the development of this field.

Particular attention is paid to the variable rheological properties of the medium, as an increase in the solid component concentration changes the viscosity and manifests thixotropic effects. Such changes directly affect the development of turbulent structures, altering the local fluctuation energy and determining the stability of circulation loops over time.

Expanding computational models to include chemical reactions in a multiphase medium opens the possibility to describe not only hydrodynamic but also kinetic aspects of mixing. The interaction of flow and reaction processes in a combined computational scheme creates the basis for the development of new types of technological systems, where the optimization of energy and material resource usage becomes an integrated part of the overall dynamics of production.

References

1. Kasat G., Khopkar A.R., Ranade V.V. & Pandit A.B. (2008). CFD Simulation of Liquid-Phase Mixing in Solid–Liquid Stirred Reactor. *Chemical Engineering Science.* 63(15). 3877-3885. https://www.researchgate.net/publication/223618439_CFD_Simulation_of_Liquid-Phase_Mixing_in_Solid-Liquid_Stirred_Reactor
2. Wang S. & Shen Y. (2025). CFD-DEM modelling of dense gas-solid reacting flow: Recent advances and challenges. *Progress in Energy and Combustion Science.* 109. 101221. https://doi.org/10.1016/j.pecs.2025.101221
3. Duan X., Feng X., Peng C., Yang C. & Mao Z. (2020). Numerical simulation of micro-mixing in gas–liquid and solid–liquid stirred tanks with the coupled CFD-E-model. *Chinese Journal of Chemical Engineering.* 28(9). 2235-2247. https://doi.org/10.1016/j.cjche.2020.06.016
4. Zapata Rivera A.M., Ducoste J., Peña M.R. & Portapila M. (2021). Computational Fluid Dynamics Simulation of Suspended Solids Transport in a Secondary Facultative Lagoon Used for Wastewater Treatment. *Water.* 13(17). 2356. https://doi.org/10.3390/w13172356
5. Білецький В.С. (2021). Моделювання у нафтогазовій інженерії: навчальний посібник. Львів: Видавництво «Новий Світ 2000», Харків: НТУ «ХПІ». 306 с. https://ev.vue.gov.ua/wp-content/uploads/2023/10/Modeliuvannia-u-naftohazoviy-inzhenerii-17.08.2021-5-do-druku-1.pdf
6. Alaita, D.A. (2021). Computational fluid dynamics modelling of multi-phase flow transition in presence of solid particles. Robert Gordon University, PhD thesis. *Hosted on OpenAIR* https://doi.org/10.48526/rgu-wt-1603672

1. Kasat G., Khopkar A.R., Ranade V.V. & Pandit A.B. (2008). CFD Simulation of Liquid-Phase Mixing in Solid–Liquid Stirred Reactor. *Chemical Engineering Science.* 63(15). 3877-3885. https://www.researchgate.net/publication/223618439_CFD_Simulation_of_Liquid-Phase_Mixing_in_Solid-Liquid_Stirred_Reactor
2. Wang S. & Shen Y. (2025). CFD-DEM modelling of dense gas-solid reacting flow: Recent advances and challenges. *Progress in Energy and Combustion Science.* 109. 101221. https://doi.org/10.1016/j.pecs.2025.101221
3. Duan X., Feng X., Peng C., Yang C. & Mao Z. (2020). Numerical simulation of micro-mixing in gas–liquid and solid–liquid stirred tanks with the coupled CFD-E-model. *Chinese Journal of Chemical Engineering.* 28(9). 2235-2247. https://doi.org/10.1016/j.cjche.2020.06.016
4. Zapata Rivera A.M., Ducoste J., Peña M.R. & Portapila M. (2021). Computational Fluid Dynamics Simulation of Suspended Solids Transport in a Secondary Facultative Lagoon Used for Wastewater Treatment. *Water*. 13(17). 2356. https://doi.org/10.3390/w13172356

5. Biletskyi V.S. (2021). Modelling in oil and gas engineering: textbook. Lviv: Nova Svit 2000 Publishing House, Kharkiv: NTU «KhPI». 306 p. https://ev.vue.gov.ua/wp-content/uploads/2023/10/Modeliuvannia-u-naftohazoviy-inzhenerii-17.08.2021-5-do-druku-1.pdf

6. Alaita, D.A. (2021). Computational fluid dynamics modelling of multi-phase flow transition in presence of solid particles. Robert Gordon University, PhD thesis. *Hosted on OpenAIR* https://doi.org/10.48526/rgu-wt-1603672

7. Liu, P.; Wang, Q.; Luo, Y.; He, Z.; Luo, W. Study on a New Transient Productivity Model of Horizontal Well Coupled with Seepage and Wellbore Flow. *Processes* 2021, 9, 2257.
https://doi.org/10.3390/pr9122257
8. Friso, D. Mathematical Modelling of the Entrainment Ratio of High Performance Supersonic Industrial Ejectors. P*rocesses* 2022, 10, 88.
https://doi.org/10.3390/pr10010088
9. Wullenweber, M.S.; Kottmeier, J.; Kampen, I.; Dietzel, A.; Kwade, A. Simulative Investigation of Different DLD Microsystem Designs with Increased Reynolds Numbers Using a Two-Way Coupled IBM-CFD/6-DOF Approach. *Processes* 2022, 10, 403.
https://doi.org/10.3390/pr10020403

7. Liu, P.; Wang, Q.; Luo, Y.; He, Z.; Luo, W. Study on a New Transient Productivity Model of Horizontal Well Coupled with Seepage and Wellbore Flow. *Processes* 2021, 9, 2257
https://doi.org/10.3390/pr9122257
8. Friso, D. Mathematical Modelling of the Entrainment Ratio of High Performance Supersonic Industrial Ejectors. *Processes* 2022, 10, 88.
https://doi.org/10.3390/pr10010088
9. Wullenweber, M.S.; Kottmeier, J.; Kampen, I.; Dietzel, A.; Kwade, A. Simulative Investigation of Different DLD Microsystem Designs with Increased Reynolds Numbers Using a Two-Way Coupled IBM-CFD/6-DOF Approach. *Processes* 2022, 10, 403.
https://doi.org/10.3390/pr10020403

Тойстер Р.В.*
Національний університет «Полтавська політехніка імені Юрія Кондратюка»
https://orcid.org/0009-0006-6201-7811

Храпач А.В.
Національний університет «Полтавська політехніка імені Юрія Кондратюка»
https://orcid.org/0009-0005-2763-4542

Комп’ютерне моделювання структури потоку у комбінованому змішувачі для водних суспензій з твердою та газовою фазами

У статті виконано огляд процесів комп’ютерного моделювання структури багатофазного потоку у змішувачах для водних суспензій із твердою та газовою фазами. Проаналізовано особливості взаємодії рідкої, твердої та газової фаз у змішувальних системах, а також визначено, як локальні швидкості, турбулентні флуктуації та реологічні властивості середовища впливають на характер циркуляції і масообміну. Починаючи з розвитку CFD-DEM методів, моделювання дозволило наблизити реконструкцію реальних процесів у змішувачах до тривимірної картини, однак складність реальної динаміки середовища досі вимагає вдосконалення моделей. Дослідження показують, що газова фаза не лише підтримує циркуляційні процеси, а й змінює локальні структури швидкості, і таким чином впливає на розподіл твердих частинок у потоці. Крім того, в процесі аналізу виявлено, що деформація бульбашок газу, їхня коалесценція і руйнування, а також агрегація твердого компонента призводять до утворення зон із різною інтенсивністю масообміну та локальними нерівномірностями концентрації фаз. Робота змішувача залежить від співвідношення висоти камери, діаметра ротора і швидкості його обертання, що визначає стабільність циркуляційних контурів і рівномірність розподілу фаз. Відхилення від оптимальних режимних характеристик призводить до розвитку нестійких зон, де накопичення твердих частинок і газових бульбашок порушує загальну ефективність процесу змішування. Окрему увагу приділено питанню впливу реологічних властивостей суспензії на турбулентні характеристики потоку, оскільки підвищення концентрації твердого компонента змінює в’язкість і впливає на локальну стійкість циркуляційних структур. У статті також розглянуто перспективи інтеграції хімічно-кінетичних процесів у обчислювальні моделі змішування, що відкриває можливості для створення нових технологічних рішень у промисловості. Таким чином чисельне моделювання змішувальних систем із багатофазним середовищем залишається ефективним інструментом для оптимізації сучасних виробничих процесів, спрямованих на підвищення енергоефективності та зниження технологічних втрат.

Ключові слова: CFD-DEM моделювання, багатофазні потоки, комбінований змішувач, масообмін, газові бульбашки, циркуляційні структури.

*Адреса для листування E-mail: rtoister.cv@gmail.com

Збірник наукових праць. Галузеве машинобудування, будівництво
Academic journal. Industrial Machine Building, Civil Engineering
http://journals.nupp.edu.ua/znp
https://doi.org/10.26906/znp.2024.63.3879

UDC 693.546.3:621.928.1

Ievhen Vasyliev *
National University «Yuri Kondratyuk Poltava Polytechnic»
https://orcid.org/0000-0001-5133-3989

Dmytro Taranenko
National University «Yuri Kondratyuk Poltava Polytechnic»
https://orcid.org/0009-0009-8680-749X

Mobile compact gravity-force concrete mixer

The article discusses the design of a compact gravity-force concrete mixer, which combines the advantages of gravity and forced mixers. An analysis of existing designs and the mixing processes within them was conducted. The proposed design is promising due to its high energy efficiency, reliability, and compactness. Its small size simplifies transportation, and its versatility allows it to be placed at any construction site, which increases its flexibility of use. The mixer ensures high-quality mixing of solutions and adapts to various conditions.

Keywords: mixer, gravitational, forced, mixture, small size, blade, axis, shaft, energy efficiency, productivity, mixture homogeneity

*Corresponding author E-mail: vas.eugene@gmail.com

Introduction.

Every day, the construction industry in Ukraine faces significant challenges in the modern world. The constant destruction of private households or low-rise buildings is causing increased demand for restoration and new construction in the country. This, in turn, leads to an increase in demand for the manufacture of concrete structures, which cannot always be met due to the lack of affordable and practical tools. Therefore, it would be advisable to consider the potential functionality of existing concrete mixing equipment and its parameters, as well as to propose a design idea that offers a modern solution for such cases. It should be noted that the compact size and energy efficiency of the future design are key factors, since possible damage to power grids leads to an unstable supply of electricity to people's homes, which requires the design to operate in such a mode that it achieves the maximum amount of concrete mix produced in the shortest possible time. Another critical parameter is compactness, which is a personalised solution for moving and storing concrete mixers. It is believed that larger models of concrete mixers can be used; however, due to their high metal content and size, they are not always advisable for use in low-rise and private households.

However, ensuring productivity while reducing dimensions should remain comparable to analogues, while maintaining the cost of manufacturing and using this design. It is also advisable to pay attention to the reliability of the design and reduce the number of potentially vulnerable components of the concrete mixer [1].

Review of the research sources and publications. During the study of other publications on this topic, the works of prominent scientists who have dealt with solving problems related to operating modes and parameter selection for this type of equipment were analysed [1-11]. In their works, considerable attention was paid not only to the principle of operation of mixers, but also to achieving adequate mixing of ready-made mixtures, which significantly influences further research. It is worth distinguishing the comparative assessment of the efficiency of various mixers in terms of design, as studied in the work of Rogozin I.A. [11], since a universal indicator has been developed that allows evaluating the performance of mixers based on their design, which in turn provides a basis for a simplified analysis of the feasibility of design options for new construction equipment. His work also examines the efficiency coefficient of the mixer, which is determined by the machine's design features and parameters, resulting in the achievement of process efficiency through the parameter of mixing homogeneity. It is noted that this parameter can be achieved in several ways, namely by adjusting the coefficients of heterogeneity of the mixture concentration components, the degree of mixture

separation, or the values of the limit shear stress of the solution, which still result in an exponential dependence of the building material preparation process. A quality mixing process for a construction mortar will involve macro-mixing and micro-mixing. Meeting the quality conditions for mixing will result in a symmetric mixture structure with a homogeneous distribution throughout the entire volume of the drum's working space.

The requirements of DSTU standards [12, 13] for construction equipment, as well as the quality and speed of preparing ready-mixed concretes, were taken into account. Specifically, about general points, we can highlight ergonomics, safety, transportability, resistance to dynamic loads, and resistance to vibrations. Based on the standards above, further research on the gravity-fed mixer should consider an optimal layout of working parts, a reduction in material consumption, and a unified overall design..

a)

b)

c)

Figure 1 - Forced-action concrete mixers,
a) RSP-800,
b) SGSh-500,
c) BP2-100.

In addition, the rheology of construction mixtures, namely the hydrodynamics of viscous substances, was analysed. This is one of many initial factors for quickly and reliably achieving mixture homogeneity [9, 10]. Construction mixtures, particularly concrete, are non-Newtonian viscous fluids. Their behaviour, like that of all sand-cement mixtures, depends not only on the water content, but also on the combinations of interactions between the binder and different fractions of the aggregate. Parameters of the rheological model, such as yield stress, plastic viscosity, and thixotropy, are crucial for designing mixers and selecting optimal operating modes. Hydrodynamics in mixing enable the determination of the distribution of velocities, flow vectors, and stresses in the liquid or semi-liquid phases of a cement-sand mixture [4].

An analysis of the main model designs currently available on the Ukrainian market has revealed that several distinct concrete mixers and their operating principles can be identified, which can serve as a basis for developing a new design, as they are the most common representatives in their category.

Most forced-action concrete mixers [15, 16, 17] are continuous in operation; their design includes a stationary drum and working blades that rotate relative to the drum axis. The working mixture is loaded into the stationary drum, and the blades, performing a rotational movement, ensure the mixture is thoroughly mixed. The finished mixture is discharged through an opening located at the bottom of the drum, which does not always meet operational requirements. In addition, complete unloading of such a mixer is complicated [3, 4, 5, 8].

A unique feature of the design is that the mixer drive can be located under the drum, above the drum, or, in the case of horizontal shafts, on the side. A drive shaft transmits the torque through a pipe to a traverse, to which the blades are attached. The pipe is rigidly and hermetically fixed to the lower plane of the drum, ensuring that there is no contact between the rotating drive shaft and the working medium, thereby providing greater reliability to the structure. However, this type of concrete mixer design is metal-intensive and, accordingly, heavy and expensive, which limits its mobility [2, 3].

Gravity mixers [17, 18] operate on the principle of the natural collapse of the mixture in the drum, under the influence of gravity. In such a mixer, the blades are rigidly fixed to the inner surface of the drum. As the drum rotates, the components of the mixture are prevented from sliding along the drum walls. The advantages of this mixer are its simple design, high reliability, and consequently, lower material consumption and cost, as well as its compactness and ease of transport.

In addition, complete unloading of the mixer is not problematic. Therefore, its design is the most common among mobile concrete mixers. However, this mixer design also has the disadvantages characteristic of

gravity mixers, namely the difficulty of obtaining a uniform mixture composition [1, 4, 5, 8].

Figure 2 - Gravity-type concrete mixers.
a) Skif BSM-200,
b) Forte EW9180P.

Definition of unsolved aspects of the problem. This study aims to optimise the parameters of a small-sized concrete mixer that combines the advantages of different operating principles, including gravity and forced action mixers.

Among the main parameters studied, special attention was paid to energy efficiency and mixing quality. The general parameters included compact size, reliability of components, and metal intensity, which also took into account the manufacture of special concrete mixer components.

Problem statement.

One of the key problems with this type of equipment is maintaining a balance between mixing quality and energy efficiency. It is believed that further research on this topic, combining the design features of gravity and forced action mixers, will result in improved mixture quality with significantly lower energy consumption.

From the perspective of insufficient justification of the parameters of similar equipment, it stimulates further possible research on this topic.

Basic material and results.

The mixing process itself is much more complicated than it may seem at first glance. To obtain a homogeneous mixture, it is necessary to distribute its components evenly throughout the entire volume of the mixing drum and to achieve dispersion of liquid droplets and air bubbles, while maintaining a uniform shear stress in the mixture during circulation. To accurately study the mixing process, a parameter is needed that can summarise and evaluate the quality of the prepared mixture. The most accurate and fair criterion for construction mixtures is the heterogeneity criterion, also known as the coefficient of variation; as this parameter increases, the heterogeneity of the mixture increases [1-7].

$$K_{var} = \frac{100}{\overline{c}} \sqrt{\frac{1}{n-1} \sum_{i=1}^{n} \left(c_i - \overline{c}\right)^2} \qquad (1)$$

where $\overline{c}$ – arithmetic mean value of the concentration of the key component in all n samples of the mixture, %;

c –concentration of the key component in the i-th sample of the mixture, %.

Among the main parameters, mixing performance will also be taken into consideration.

$$П_{експл} = V_{заг} \cdot Z_ц, \ m^3 / hour. \qquad (2)$$

$$П_{експл} = V_{заг} \cdot Z_ц \cdot \rho_0, \ m^3 / hour. \qquad (2)$$

$V_{заг.}$ – total volume of the mixture in the mixer body, m^3;

ρ_0 – average density of concrete mix, kg/m^3;

$Z_ц = 3600/t_ц$ number of machine cycles per hour;

$t_ц$- duration of one cycle, which consists of the sum of the duration of loading components t_1, and their movement [7, 8].

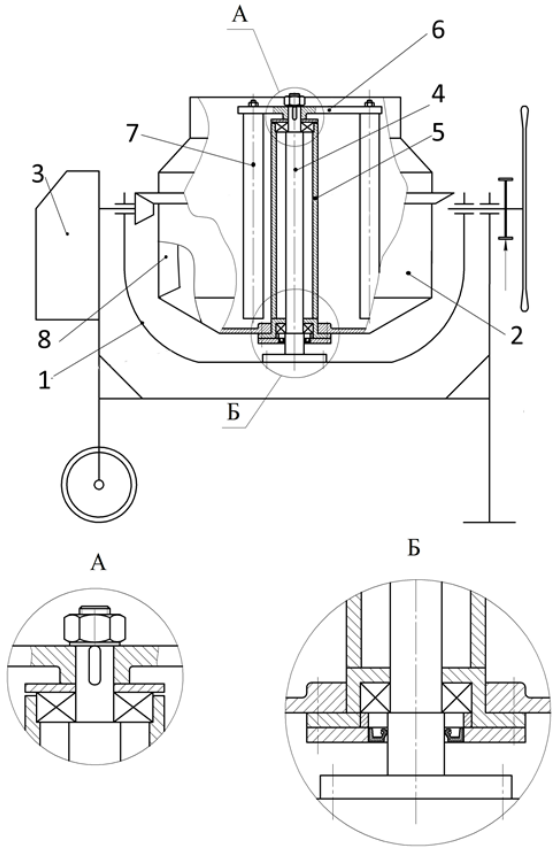

Figure 3 - Compact mixer

An analysis of the main model designs currently available on the market has revealed several separate concrete mixers that can serve as the basis for a theoretical design. During construction or renovation work, both forced-action and gravity concrete mixers can be used. After reviewing existing mixers and considering the necessary calculations, the following model is proposed [19].

The design kinematic diagram of the mixer for a rotating drum entirely coincides with that of a conventional gravity mixer. The mechanical energy of rotation from the electric motor drive 1 is transmitted through a bevel gear to the rim of drum 2, causing it to rotate. The drum, as before, rotates freely around the central axis. The central axis 4 is rigidly fixed to the movable frame 1, and the movable frame 1 can tilt, tilting the drum 2 to the required position. The central axis 4 runs along the axis of the drum 2, coaxially in the central pipe 5. In the central pipe 5, bearings are located at the upper and lower ends, on which the central axis 4 is fixed. The central pipe 5 is hermetically sealed to the lower part of the drum 2, which allows the drum 2 to rotate freely on the bearings of the central axis 4. At the same time, the mixture cannot directly contact the central axis 4, which ensures the proper reliability of the drive. A traverse 6 is installed on the upper end of the central axis 4 using a spline connection, so it cannot rotate with the drum 2. The blades 7 are attached to the traverse 6, allowing for the necessary radial positioning relative to the axis of the hollow pipe 5.

The mixer operates as follows. Drum 6 contains a preloaded mixture that is to be mixed.

Depending on the technological needs (mixture recipe), the number and location of the replaceable blades 5 are set (mixing can also occur without the blades 5 in gravity mode). By changing the position of the movable frame 1, the required tilt angle of the drum 2 is set. The position must be such that the mixture inside the tank covers the blades of the drum, allowing the mixture to rotate with the drum. The blades 8 prevent the mixture from sliding along the inner walls of the drum 2. The mixture moves with the drum 2, while the blades 7 of the traverse 6 remain stationary and begin to forcibly mix the mixture. Simultaneously, in addition to the forced mixing provided by the blades 7 of the traverse 6, the gravity mixing process continues with the help of the blades 8 of the drum 2. This makes it possible to ensure high mixing efficiency in a shorter period.

Conclusion. after considering the advantages of the proposed design for a mobile compact gravity-force concrete mixer, we found that despite its low material consumption, the design is highly reliable. The drum 2 rotates on a rigidly mounted axis 4 and rests on two bearings, which are spaced as far apart as possible. This ensures extremely stable operating conditions for the bevel gear, especially under a full load. Additionally, the design is compact and easy to transport. If needed (for example, when manually moving the mixer from one floor to another), drum 2, along with traverse 6, can be easily detached from movable frame 1, which significantly simplifies transportation, as reinstalling drum 2 is not difficult.

References

1. Desai, A., Bhutani, H., Chavan, A., Chitnis, A., & Chowdhary, D. (2021). Design and analysis of a portable concrete mixer. *International Research Journal of Engineering and Technology*, 8(7), 4371–4376.
2. Stolz, C. M., & Masuero, A. B. (2018). Influence of grains distribution on the rheological behavior of mortars. *Construction and Building Materials*, 177(1), 261–271. https://doi.org/10.1016/j.conbuildmat.2018.05.131
3. Korobko, B., Zadvorkin, D., & Vasyliev, I. (2018). Energy efficiency of a hydraulically actuated plastering machine. *International Journal of Engineering & Technology,* 7(3.2), 203–208. https://doi.org/10.14419/ijet.v7i3.2.14403
4. Онищенко, О. Г., Пічугін, С.Ф., Онищенко, В. О., Стороженко, Л. І., Семко, О. В., Слюсаренко Ю. С., & Ємельянова, І. А. (2011). *Високоефективні технології та комплексні конструкції в промисловому й цивільному будівництві*. Полтава: ТОВ АСМУ.
5. Ємельянова, І. А., Гордієнко, А. Т., & Субота, Д. Ю. (2018). Особливості виконання бетонних робіт в умовах будівельного майданчика. *Будівництво. Науковий вісник будівництва,* 3(93), 205–214. https://doi.org/10.29295/2311-7257-2018-93-3-205-214
6. Вірченко, В. В. (2015). *Підвищення ефективності роботи мобільного малогабаритного штукатурного агрегату* (Дисертація кандидата технічних наук,

1. Desai, A., Bhutani, H., Chavan, A., Chitnis, A., & Chowdhary, D. (2021). Design and analysis of a portable concrete mixer. *International Research Journal of Engineering and Technology*, 8(7), 4371–4376.
2. Stolz, C. M., & Masuero, A. B. (2018). Influence of grains distribution on the rheological behavior of mortars. *Construction and Building Materials*, 177(1), 261–271. https://doi.org/10.1016/j.conbuildmat.2018.05.131
3. Korobko, B., Zadvorkin, D., & Vasyliev, I. (2018). Energy efficiency of a hydraulically actuated plastering machine. *International Journal of Engineering & Technology,* 7(3.2), 203–208. https://doi.org/10.14419/ijet.v7i3.2.14403

4. Onyshchenko, O. G., Pichugin, S. F., Onyshchenko, V. O., Storozhenko, L. I., Semko, O. V., Slyusarenko, Y. S., & Emelyanova, I. A. (2011*). Highly efficient technologies and complex structures in industrial and civil construction*. Poltava: ASMU LLC.
5. Yemelianova, I. A., Gordienko, A. T., & Subota, D. Y. (2018). Features of concrete works in construction site conditions. Scientific Bulletin of Construction, 3(93), 205–214. https://doi.org/10.29295/2311-7257-2018-93-3-205-214
6. Virchenko, V. V. (2015). *Improving the efficiency of a mobile small-sized plastering unit* [Candidate's

Харківський національний університет будівництва та архітектури).

7. Онищенко, О. Г., & Ващенко, К. М. (2006). Розрахунок потужності та визначення опорів, що виникають при роботі стрічкового шнекового розчинозмішувача. *Вісник КДПУ: Збірник наукових праць*, *(1)36*, 58–63.

8. Korobko, B., & Vasyliev, I. (2017). Test method for rheological behaviour of mortar for building work. *Acta Mechanica et Automatica*, 11(3), 173–177. https://doi.org/10.1515/ama-2017-0025

9. Ковальов, І. О., Ратушний, О. В., & Колісніченко, Е. В. (2023). *Інтегральний курс механіки рідини й газу: навчальний посібник*. Суми: СумДУ.

10. Панченко, В. О., Івченко, О. В., Мелейчук, С. С. та ін. (2021). *Спеціальні гідромашини: навчальний посібник* (В. О. Панченко, ред.). Суми: СумДУ.

11. Рогозін, І. А. (2019). *Обґрунтування параметрів штукатурно-змішувальної установки з вертикальним шнеком* (Дисертація кандидата технічних наук, Полтавський національний технічний університет імені Юрія Кондратюка).

12. ДСТУ Б В.2.7-46:2010. (2011). *Будівельні матеріали. Цементи загальнобудівельного призначення. Технічні умови.* Київ: Мінрегіон України.

13. ДСТУ Б В.2.8-19:2009. (2009). *Будівельна техніка, оснастка, інвентар та інструмент. Рівні будівельні. Технічні умови*. Київ: Держспоживстандарт України.

14. Бетонозмішувач примусовий РСП-800. (н.д.). Машини та обладнання для будівельних робіт. https://budprom.in.ua/uk/stroitelnoye-oborudovaniye/betonomeshalki-i-rastvoromeshalki/betonosmesitel-prinuditelnyy-rsp-800 (дата звернення: 25.01.2024).

15. Горизонтальний шнековий змішувач СГШ-500. *Машини та обладнання для будівельних робіт* : веб-сайт. URL: https://4build.biz/gorizontalnyj-shnekovyj-smesitel-sgsh-500 (дата звернення: 25.01.2024).

16. Примусовий бетонозмішувач БП2-100 *Машини та обладнання для будівельних робіт* https://4build.biz/prinuditelnyj-betonosmesitel-bp2-100 (дата звернення: 25.01.2024).

17. Бетонозмішувач Скіф БСМ-200 з редуктором перевороту. *Машини та обладнання для будівельних робіт*: веб-сайт. URL: https://skif.ua/betonomeshalka-skif-bsm-200-s-reduktorom-perevorota (дата звернення: 25.01.2024).

18. Бетонозмішувач Forte EW9180P 180 л. *Машини та обладнання для будівельних робіт*: веб-сайт. URL: https://epicentrk.ua/ua/shop/betonomeshalka-forte-ew9180p.html (дата звернення: 25.01.2024).

19. Васильєв, Є. А., & Тараненко, Д. В. (2024). Мобільний гравітаційний бетонозмішувач примусової дії (Патент України № 156153). Національний університет «Полтавська політехніка імені Юрія Кондратюка». https://uapatents.com/20-2024

dissertation, Kharkiv National University of Construction and Architecture].

7. Onyshchenko, O. G., & Vashchenko, K. M. (2006). Calculation of power and determination of resistances arising during the operation of a belt screw mortar mixer. *Bulletin of KDPU*, 1(36), 58–63.

8. Korobko, B., & Vasyliev, I. (2017). Test method for rheological behaviour of mortar for building work. *Acta Mechanica et Automatica*, 11(3), 173–177. https://doi.org/10.1515/ama-2017-0025

9. Kovalov, I. O., Ratushny, O. V., & Kolisnichenko, E. V. (2023). *Integral course in fluid and gas mechanics: Textbook.* Sumy: Sumy State University.

10. Panchenko, V. O., Ivchenko, O. V., Meleychuk, S. S., et al. (2021). *Special hydraulic machines: Textbook* (V. O. Panchenko, Ed.). Sumy: Sumy State University.

11. Rohozin, I. A. (2019). *Justification of the parameters of a plaster mixing plant with a vertical screw* [Candidate's dissertation, Poltava National Technical Yuri Kondratyuk University].

12. Ministry of Regional Development of Ukraine. (2011). *DSTU B V.2.7-46:2010. Building materials. Cements for general construction purposes. Technical conditions.*

13. State Consumer Standards of Ukraine. (2009). *DSTU B V.2.8-19:2009. Construction machinery, equipment, inventory and tools. Construction levels. Technical conditions.*

14. RS-800 forced concrete mixer. (2024). *Machinery and Equipment for Construction Works*. https://budprom.in.ua/uk/stroitelnoye-oborudovaniye/betonomeshalki-i-rastvoromeshalki/betonosmesitel-prinuditelnyy-rsp-800

15. Horizontal screw mixer SGSh-500. (2024). *Machinery and Equipment for Construction Works.* https://4build.biz/gorizontalnyj-shnekovyj-smesitel-sgsh-500

16. BP2-100 compulsory concrete mixer. (2024). *Machinery and Equipment for Construction Works*. https://4build.biz/prinuditelnyj-betonosmesitel-bp2-100

17. Skif BSM-200 concrete mixer with reverse gear. (2024). *Machinery and Equipment for Construction Works.* https://skif.ua/betonomeshalka-skif-bsm-200-s-reduktorom-perevorota

18. Forte EW9180P 180 L concrete mixer. (2024). Machinery and Equipment for Construction Works. https://epicentrk.ua/ua/shop/betonomeshalka-forte-ew9180p.html

19. Vasilyev, Y. A., & Taranenko, D. V. (2024). Mobile forced-action gravity concrete mixer (Patent No. 156153, Ukraine). National University "Yuri Kondratyuk Poltava Polytechnic". https://uapatents.com/uk/patents/156153

Васильєв Є.А.*
Національний університет «Полтавська політехніка імені Юрія Кондратюка»
https://orcid.org/0000-0001-5133-3989

Тараненко Д.В.
Національний університет «Полтавська політехніка імені Юрія Кондратюка»
https://orcid.org/0009-0009-8680-749X

Мобільний гравітаційний бетонозмішувач примусової дії

У статті розглянуто конструкцію малогабаритного гравітаційний бетонозмішувач примусової дії, який міг би бути ефективним у приготуванні бетонних сумішей за рахунок поєднання принципів роботи бетонозмішувачів гравітаційної і примусової дії. Припускається, що зазначена конструкція малогабаритного гравітаційно-примусового бетонозмішувача виявиться перспективною та інноваційною у сфері приготування будівельних сумішей. Її унікальність полягає в тому, що вона успішно поєднує переваги як гравітаційних, так і примусових бетонозмішувачів, а також ефективно вирішує проблеми, що виникають при їхньому застосуванні на будівельних майданчиках. Також у статті проаналізовано аналоги існуючих бетонозмішувачів гравітаційної дії і примусової дії. Досліджено процеси виникаючі при обох видах змішування сумішей в існуючих аналогах, які виконують дані операції перемішування на будівельних майданчиках. Передбачається, що дана конструкція забезпечує високу ефективність змішування, має покращену енергоефективність серед аналогів, надійність своїм розташуванням вузлів. Один із головних плюсів запропонованої конструкції полягає в малогабаритності конструкції, що сприяє полегшенню транспортування її по будівельному майданчику. Це не тільки збільшує ефективність робіт, але й робить процес будівництва економічно вигіднішим. Розроблена конструкція є достатньо компактною та універсальною. Додатковою перевагою є універсальність конструкції, яка дозволяє розміщувати обладнання в будь-якому місці будівельних робіт. Це робить змішувач гнучким і адаптованим до різних умов та завдань на будівельному майданчику. Вона забезпечує ефективне змішування будівельних розчинів у встановленому об'ємі, забезпечуючи при цьому енергоефективність змішування. Однак вона також має переваги завдяки об'єднанні виникаючих процесах в обох видах змішувачів, а також можливості розміщення обладнання в будь-якому місці будівельних робіт. Загалом, дана конструкція гравітаційно-примусового бетонозмішувача видається перспективною і обіцяючою, вирішуючи численні технічні та економічні аспекти, пов'язані з будівництвом

Ключові слова: змішувач, гравітаційний, примусовий, суміш, малогабаритність, лопатка, вісь , вал, енергоефективність, продуктивність, однорідність суміші.

*Адреса для листування E-mail: vas.eugene@gmail.com

Збірник наукових праць. Галузеве машинобудування, будівництво
Academic journal. Industrial Machine Building, Civil Engineering
http://journals.nupp.edu.ua/znp
https://doi.org/10.26906/znp.2024.63.3887

UDC 666.97.035

Volodymyr Gerasymenko *
O. M. Beketov National University of Urban Economy in Kharkiv
https://orcid.org/0000-0002-7874-1322

Olena Protsenko
O. M. Beketov National University of Urban Economy in Kharkiv
https://orcid.org/0000-0002-2478-4781

Volodymyr Lus
O. M. Beketov National University of Urban Economy in Kharkiv
https://orcid.org/0009-0007-5540-8651

Iryna Bielykh
O. M. Beketov National University of Urban Economy in Kharkiv
https://orcid.org/0009-0005-9232-9683

Calculation of structural parameters of a vibratory machine

The article is dedicated to the development of a vibratory machine for compacting concrete mixtures, ensuring the adaptation of vibration modes to the mixture's condition to enhance energy efficiency and concrete quality. The study was conducted through literature analysis, vibration parameter modeling, and calculation of structural characteristics. It was established that modern methods, such as DEM and CFD, highlight the need for flexible vibration control to prevent microstructure defects. A machine design based on elastic pneumatic shells operating in resonant mode is proposed. Key formulas for calculating the vibratory platform are provided. The design achieves a 15% reduction in energy consumption compared to traditional machines, stable compaction, and adaptability to various mixture types. The results confirm the effectiveness of the proposed solution for forming a dense concrete microstructure. Further research involves experimental validation and parameter optimization.

Keywords: vibratory machine, concrete compaction, resonant mode, elastic shells, energy efficiency, concrete quality, concrete mixture

*Corresponding author E-mail: vladimirg54213@gmail.com

Introduction

The quality of hardened concrete significantly depends not only on the control of preliminary technological operations, such as the scientifically grounded selection of components (cement, aggregates of various fractions, water, chemical admixtures) [1], precise dosing to achieve the required granulometric composition and to ensure high homogeneity of the mixture during mixing [2], but also on the efficiency of vibration compaction [3]. The optimization of its parameters (frequency, amplitude, duration) plays a decisive role in the formation of a dense microstructure [4] and in achieving the required physical and mechanical properties of the final product [5]. The aim of this study is to develop the design of a vibration machine that allows the adaptation of vibration parameters to the state of the concrete mixture, while ensuring energy efficiency and stability of quality.

Review of Research Sources and Publications

The process of compacting a concrete mixture by vibration is the central stage in the entire technological chain of concrete and reinforced concrete production. The efficiency of this stage directly determines not only the strength, but also the overall structural stability, durability, and absence of internal defects [5], [6]. Although vibration compaction has been studied for many years, its true intricacies have been revealed only with the introduction of digital simulations, sensor technologies, and artificial intelligence-based algorithms [3], [7], [8]. These tools enable, for the first time, an in-depth understanding of the behavior of a concrete mixture at the moment of dynamic disturbance—precisely where micropores close and aggregate grains rearrange [4], [9].

One of the key approaches in recent studies has been the discrete element method (DEM), which allows for modeling the behavior of each individual element within the system. In [3], DEM was used to visually

demonstrate the response of fresh concrete particles to vibrational loading—how they move, interact with one another, and how contact configurations change. These visualizations effectively transform abstract assumptions into comprehensible models. Continuing in this direction, [7] combined DEM with CFD (computational fluid dynamics) modeling, making it possible not only to observe particle motion but also to track changes in the rheological characteristics of the mixture under vibration.

Another important aspect is the settlement of aggregates, which directly affects the homogeneity and strength of the concrete structure. Study [9] found that vibration causes local concentrations of aggregate that disturb structural balance and may lead to internal defects. An alternative approach, presented in [4], proposes a method of precise vibration control, enabling the optimization of vibration parameters according to the actual state of the mixture, thereby reducing the risk of uneven compaction and pore formation.

The duration of vibration also lacks a universal optimum. In particular, for high-density and high-strength concretes (so-called UHPC—ultra-high-performance concretes), even slight over-compaction leads to the destruction of the delicate microstructure. Authors of [6] concluded that microcracks emerge at a stage that visually appears fully satisfactory. A similar sensitivity is observed in slipform systems [5], where both insufficient and excessive vibration duration reduce compactness, leading to premature structural wear.

On the other hand, new approaches to evaluating the energy efficiency of compaction—such as the model proposed in [2]—enable quantitative analysis of how much energy is transferred to the concrete mass and how it correlates with the degree of compaction. This allows moving away from empirical parameters toward a scientifically grounded compaction control system.

Another current trend is the changing nature of concrete mixtures themselves. With the introduction of composites, nanodispersed additives, and complex forms, traditional visual control methods for compaction have largely lost their effectiveness. Here, machine learning and artificial intelligence technologies are coming into play. In [10], a method for evaluating vibrational effects in nanocomposite structures was proposed, opening prospects for adaptive compaction control based on real-time data.

Studies [8] and [11] focus directly on real-time algorithms capable of analyzing sensor readings during compaction and automatically detecting deviations—such as reduced density, incomplete settlement, or excessive porosity. These systems are integrated into production processes and can potentially adjust vibration parameters in real time.

Problem Statement

Based on the above, it becomes clear that vibration parameters cannot be considered fixed values but should be adjusted depending on the current state of the mixture. Rigidly set parameters are no longer effective. Without adaptation and flexible regulation, quality instability, resource overuse, and ultimately, risks of structural failure arise.

The use of vibration machines in near-resonant modes makes it possible to significantly reduce loads on the drive mechanism and, accordingly, lower the overall energy consumption of the equipment. This is because, when operating close to the natural frequency of the oscillatory system, energy is spent only on compensating for losses, rather than on forced excitation—the coefficient of dynamic efficiency here plays a key role [1; 3, 12]. Under such conditions, the energy required to maintain stable oscillations decreases in proportion to the dynamic sensitivity of the system, making resonance mode highly attractive for energy-efficient compaction of concrete mixtures.

However, ensuring stable operation in this range requires a highly accurate control system—specifically, maintaining the imbalance rotation frequency within a very narrow band around the resonance peak. Implementing such functions necessitates complex electronic circuits, digital controllers, and feedback loops based on acceleration, strain, or density sensors [6; 8]. From a technical standpoint, this is feasible, but from an economic perspective, it is not always practical: the cost of the control system often rises faster than the productivity of the equipment itself. This is especially noticeable in large-scale vibration platforms, where electronics can represent a significant share of total system costs [1].

Additionally, as machine power increases, the dynamic forces to be compensated by the control system also grow. This demands more reliable components, backup algorithms, and maintenance by highly qualified personnel. As a result, the energy savings achieved through resonance mode are partially or fully offset by the costs of maintaining high-tech control systems [11].

A second important aspect of efficient vibration compaction of concrete mixtures is the use of vibro-impact mode. Initially, the mixture must be vigorously agitated, which requires large amplitude and low frequency. Subsequently, for effective compaction, frequency increases while amplitude decreases [13].

Main Material and Results

Based on the identified issues and the analysis of the literature, a design of a vibration machine was developed that adapts vibration regimes to the state of the mixture, ensuring both energy efficiency and operational stability. Its core is a movable upper platform (pos. 2), on which a mold with the concrete mixture (pos. 1) is placed. It interacts with the lower stationary support (pos. 5). Between these elements, elastic pneumatic shells (pos. 6) are installed, serving as the source of reciprocating motion. To prevent unwanted horizontal displacements of the moving part, guides (pos. 4) are provided.

Compressed air is supplied from a compressor (pos. 10) or from the plant's main pneumatic line. Its

distribution is controlled by spool pneumatic distributors (pos. 7), which regulate air delivery to the pneumatic shells. To reduce pressure fluctuations in the system, a receiver (pos. 9) is installed. A controlled valve (pos. 8) allows rapid interruption or initiation of air supply.

The operating frequency of the pneumatic distributors is regulated by an electric drive (pos. 11), which controls the rotation speed. To enhance the downward movement of the platform, additional elastic elements (pos. 3) are used, accumulating the energy of the return impulse.

The asynchronous motor 11 is controlled via frequency converters, allowing smooth adjustment of rotational speed over a wide range while maintaining high efficiency. The use of such a frequency converter eliminated the need for a more expensive DC motor.

In the presented schematic, cylindrical compression springs with constant stiffness are used as springs (pos. 3). As noted in [14], the vibration platform operates steadily in resonance mode. To ensure resonance in this design, variable stiffness of the elastic shells (pos. 6) and springs (pos. 3) is required.

The stiffness of the shells is determined by the following formula:

$$C=C_1+C_2+C_3 \quad (1)$$

where: C_1 – stiffness of the elastic layer of compressed air (N/m); C_2- stiffness determined by the effective area (N/m); C_3 – stiffness of the elastic rubber–cord shell (N/m).

As follows from formula (1), the stiffness values C_2 and C_3 for a structurally selected elastic shell vary only within narrow limits. The stiffness value C_1 is determined as:

$$C_1 = n\,(b_к + L_к)\,p \quad (2)$$

де: n – number of elastic shells;

$b_к = \frac{\pi\left(r-\frac{y}{2}\right)}{2}\left(1 + k_1\frac{y}{2} + k_2\left(\frac{y}{2}\right)^2\right)$ – width of contact of the elastic shell in the transverse cross-section with the table (m); $L_к$ – length of contact between the elastic shell and the table (m); p – compressed air pressure (Pa).

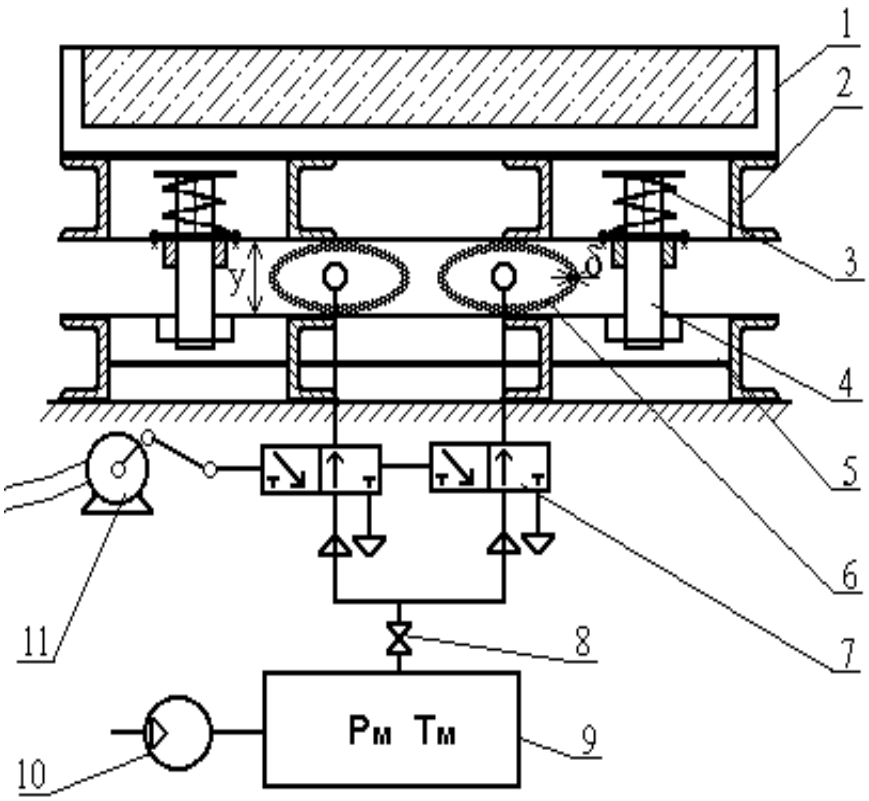

Figure 1 – Schematic diagram of a vibrating platform on elastic shells
1 – mold with concrete mix; 2 – upper movable table; 3 – springs; 4 – guides; 5 – fixed table; 6 – elastic shells; 7 – pneumatic distributor; 8 – valve; 9 – receiver; 10 – compressor; 11 – electric motor.

Taking into account the width of contact between the shell and the table surface, expression (2) takes the form:

$$C_1 = n\,p\left[\frac{\pi(r-\frac{y}{2})}{2}(1 + k_1\frac{y}{2} + k_2(\frac{y}{2})^2 + L_к\right] \quad (3)$$

where: r - inner radius of the shell in the initial state (m); y – radial deformation of the shell (m); k_1, k_2 - empirical or experimentally selected coefficients accounting for the geometry and elasticity of the material.

On the basis of expression (2), under the given constructive length of the table and the size of the elastic shell, the change in stiffness C_1 will be determined by the variation in compressed air pressure.

The stiffness C_3 in this case can be approximated through the radial stiffness of a cylinder compressed between two planes, according to the formula:

$$C_3 = \frac{E_{гк} L_к}{\ln(\frac{8R}{t})} \quad (4)$$

where: $E_{гк}$ - elastic modulus of the rubber–cord; R - outer radius of the shell (m); $L_к$ – length of the shell (along the guiding axis, i.e., its "length lying on the table") (m).

The stiffness determined by the effective area C_2 constitutes about 6–8% of the sum of stiffnesses C_1 and C_3.

The stiffness of the upper springs and lower elastic shells is found from the resonance amplitude condition:

$$C = \frac{F_{ін} \pm G}{2 * A_{рез}} \quad (5)$$

The energy expended for the displacement of inertial masses of the vibration platform (primarily the moving table (2) with the mold and the concrete mixture (1)) is described by the power balance equation. This equation accounts for the work of resistive forces that dissipate energy. For harmonic oscillations in steady-state mode, viscous damping forces proportional to velocity play a key role.

The general power balance equation is:

$$P_{прив} = P_{демп} + P_{терт} + P_{бет} + P_{інш} \quad (6)$$

where: $P_{демп}$- power dissipated through system damping; $P_{терт}$ - power lost to overcome friction in guides; $P_{бет}$- power transmitted into the concrete mixture to overcome its viscous resistance; $P_{інш}$- power dissipated in other elements.

For energy over a vibration period T:

$$E_{прив} = \int_0^T P_{прив} dt = E_{демп} + E_{терт} + E_{бет} + E_{інш} \quad (7)$$

The dissipative energy due to damping per period T:

$$E_{демп} = \int_0^T b_{екв} (x'(t))^2 dt \quad (8)$$

where: $b_{екв}$- equivalent viscous damping coefficient of the system (N·s/m); $x'(t)$- velocity of the moving table (m/s).

Thus, the instantaneous energy dissipated by damping is:

$$E_{демп}(t) = F_{демп} x'(t) = b_{екв} (x'(t))^2 \quad (9)$$

where: $F_{демп} = b_{демп} x'(t)$ - damping force.

For harmonic oscillations:

$$x(t) = A sin(\omega t) \quad (10)$$

$$x'(t) = A\omega cos(\omega t) \quad (11)$$

where: A- amplitude (m); ω - angular frequency (rad/s).

Then the energy dissipated by the damper per period is:

$$E_{демп} = b_{екв} \int_0^T (A\omega cos(\omega t))^2 dt = b_{екв} A^2 \omega^2 \int_0^T cos^2(\omega t) dt$$

$$E_{демп} = \pi b_{екв} A^2 \omega \quad (12)$$

The equivalent damping coefficient is defined as:

$$b_{екв} = b_р + b_{пр} + b_{напр} + b_{бет} + b_{інш} \quad (13)$$

where: $b_р = \frac{\eta Кос(P)}{\omega}$ - equivalent damping of elastic shells, proportional to air pressure P; $b_{пр}$- damping in metal springs (small, since $\eta_{ст} \approx 0.001 - 0.01$); $b_{напр} = \frac{4 F_{терт}}{\pi A \omega}$ - damping associated with friction in guides (for harmonic oscillations);

$b_{бет} = \beta \mu_{бет} V_{бет}$- damping due to concrete, β- experimentally determined proportionality coefficient, $\mu_{бет}$ - dynamic viscosity of the concrete mixture, $V_{бет}$ - volume of concrete in the mold;

$b_{інш}$- other damping (supports, joints, etc.), typically 5–7% of the equivalent damping.

Energy dissipated by friction in guides:

$$E_{терт} = 4 F_{терт} A = 4 \mu N A \quad (14)$$

where: $F_{терт} = \mu N$- friction force; μ- friction coefficient; N- normal force.

Energy consumed for compaction of concrete is determined by:

$$E_{бет} = \int_0^T P_{бет} dt = \frac{1}{2} k \mu_{бет} A^2 \omega^2 V_{бет} T \quad (15)$$

where: k- empirical coefficient accounting for mold geometry and distribution of the concrete mixture within it.

The influence of concrete on the dynamics of the vibration platform is a well-known problem considered in studies [15–17].

Key advantages of the proposed design include:

- *universality*: the machine adapts to different types of concrete mixtures thanks to adjustable vibration parameters, allowing optimization of the compaction process depending on material composition.
- *energy efficiency*: resonance mode operation with elastic elements reduces energy consumption by 10–20% compared with similar machines.
- *compaction quality*: uniform distribution of vibrational energy ensures high density and homogeneity of concrete products while minimizing defects.

Conclusions

This paper presents the development of a vibration machine design that enables the adaptation of vibration regimes to the state of the concrete mixture, ensuring both energy efficiency and quality stability. Based on the analysis of modern studies, the need for flexible control of vibration parameters was identified, which formed the basis for problem formulation. The proposed design on elastic shells, with stiffness calculated for resonance mode, demonstrates the

feasibility of achieving optimal compaction conditions. The results confirm that the developed machine reduces energy consumption and provides high-quality concrete products. Future research may focus on experimental validation of the design and optimization of its parameters for different types of concrete mixtures.

References

1. Zhao X., Huang Y., Dong W., Liu J., Ma G. A review of compaction mechanisms, influencing factors, and advanced methods in concrete vibration technology // Journal of Building Engineering. – 2024. – № 109847. – DOI: https://doi.org/10.1016/j.jobe.2024.109847.
2. Li J., Tian Z., Yu X., Xiang J., Fan H. Vibration quality evaluation of reinforced concrete using energy transfer model // Construction and Building Materials. – 2023. – Vol. 373. – Article 131247. – DOI: https://doi.org/10.1016/j.conbuildmat.2023.131247.
3. Yan W., Cui W., Qi L. DEM study on the response of fresh concrete under vibration // Granular Matter. – 2022. – DOI: https://doi.org/10.1007/s10035-021-01199-y.
4. Yu Z., Dong W., Wang F., Huang Y., Ma G. Enhancing concrete strength through precision vibration engineering: Aggregate settlement and pore stats // Construction and Building Materials. – 2025. – Vol. 464. – Article 140117. – DOI: https://doi.org/10.1016/j.conbuildmat.2025.140117.
5. Chai M., Hu C., Cheng M. Study on the effect of vibrating process on the compactness of slipform concrete // Applied Sciences. – 2023. – Vol. 13(14). – Article 8421. – DOI: https://doi.org/10.3390/app13148421.
6. Liu J., An M., Huang L., Wang Y., Han S. Influence of vibrating compaction time on the strength and microstructure of ultra-high performance concrete // Construction and Building Materials. – 2023. – DOI: https://doi.org/10.1016/j.conbuildmat.2023.133584.
7. Cao G., Bai Y., Shi Y., Li Z., Deng D., Jiang S., Xie S., Wang H. Investigation of vibration on rheological behavior of fresh concrete using CFD-DEM coupling method // Construction and Building Materials. – 2024. – DOI: https://doi.org/10.1016/j.conbuildmat.2024.135908.
8. Quan Y., Wang F. Machine learning-based real-time tracking for concrete vibration // Automation in Construction. – 2022. – Vol. 139. – Article 104343. – DOI: https://doi.org/10.1016/j.autcon.2022.104343.
9. Cai Y., Liu Q., Yu L., Meng Z., Hu Z., Yuan Q., Šavija B. An experimental and numerical investigation of coarse aggregate settlement in fresh concrete under vibration // Cement and Concrete Composites. – 2021. – Vol. 122. – Article 104153. – DOI: https://doi.org/10.1016/j.cemconcomp.2021.104153.
10. Lin Y., Ibraheem A. A. Machine learning method as a tool to estimate the vibrations of the concrete structures reinforced by advanced nanocomposites // Mechanics of Advanced Materials and Structures. – 2024. – DOI: https://doi.org/10.1080/15376494.2024.2355517.
11. Fan S., He T., Li W., Zeng C., Chen P., Chen L., Shu J. Machine learning-based classification of quality grades for concrete vibration behaviour // Automation in Construction. – 2024. – Vol. 167. – Article 105694. – DOI: https://doi.org/10.1016/j.autcon.2024.105694.
12. Назаренко І.І. Вібраційні машиниі процеси будівельної індустрії: Навчальний посібник.–К.: КНУБА, 2007.-230с
13. Nazarenko, I. and Slipetskyi, V. (2019). Analysis and Synthesis of Creation of Vibration Machines with an Estimation of Their Efficiency and Reliability. Technology audit and production reserves, 6(1(50)). https://doi.org/10.15587/2312-8372.2019.189057

1. Zhao X., Huang Y., Dong W., Liu J., Ma G. A review of compaction mechanisms, influencing factors, and advanced methods in concrete vibration technology // Journal of Building Engineering. – 2024. – № 109847. – DOI: https://doi.org/10.1016/j.jobe.2024.109847.
2. Li J., Tian Z., Yu X., Xiang J., Fan H. Vibration quality evaluation of reinforced concrete using energy transfer model // Construction and Building Materials. – 2023. – Vol. 373. – Article 131247. – DOI: https://doi.org/10.1016/j.conbuildmat.2023.131247.
3. Yan W., Cui W., Qi L. DEM study on the response of fresh concrete under vibration // Granular Matter. – 2022. – DOI: https://doi.org/10.1007/s10035-021-01199-y.
4. Yu Z., Dong W., Wang F., Huang Y., Ma G. Enhancing concrete strength through precision vibration engineering: Aggregate settlement and pore stats // Construction and Building Materials. – 2025. – Vol. 464. – Article 140117. –DOI: https://doi.org/10.1016/j.conbuildmat.2025.140117.
5. Chai M., Hu C., Cheng M. Study on the effect of vibrating process on the compactness of slipform concrete // Applied Sciences. – 2023. – Vol. 13(14). – Article 8421. – DOI: https://doi.org/10.3390/app13148421.
6. Liu J., An M., Huang L., Wang Y., Han S. Influence of vibrating compaction time on the strength and microstructure of ultra-high performance concrete // Construction and Building Materials. – 2023. – DOI: https://doi.org/10.1016/j.conbuildmat.2023.133584.
7. Cao G., Bai Y., Shi Y., Li Z., Deng D., Jiang S., Xie S., Wang H. Investigation of vibration on rheological behavior of fresh concrete using CFD-DEM coupling method // Construction and Building Materials. – 2024. – DOI: https://doi.org/10.1016/j.conbuildmat.2024.135908.
8. Quan Y., Wang F. Machine learning-based real-time tracking for concrete vibration // Automation in Construction. – 2022. – Vol. 139. – Article 104343. – DOI: https://doi.org/10.1016/j.autcon.2022.104343.
9. Cai Y., Liu Q., Yu L., Meng Z., Hu Z., Yuan Q., Šavija B. An experimental and numerical investigation of coarse aggregate settlement in fresh concrete under vibration // Cement and Concrete Composites. – 2021. – Vol. 122. – Article 104153. – DOI: https://doi.org/10.1016/j.cemconcomp.2021.104153.
10. Lin Y., Ibraheem A. A. Machine learning method as a tool to estimate the vibrations of the concrete structures reinforced by advanced nanocomposites // Mechanics of Advanced Materials and Structures. – 2024. – DOI: https://doi.org/10.1080/15376494.2024.2355517.
11. Fan S., He T., Li W., Zeng C., Chen P., Chen L., Shu J. Machine learning-based classification of quality grades for concrete vibration behaviour // Automation in Construction. – 2024. – Vol. 167. – Article 105694. – DOI: https://doi.org/10.1016/j.autcon.2024.105694.

12. Nazarenko, I Vibratory Machines and Processes of the Construction Industry: Textbook. – Kyiv: Kyiv National University of Construction and Architecture, 2007. – 230 p.

13. Nazarenko, I. and Slipetskyi, V. (2019). Analysis and Synthesis of Creation of Vibration Machines with an Estimation of Their Efficiency and Reliability. Technology audit and production reserves, 6(1(50)). https://doi.org/10.15587/2312-8372.2019.189057

14. Герасименко В.В, Віброплощадка з управляючим впливом на суміш яка ущільнюється автореф. дис. на здобуття наук. ступеня канд. техн. наук : спец. 05.05.02 – машини для виробництва будівельних матеріалів та конструкцій / В.В. Герасименко. – Харків, 2002.- 17 с. http://www.irbis-nbuv.gov.ua/aref/20081124004459
15. Maslov A., Savielov D., Salenko Y., Puzyr R. Research process of vibration platform movement for compacting polymer concrete mixtures // *AIP Conference Proceedings*. – 2022. – Vol. 2577. – Article ID: 050013. – DOI: 10.1063/5.0101309.
16. Назаренко І., Дьяченко О., Нестеренко М. Аналіз параметрів процесу ущільнення бетонного розчину і обґрунтування конструкцій дебалансного віброзбудника зі змінними параметрами // Техніка будівництва. – 2025. – № 42. – С. 102–115. https://doi.org/10.32347/tb.2025-42.0511
17. Bazhenov, V., Pogorelova, O. & Postnikova, T. (2021). Coexisting Regimes in Hysteresis Zone in Platform-Vibrator with Shock. Strength of Materials and Theory of Structures, (107), 3–19. https://doi.org/10.32347/2410-2547.2021.107.3-19

14. Gerasymenko, V.V. Vibratory Platform with Controlled Impact on the Compacted Mixture: Abstract of the Dissertation for the Degree of Candidate of Technical Sciences: Specialty 05.05.02 – Machines for the Production of Construction Materials and Structures / V.V. Gerasimenko. – Kharkiv, 2002. – 17 p. http://www.irbis-nbuv.gov.ua/aref/20081124004459
15. Maslov A., Savielov D., Salenko Y., Puzyr R. Research process of vibration platform movement for compacting polymer concrete mixtures // *AIP Conference Proceedings*. – 2022. – Vol. 2577. – Article ID: 050013. – DOI: 10.1063/5.0101309.
16. Nazarenko, I., Dyachenko, O., Nesterenko, M. Analysis of the Parameters of the Concrete Mixture Compaction Process and Justification of the Design of an Unbalanced Vibration Exciter with Variable Parameters // Construction Engineering. – 2025. – No. 42. – pp. 102–115.https://doi.org/10.32347/tb.2025-42.0511Bazhenov,
17. V., Pogorelova, O. & Postnikova, T. (2021). Coexisting Regimes in Hysteresis Zone in Platform-Vibrator with Shock. Strength of Materials and Theory of Structures, (107), 3–19. https://doi.org/10.32347/2410-2547.2021.107.3-19

Герасименко В.В.*
Харківський національний університет міського господарства імені О. М. Бекетова
https://orcid.org/0000-0002-7874-1322

Проценко І.М.
Харківський національний університет міського господарства імені О. М. Бекетова
https://orcid.org/0000-0002-2478-4781

Лусь В.І.
Харківський національний університет міського господарства імені О. М. Бекетова
https://orcid.org/0009-0007-5540-8651

Бєлих І.М.
Харківський національний університет міського господарства імені О. М. Бекетова
https://orcid.org/0009-0005-9232-9683

Розрахунок конструктивних параметрів вібраційної машини

Стаття присвячена розробці вібраційної машини для ущільнення бетонної суміші, що забезпечує адаптацію режимів вібрації до її стану для підвищення енергоефективності та якості бетону. Дослідження проводилося шляхом аналізу літератури, моделювання параметрів вібрації та розрахунку конструктивних характеристик. Встановлено, що сучасні методи, такі як DEM та CFD, вказують на потребу гнучкого управління вібрацією для уникнення дефектів мікроструктури. Запропоновано конструкцію машини на еластичних пневмооболонках, яка працює в режимі. Наведені основні формули для розрахунку запропонованого вібромайданчику. Конструкція забезпечує зниження енерговитрат до 15% порівняно з традиційними машинами, стабільність ущільнення та адаптацію до різних типів сумішей. Результати підтверджують ефективність запропонованого рішення для формування щільної мікроструктури бетону. Подальші дослідження передбачають експериментальну перевірку та оптимізацію параметрів.

Ключові слова: вібраційна машина, ущільнення бетону, резонансний режим, еластичні оболонки, енергоефективність, якість бетону, бетонна суміш.

* Адреса для листування E-mail: vladimirg54213@gmail.com

Збірник наукових праць. Галузеве машинобудування, будівництво
Academic journal. Industrial Machine Building, Civil Engineering
http://journals.nupp.edu.ua/znp
https://doi.org/10.26906/znp.2024.63.3888

UDC 666. 983

Vladimir Blazko
O. M. Beketov National University of Urban Economy in Kharkiv
https://orcid.org/0000-0002-5649-9379

Anna Anishchenko*
O. M. Beketov National University of Urban Economy in Kharkiv
https://orcid.org/0000-0002-3411-0385

Stanislav Kostenko
O. M. Beketov National University of Urban Economy in Kharkiv
https://orcid.org/0000-0003-0268-8008

Volodymyr Gerasymenko
O. M. Beketov National University of Urban Economy in Kharkiv
https://orcid.org/0000-0002-7874-1322

Determination of the Main Performance Indicators of a Forced-Action Concrete Mixer Using Similarity Criteria

The study focuses on the improvement of a forced-action concrete mixer designed for the preparation of low-workability concrete mixtures. The methodology is based on the application of dimensionless similarity criteria and mathematical modeling. Analytical dependencies for calculating the output rate and drive power were derived based on the geometric and kinematic parameters of the mixer, considering the dynamics of multi-loop mixing. The obtained results enable model scaling without the need for full-scale testing. Further research is planned to optimize operational modes for continuous mixing machines.

Keywords: concrete mixer, drive power, energy consumption, forced-action mixing, low-workability mixture, mixing modeling, output rate, similarity criteria

*Corresponding author E-mail: Aanishchenko@ukr.net

Introduction

In the context of modern construction technologies, the problem of improving the efficiency and reliability of equipment for concrete mixture preparation is gaining particular relevance [1–3]. One of the key units in this process is the forced-action concrete mixer, which ensures high mixing quality and consistency of mixture parameters. Despite their advantages, such mixers are characterized by complex kinematics and significant energy consumption. Therefore, their design solutions must rely not only on empirical approaches but also on scientifically grounded calculation methods that enable adaptation to specific operational conditions [4].

Review of the research sources and publications

Currently, the mixing equipment market offers a wide variety of technical solutions, with twin-shaft horizontal, turbulent, and planetary mixers being the most common. However, most of these machines demonstrate limited efficiency when operating with stiff and low-workability mixtures, thus necessitating specialized equipment for producing such concrete compositions [5]. A significant contribution to the formalization of mixing processes has been made through the application of similarity theory. Both domestic and foreign studies have explored the transition from model-scale to full-scale systems using dimensionless criteria. These criteria account for the physical and mechanical properties of mixtures, the geometric parameters of mixers, and the interaction dynamics between the mixing elements and the medium [6–9]. A systematic modeling approach has been shown to reduce the scope of experimental studies while maintaining the accuracy of technical assessments. Several studies propose criteria characterizing mixing power, dispersion level, and homogenization degree. Their application in the design of equipment for stiff mixtures enables the formulation of universal dependencies for predicting productivity and energy consumption [10].

Definition of unsolved aspects of the problem

Despite evident advantages, the use of similarity criteria in industrial equipment design has not yet become standard practice. This is due to the complexity of building accurate models and the need for a high level of specialist training. Therefore, studies combining experimental methods and theoretical modeling remain relevant and require further development [8].

Problem statement

The aim of this study is to determine the main performance indicators of a new-design forced-action concrete mixer based on the analysis of its structural and operational characteristics using similarity criteria. This approach enables scaling and parameter optimization during the transition from a laboratory prototype to an industrial-scale unit.

Basic material and results

The novelty of the research lies in the first-time adaptation and application of a system of dimensionless similarity criteria to a concrete mixer whose design is protected by a Ukrainian patent [11]. This system of criteria had previously been used in general form for evaluating processes in mixing devices but had not been applied to the calculation of output rate and energy consumption for a mixer with a triple-circuit mixing scheme. In this study, the similarity criteria were employed to derive formulas for determining the output rate and drive power without the need for full-scale experiments.

The mixer's working unit incorporates three horizontal shafts: the upper and lower blade shafts ensure the movement of mixture components and the breakdown of small agglomerates composed of soluble particles. The middle shaft, operating in zones I and II of the mixing chamber, first transports dry components and subsequently the prepared concrete mixture to the discharge zone (Figure 1).

All three shafts are involved in organizing multi-circuit material flow inside the mixer, resulting in a significant increase in the effective working volume, where intensive mixing occurs—up to the full volume of the mixing chamber. To utilize gravitational forces and enhance the cascading multi-circuit movement of the concrete mixture particles, the shafts are installed at an angle β at different vertical levels (Figure 1b)

For this mixer design, a system of dimensionless similarity criteria [12–15] was proposed and adapted to the specific features of a machine with a triple-circuit mixing scheme. For the first time, the combined influence of gravitational, inertial, elastic, surface-active, and turbulent effects was generalized and expressed through five criteria, C_{P1}–C_{P5}.

- **C_{P1}** – The ratio between the generalized pressure exerted by the mixing element and the dynamic pressure of the medium. It indicates the intensity of energy transfer to the mixture.

$$C_{P1} = \frac{P}{\rho \cdot v^2} \quad (1)$$

- **C_{P2}** – The ratio of gravitational force to the kinetic energy of the medium. It is an analogue of the Froude number (Fr), representing the effect of gravity on flow behavior.

$$C_{P2} = \frac{g \cdot l}{v^2} \quad (2)$$

- **C_{P3}** – The ratio of the medium's resistance to deformation (expressed via Pi) to its elastic recovery ability (modulus of elasticity, *E*). It characterizes how strongly the medium resists the mixing element.

$$C_{P3} = \frac{P_i}{E \cdot l^2} \quad (3)$$

- **C_{P4}** – The ratio of surface activity to external pressure. This criterion accounts for interfacial interactions in mixtures containing additives or surfactants.

$$C_{P4} = \frac{\sigma_\alpha \cdot l^2}{P} \quad (4)$$

- **C_{P5}** – A generalized Reynolds number adapted for concrete mixing. It reflects the ratio of inertial to viscous forces in the process.

$$C_{P5} = Re = \frac{\rho \cdot n}{P} \quad (5)$$

Where:

P – generalized specific pressure from the mixing element;

ρ – density of the medium;

ν – velocity of medium (concrete mix) movement;

g – gravitational acceleration;

l – characteristic cross-section of the loaded microvolume;

Pi – generalized resistance of the medium;

E – modulus of elasticity of the medium;

σ_α – surface activity of the substance.

These criteria, established based on general laws governing the interaction between working elements and the surrounding medium, allowed the derivation of scale transition coefficients from a baseline model to a full-scale industrial machine.

To solve the system of equations and obtain the transition coefficients, the following structural parameters were used:

r – blade rotation radius;

d – blade width;

b – blade height;

as well as operating parameters:

ω – angular velocity of the mixing unit;

W – total mixing energy of the baseline model;

and the physical-technical characteristics of low-workability concrete mixtures.

$$C_{P1} = \frac{P}{\rho \cdot v^2} = 2{,}18; \quad (5)$$

$$P = dF \cdot z_b;$$

$$dF = c \cdot \rho \cdot d \cdot b \cdot r \cdot \frac{\omega^2 \cdot r^2}{2};$$

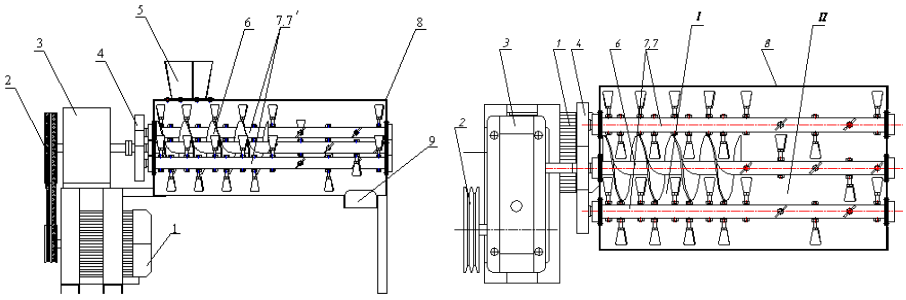

a)

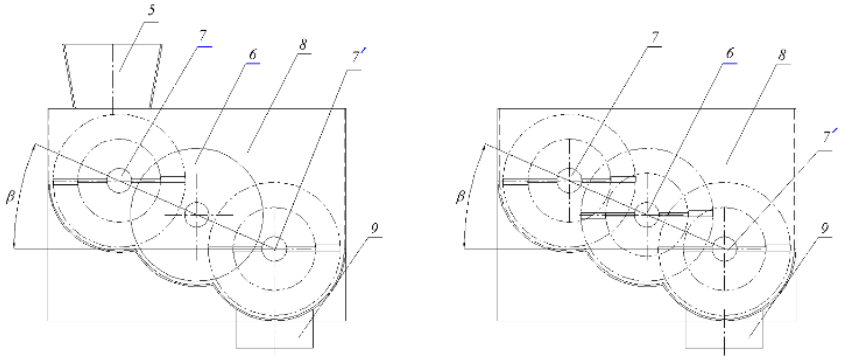

b)

Figure 1 – Structural diagram of the concrete mixer
a) concrete mixer; b) arrangement of shafts inside the mixer housing; 1 – electric motor; 2 – V-belt drive; 3 – gearbox; 4 – open gear transmission; 5 – loading hopper; 6 – screw shaft; 7, 7′ – upper and lower blade shafts; 8 – mixer housing; 9 – discharge pipe with gate valve; I – dry component mixing zone; II – concrete preparation zone with a specified water-cement ratio.

$$C_{P2} = \frac{g \cdot l}{v^2} = 32\ ; \qquad (6)$$

$$C_{P3} = \frac{P_i}{E \cdot l^2} = 10{,}56\ ; \qquad (7)$$

$$P_i = c \cdot \rho \cdot b \cdot \frac{\omega^2}{2} \int_{r_{in}}^{r_{ex}} r^2 \cdot dr\ ;$$

$$P_i = \cdot \rho \cdot b \cdot \frac{\omega^2}{2} \cdot \left(\frac{{r_{ex}}^3 - r_{in}}{3}\right);$$

$$C_{P4} = \frac{\sigma_\alpha \cdot l^2}{P} = 0{,}68; \qquad (8)$$

$$\sigma_\alpha = \frac{\sum W}{\sum P_{w.b}};$$

$$C_{P5} = Re = \frac{\omega \cdot r \cdot i \cdot \rho}{\mu} = 46{,}1\ . \qquad (9)$$

Eqs (6)–(9) describe the derived relationships. Based on the analysis and obtained results, a series of calculations were carried out using an established methodology for determining the key parameters of the working machine.

Productivity (PR) for the concrete mixer:

For the **baseline model** (laboratory mixer):

$$PR_{tech} = 3600 \cdot \frac{\pi}{4} \cdot (D^2 - d^2) \cdot b \cdot n \cdot z_b \cdot sin\alpha \cdot k_l^{av} \cdot k_{ex}^{II} = 4{,}28 m^3/h \qquad (10)$$

For the **industrial mixer**:

$$PR_{tech} = 3600 \cdot \frac{\pi}{4} \cdot (D^2 \cdot C_{P1} - d^2 \cdot C_{P1}) \cdot (b \cdot C_{P1}) \cdot n \cdot z_b \cdot sin\alpha \cdot k_l^{av} \cdot k_{ex}^{II} = 31 m^3/h \qquad (11)$$

Formulas (10) and (11) consider the geometric characteristics of the working volume and kinematic parameters, incorporating analogues of similarity criteria: namely, inertial effects (via Re), gravitational influence (via Fr), and interactions involving surface-active components.

In formulas (12) and (13), used to determine the **drive power**, the following components are considered:

DP₁ – energy expenditure to overcome gravitational forces (related to Fr);

DP₂ – energy required to move the mixture within the volume (related to Re and CP1);

DP₃ – energy consumed by shear deformation and elastic resistance (related to CP3).

Drive power (DP)for the concrete mixer:

Baseline model:

$$DP = \frac{\lambda(DP_1 + DP_2 + DP_3)}{1000 \cdot \eta}; \qquad (12)$$

$$DP = \frac{1{,}2(803 + 1537 + 1591)}{1000 \cdot 0{,}85} = 5{,}53\ kW.$$

Industrial mixer:

$$DP = \frac{\lambda(DP_1 + DP_2 + DP_3)}{1000 \cdot \eta}; \qquad (13)$$

$$DP = \frac{1{,}2(1318 + 5672 + 11460)}{1000 \cdot 0{,}85} = 21\ kW.$$

Where:

λ – power reserve coefficient of the electric motor;

η – efficiency of the drive system;

DP₁, DP₂, DP₃ – generalized power components.

Conclusions

This study proposes a validated approach for evaluating the main performance characteristics of a

newly designed concrete mixer through the use of an adapted system of dimensionless similarity criteria. Unlike previous studies, the criteria referenced in [12–15] were, for the first time, integrated into a calculation methodology for determining both output rate and drive power of a machine with a triple-circuit mixing mechanism, implemented in a patented design [11].

This approach enables the transition from a laboratory-scale model to an industrial prototype without the need for full-scale testing.

References

1.Valigi, M. C., et al. (2019). Twin-Shaft Mixers' Mechanical Behavior: Power Consumption and Exchanged Forces.

2. Emelyanova, I. A. (2008). Features of Preparation of Inactive Mortars in Concrete Mixers with Horizontal Blade Shafts.

3. Волянський О. А. Технологія бетонних і залізобетонних конструкцій : підручник : у 2 ч. - К. : Вища шк., 1994. – Ч. 1. Технологія бетону. – 271с.

4. Ващенко К.М., Пархітько Г.С. Дослідження впливу геометричних характеристик робочих органів на ефективність роботи роторного змішувача. Збірник наукових праць (галузеве машинобудування, будівництво). 2012. Вип. 1 (31). С. 97-103.

5. Будівельна техніка: підручник / В.О. Онищенко та ін. Київ: Кондор-Видавництво, 2017. 416 с.

6. Сидоров В.П. Змішувальні машини в будівництві. – Київ: Вища школа, 2015. – 208 с.

7. Назаренко М.С., Петренко І.В. Дослідження ефективності змішування бетонних сумішей // Вісник будівництва. – 2020. – №2. – С. 65–71.

8.Бойко І.П., Павленко С.А. Особливості роботи багатовальних змішувачів // Машини і механізми. – 2018. – №3. – С. 44–49.

9. Гришко О.М. Фізичне моделювання в інженерній справі. – Львів: ЛП, 2017. – 146 с.

10. Siddique, R., et al. (2024). Control of Concrete Segregation and Quality Enhancement Using Continuous Mixers. Advances in Civil Engineering, 2024, 6849967.

11. Емельянова І.А., Баранов А.М., Блажко В.В., Тугай В.В. Змішувач для приготування будівельної суміші : пат. №74444 Україна, МПК B28C5/14 / заявл. 15.12.2005. – Держ. департамент інтелектуальної власності України. – Опубл. в бюл. №12, 2006.

12. Kliukas, R.; Vadlūga, R. Analysis of Structural Spun Concrete properties. In Proceedings of the 3rd International Conferences SDSMS'03, Klaipėda, Lithuania, 17–19 September 2003; pp. 141–150.

13. Kudzys, A.; Kliukas, R. The resistance of compressed spun constrete members reinforced by high-strength steel bars. Mater. Struct. 2008, 41, 419 – 430.

14. Ferraris, C. F. (2001). Concrete Mixing Methods and Concrete Mixers: State of the Art. Journal of Research of the National Institute of Standards and Technology, 106(2), 391 – 399.

15 Galletti, C., et al. (2023). Numerical Mixing Index: Definition and Application on Concrete Mixer. Fluids, 10(3), 72.

1. Valigi, M. C., et al. (2019). Twin-Shaft Mixers' Mechanical Behavior: Power Consumption and Exchanged Forces.

2. Emelyanova, I. A. (2008). Features of Preparation of Inactive Mortars in Concrete Mixers with Horizontal Blade Shafts.

3. Volianskyi, O. A. (1994). Technology of Concrete and Reinforced Concrete Structures: Textbook in Two Parts. Part 1. Concrete Technology. Kyiv: Vyshcha Shkola. (in Ukrainian)

4. Vashchenko, K. M., Parkhitko, H. S. (2012). Study of the Influence of the Geometric Characteristics of Working Bodies on the Efficiency of a Rotary Mixer. Collection of Scientific Papers (Sectoral Mechanical Engineering, Construction), Issue 1(31), 97–103. (in Ukrainian)

5. Onyshchenko, V. O., et al. (2017). Construction Equipment: Textbook. Kyiv: Kondor-Vydavnytstvo. (in Ukrainian)

6. Sydorov, V. P. (2015). Mixing Machines in Construction. Kyiv: Vyshcha Shkola. (in Ukrainian)

7. Nazarenko, M. S., Petrenko, I. V. (2020). Study of the Efficiency of Mixing Concrete Mixtures. Bulletin of Construction, 2, 65–71. (in Ukrainian)

8. Boiko, I. P., Pavlenko, S. A. (2018). Peculiarities of Multishaft Mixers Operation. Machines and Mechanisms, 3, 44–49. (in Ukrainian)

9. Hryshko, O. M. (2017). Physical Modeling in Engineering. Lviv: Lviv Polytechnic. (in Ukrainian)

10. Siddique, R., et al. (2024). Control of Concrete Segregation and Quality Enhancement Using Continuous Mixers. Advances in Civil Engineering, 2024, Article ID 6849967.

11. Emelianova, I. A., Baranov, A. M., Blazhko, V. V., Tuhai, V. V. (2006). Mixer for Preparing Construction Mixture: Patent of Ukraine No. 74444, IPC B28C5/14. Application date: 15.12.2005. State Department of Intellectual Property of Ukraine. Published in Bulletin No. 12. (in Ukrainian)

12. Kliukas, R., & Vadlūga, R. (2003). Analysis of Structural Spun Concrete Properties. Proceedings of the 3rd International Conference SDSMS'03, Klaipėda, Lithuania, September 17–19, pp. 141–150.

13. Kudzys, A., & Kliukas, R. (2008). The Resistance of Compressed Spun Concrete Members Reinforced by High-Strength Steel Bars. Materials and Structures, 41, 419–430.

14. Ferraris, C. F. (2001). Concrete Mixing Methods and Concrete Mixers: State of the Art. Journal of Research of the National Institute of Standards and Technology, 106(2), 391–399.

15. Galletti, C., et al. (2023). Numerical Mixing Index: Definition and Application on Concrete Mixer. Fluids, 10(3), 72.

Блажко В.В.
Харківський національний університет міського господарства імені О. М. Бекетова
https://orcid.org/0000-0002-5649-9379

Аніщенко А.І.*
Харківський національний університет міського господарства імені О. М. Бекетова
https://orcid.org/0000-0002-3411-0385

Костенко С.М.
Харківський національний університет міського господарства імені О. М. Бекетова
https://orcid.org/0000-0003-0268-8008

Герасименко В.В.
Харківський національний університет міського господарства імені О. М. Бекетова
https://orcid.org/0000-0002-7874-1322

Визначення основних показників роботи бетонозмішувача примусової дії з використанням критеріїв подібності

Удосконалення конструкцій змішувального обладнання для приготування жорстких бетонних сумішей є ключовим напрямом підвищення ефективності будівельного виробництва. У роботі застосовано метод теоретичного моделювання з використанням безрозмірних критеріїв подібності, що дозволяє виконати масштабування робочих параметрів від лабораторного зразка до промислового бетонозмішувача. Проведено структурно-функціональний аналіз нової триконтурної схеми перемішування, що включає роботу трьох горизонтальних валів з різними функціями транспортування та деструкції компонентів суміші. Запропоновано п’ять адаптованих критеріїв подібності (аналог Fr, Re та інших), які враховують гравітаційні, інерційні, в’язкі, пружні й міжфазні сили, що діють у робочому об’ємі змішувача. На основі отриманих критеріїв виведено формули для розрахунку продуктивності (output rate) та потужності приводу (drive power), що включають геометричні параметри мішального простору, кутову швидкість (ω) і коефіцієнти енерговитрат. Уперше обґрунтовано енергетичний баланс приводу з урахуванням втрат на гравітаційне переміщення, зсувну деформацію й опір середовища. Результати підтвердили можливість використання запропонованого підходу для проектування бетонозмішувачів з урахуванням специфіки жорстких сумішей, без проведення повномасштабних експериментів. Перспективним напрямом подальших досліджень є розширення системи критеріїв для машин неперервної дії з автоматизованим регулюванням режимів перемішування.

Ключові слова: бетонозмішувач, енергоспоживання, змішування примусової дії, критерії подібності, малорухома суміш, моделювання процесу змішування, потужність приводу, продуктивність

*Адреса для листування E-mail: Aanishchenko@ukr.net

ЗМІСТ

CONTENTS